

**EFFECTS OF POLYETHER ANTIBIOTICS ON
AUTOPHAGY**

**Thesis Submitted to
the Graduate School of Engineering and Sciences of
İzmir Institute of Technology
in Partial Fulfilment of the Requirements for the Degree of**

MASTER OF SCIENCE

in Molecular Biology and Genetics

**by
Nasar KHAN**

**June 2017
İZMİR**

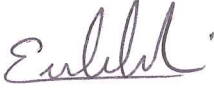
We approve the thesis of **Nasar KHAN**

Examining Committee Members




Assist. Prof. Dr. Çiğdem TOSUN

Department of Molecular Biology and Genetics, İzmir Institute of Technology



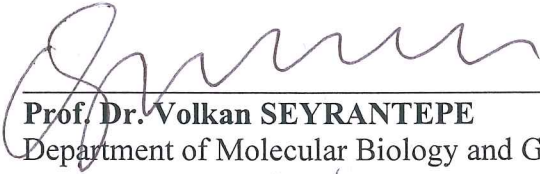
Prof. Dr. Erdal BEDİR

Department of Bioengineering, İzmir Institute of Technology



Assoc. Prof. Dr. Petek BALLAR KIRMIZIBAYRAK

Faculty of Pharmacy, Ege University



Prof. Dr. Volkan SEYRANTEPE

Department of Molecular Biology and Genetics, İzmir Institute of Technology



Assist. Prof. Dr. Özden YALÇIN ÖZUYSAL

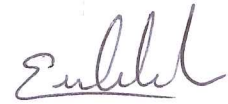
Department of Molecular Biology and Genetics,
İzmir Institute of Technology

12 June 2017



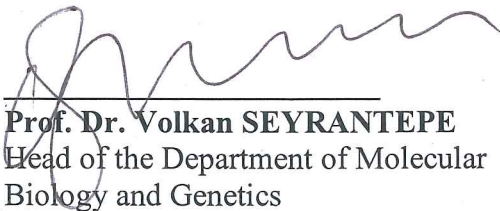
Assist. Prof. Dr. Çiğdem TOSUN

Supervisor, Department of Molecular Biology
and Genetics,
İzmir Institute of Technology



Prof. Dr. Erdal BEDİR

Co-Supervisor, Department of
Bioengineering,
İzmir Institute of Technology



Prof. Dr. Volkan SEYRANTEPE

Head of the Department of Molecular
Biology and Genetics

Prof. Dr. Aysun SOFUOĞLU

Dean of the Graduate School of
Engineering and Sciences

ACKNOWLEDGEMENTS

I feel highly privileged to express my profound gratitude to my respectable teachers and research supervisors, Assist. Prof. Dr. ıđdem TOSUN, Prof. Dr. Erdal BEDİR and Assoc. Prof. Dr. Petek BALLAR KIRMIZIBAYRAK for their devotion, support and clean interest in my research work and thesis. It was because of their inspiring guidance, dynamic supervision and financial support that I became able to complete my Master degree. I am really grateful for their worthy efforts to arrange this special project for me in order to save my future, when I was at the critical stage of my Master degree.

In parallel, again a warm thankful to Assoc. Prof. Dr. Petek BALLAR KIRMIZIBAYRAK for her valuable supervision, help and giving an opportunity to perform this research work in her laboratory during my thesis studies. I would like to extend my hearty thanks to my senior lab colleagues Assist. Prof. Dr. Burcu TEPEDELEN ERBAYKENT, Recep İLHAN, Sinem YILMAZ, Yalçın ERZURUMLU and Selin GÜNAL for their extraordinary help, sharing practical and theoretical information, friendships and moral support.

Beside this, I also want to express my thankful feelings for my previous supervisor Assist. Prof. Dr. Mustafa KÖKSAL for his kind supervision and support during the first year of my Master degree. I am also grateful of my previous laboratory colleagues Kamil OVACIK, Ebru GÜRELME, Dilara DEMİRCİ and Aysu ÖZKAN for their tremendous support and help. Over all, I would like to thanks to all faculty members of Molecular Biology and Genetics and Bioengineering departments at Izmir Institute of Technology as well as Faculty of Pharmacy at Ege University for their sincere help and support during my experimental work. Along with this, I want to extend my thanks to Turkey for giving me this dynamic opportunity to pursued my Master degree as international student.

Finally, I want to express my deep gratitude and appreciation to my family members and my beloved late father for their unconditional and eternal love, belief, motivation, enormous encouragement and endless support throughout my life.

ABSTRACT

EFFECTS OF POLYETHER ANTIBIOTICS ON AUTOPHAGY

Treatment of cancer is one of the crucial enigma for scientific world and that's why much effort needs to be put in place for the resolution of this challenge in alternative ways. Autophagy is believed to have an important role in tumor development and progression. The natural polyether antibiotics might be important chemotherapeutic agents to cure cancer by modulating autophagy.

The primary goal of this study was to investigate the cytotoxic effects and autophagic mechanism of actions of three polyether antibiotics, one of which was a new secondary metabolite isolated from the marine *Streptomyces cacaoi*. The effects of these polyether antibiotics were investigated along with previously known autophagy modulators from the same group (Monensin). To achieve this goal, cytotoxicities of these polyether type compounds on three different type of cancer cell lines along with two healthy cell lines were investigated followed by a search to reveal the effects of these compounds on autophagy in cancer cell lines. Methodology of this study consists of mammalian cell culturing, cytotoxicity screening, staining and quantification of acidic compartments inside the cells and studying different autophagy markers along with other associated proteins under various conditions by using Western blotting.

This study revealed that the tested polyether antibiotics were autophagy inhibitors as well as inducers of apoptosis in cervical, colorectal and prostate cancer cells. The obtained results will be of significance for the field of anticancer drug-development; however, before one places these secondary metabolites as potential drug candidates, further studies including *in vivo* experiments are warranted.

ÖZET

POLYETER ANTİBİYOTİKLERİN OTOFAJI ÜZERİNDEKİ ETKİSİ

Kanser tedavisi bilim dünyasının önemli gizemlerden biridir ve bu nedenle bu zorlu hastalığın çözümlenebilmesi için alternatif yolların bulunmasında büyük çaba harcanması gerekmektedir. Tümör gelişimi ve ilerlemesinde otofajinin büyük bir rolü olduğu bilinmektedir. Doğal poliyeter iyonofor antibiyotikler, kanser hücre hatlarında otofajiyi hedefler ve kanser hastaları için önemli bir kemoterapötik ajan olma potansiyelini taşır.

Bu çalışmanın temel amacı, denizel aktinomiset *Streptomyces cacaoi*'den izole edilen yeni sekonder metabolit olmak üzere üç poliyeter antibiyotiğin, sitotoksik etkilerinin ve otofaji yolağındaki çalışma mekanizmasının araştırılmasıdır. Bu poliyeter antibiyotiklerin etkileri, önceden bilinen aynı gruptaki otofaji modülatörleriyle (Monensin) birlikte araştırılmıştır. Bu hedefe ulaşmak için poliyeter tipi bileşiklerin sitotoksitesisi üç farklı kanser ve iki sağlıklı hücre hattında incelenmiş, sonrasında ise kanser hücrelerinde otofajik etkinin rolüne bakılmıştır. Bu çalışmada kullanılan teknikler; memeli hücre hattı kültürü, sitotoksitesite taramaları, hücre içinde asidik kompartmanlarının boyanması ve miktarlarının belirlenmesi ve farklı otofaji belirteçleri ile yardımcı proteinlerinin farklı koşullarda "Western blotting" tekniği ile incelenmesidir.

Bu çalışma göstermiştir ki test edilen poliyeter antibiyotikler otofaji inhibitörü olmalarını yanında apoptosisi servikal, kolorektal ve prostat kanseri hücrelerinde indükleyen ajanlardır. Elde edilen sonuçlar antikanser ilaç geliştirme alanı için önemli sonuçlar içermektedir. Fakat bu sekonder metabolitleri potent ilaç adayları olarak gösterebilmek için *in vivo* testleri de içeren ileri çalışmalara ihtiyaç vardır.

TABLE OF CONTENTS

LIST OF TABLES.....	ix
LIST OF FIGURES.....	x
CHAPTER 1. INTRODUCTION.....	1
1.1. Cancer.....	1
1.2. Polyether Antibiotics.....	2
1.2.1. Chemical structure.....	2
1.3. Mechanism of Cation Transport by Polyether Antibiotics.....	5
1.3.1. Electroneutral Mechanism.....	5
1.3.2. Electrogenic Mechanism.....	6
1.4. Application and Biological Activity of Polyether Antibiotics.....	7
1.4.1. Antimicrobial activity.....	8
1.4.2. Anticancer activity.....	9
1.5. Autophagy	11
1.6. Autophagy Signalling Pathway.....	13
1.6.1. Induction of autophagy.....	14
1.6.2. Early membrane Initiation.....	15
1.6.3. Autophagosome formation.....	16
1.6.4. Cargo recognition and selection.....	18
1.6.5. Autophagosome and lysosome fusion.....	20
1.7. Role of Autophagy in Cancer.....	22
1.7.1. Autophagy as tumor suppressor.....	23
1.7.2. Autophagy as tumor promotor.....	24
1.8. Influence of Anticancer Agents on Autophagy.....	25
1.9. Effects of Autophagy on Cancer Therapy.....	26
1.10. Polyether Antibiotics Against Autophagy	28
1.11. Aim of This Work.....	30

CHAPTER. 2. MATERIALS AND METHODS.....	31
2.1. Materials.....	31
2.2. Methods.....	31
2.2.1. Monensin Isolation and purification.....	31
2.2.1.1. Monensin containing product.....	31
2.2.1.2. Extraction and isolation.....	31
2.2.1.3. Thin layer chromatography.....	32
2.2.1.4. Structure confirmation.....	32
2.2.2. Mammalian cell culture.....	32
2.2.2.1. Cells maintenance and growth.....	32
2.2.2.2. Cells passaging.....	33
2.2.2.3. Cells freezing and thawing.....	33
2.2.2.4. Cells counting.....	34
2.2.3. Cytotoxicity analysis.....	34
2.2.3.1. Cells seeding.....	34
2.2.3.2. Preparation of compounds solution.....	34
2.2.3.3. Application of compounds on cell lines.....	35
2.2.3.4. WST-1 assay.....	35
2.2.3.5. IC ₅₀ value calculation.....	35
2.2.4. Western blotting.....	36
2.2.4.1. Cells seeding.....	36
2.2.4.2. Compounds treatment.....	36
2.2.4.3. Cells harvesting.....	39
2.2.4.4. Cells lysis.....	40
2.2.4.5. BCA analysis.....	40
2.2.4.6. SDS PAGE.....	40
2.2.4.7. Membrane transfer.....	40
2.2.4.8. Blotting.....	41
2.2.4.9. ECL Imaging.....	41
2.2.5. Acridine Orange staining.....	41
2.2.6. MDC staining.....	42
2.2.7. MDC Fluorometry analysis.....	42
2.2.8. Statistical Analysis.....	43

CHAPTER. 3. RESULTS.....	44
3.1. Polyether Antibiotics Isolation and Purification.....	44
3.2. Monensin Isolation and Purification.....	45
3.2.1. Monensin Isolation.....	45
3.2.2. Monensin purification.....	45
3.2.3. Structure confirmation of Monensin.....	46
3.3. Polyether Antibiotics Activity Against Cancer Cell lines.....	48
3.4. Polyether Antibiotics Activity Against Healthy Cell lines.....	52
3.5. Polyether Antibiotics Increase Expression Level of Autophagy Markers.....	54
3.6. Autophagy Markers Accumulation Dependent on Polyether Antibiotics Concentration.....	57
3.7. Polyether Antibiotics Increases the Synthesis of Autophagic Vacuoles.....	59
3.8. The Effects on Beclin-1 and Other Autophagy Related Genes (Atgs) Over the time.....	60
3.9. The Effects on Beclin-1 and Atgs Directly Proportional to Polyether Concentration.....	62
3.10. Effects of Polyether Antibiotics on Acidic Compartments in Cytosol.....	63
3.11 Quantification of Acidic Vacuoles inside the Cells.....	67
3.12. Polyether Antibiotics Activate Apoptosis.....	68
 CHAPTER. 4. DISSCUSSION.....	 72
 CHAPTER. 5. CONCLUSION.....	 77
 REFERENCES.....	 79
 APPENDIX A. MATERIALS, SOLUTIONS, SUPPLEMENTARY IMAGES	 98

LIST OF TABLES

<u>Table</u>	<u>Page</u>
Table 2.1. Time course treatment experimental design.....	37
Table 2.2. Dose response treatment experimental design.....	38
Table 2.3. Combine treatment experimental design.....	39
Table 2.4. AO, MDC staining and Fluorometry experimental compounds treatment.	42
Table 3.1. IC ₅₀ values of polyether antibiotics against cancer and healthy cell lines..	.48

LIST OF FIGURES

<u>Figure</u>	<u>Page</u>
Figure 1.1. Linear chemical structure of some important polyether antibiotics.....	4
Figure 1.2. Pseudo-cyclic structure of polyether antibiotics – Monensin	4
Figure 1.3. Mechanism of transport of ion across the membrane.....	6
Figure 1.4. Role of autophagy in the cell.....	12
Figure 1.5. Autophagy induction and autophagosome biogenesis.....	13
Figure 1.6. Substrate recognition and selective autophagy.....	19
Figure 1.7. Autophagosome and lysosomal fusion.....	21
Figure 3.1. Chemical structure of our polyether antibiotics.....	44
Figure 3.2. Solid liquid extraction system and initial chromatogram.....	45
Figure 3.3. Chemical purification system and final TLC chromatogram.....	46
Figure 3.4. LC-ESI-MS spectrum of Monensin.....	47
Figure 3.5. ¹ H NMR Spectrum of Monensin.....	47
Figure 3.6 Microscopic pictures of PC-3 cell line.....	49
Figure 3.7 Microscopic pictures of CaCo-2 cell line.....	50
Figure 3.8. Microscopic pictures of HeLa cell line.....	51
Figure 3.9. Microscopic pictures of MRC-5 cell line.....	53
Figure 3.10. W.B images of LC3 and p62 for CaCo-2 (Time course).....	55
Figure 3.11. W.B images of LC3 and p62 for HeLa (Time course).....	56
Figure 3.12. W.B images of LC3 and p62 for PC-3 (Time course).....	57
Figure 3.13. W.B images and graph of LC3 and p62 for HeLa (Dose response).....	58
Figure 3.14. W.B images and graph of LC3 and p62 for HeLa (Combine treatment).	60
Figure 3.15. Western blot images of beclin-1 and Atgs for HeLa (Time course).....	61
Figure 3.16. Western blot images of beclin-1 and Atgs for CaCo-2 (Time course)...	62
Figure 3.17. Western blot images of beclin-1 and Atgs for HeLa (Dose response).....	63
Figure 3.18. Acridine Orange staining of HeLa Cell line.....	65
Figure 3.19. MDC staining of HeLa Cell line.....	66
Figure 3.20. Graph showing quantity of acidic vacuoles inside the cells.....	68
Figure 3.21. Western blot images of caspase 9 and 3 for HeLa (Time and Dose).....	69
Figure 3.22. Western blot images of PARP for HeLa (Time and Dose).....	70
Figure 3.23. Western blot image of PARP for CaCo-2 (Time).....	71

Figure 3.24. Western blot images of ER stress markers for CaCo-2 (Time)..... 71

CHAPTER 1

INTRODUCTION

1.1.Cancer

Cancer, a generic word used for a large group of diseases characterized by abnormal cell growth that has the potential of invading or spreading to any part of the body (WHO, 2014). Malignant tumors and neoplasms are other terms used for cancer. Neoplasm or tumor referred to a group of cells that undergone unregulated growth and often form a mass or lump which may be disseminated diffusely (Birbrair et al., 2014). The hallmarks regarding cancer encompass six biological capabilities acquired by the cells during a multistep process of tumors. These include sustaining proliferative signalling, resisting cell death, evading growth suppressors, inducing angiogenesis, enabling replicative immortality and activating invasion and metastasis (Hanahan and Robert, 2011).

Risk factors associated with cancer include internal factors of the individual like inherited mutations, hormones, immune conditions and environmental/acquired factors like tobacco, alcohol, diet, obesity, radiation, chemicals and infectious agents (Anand et al., 2008). According to the World Health Organisation (WHO), cancer is the second leading cause of death in the world and approximately 8.8 million deaths occurred due to cancer in 2015. Globally, about 1 in 6 deaths is due to cancer. According to current prevalence data, it is expected that the number of new cases in cancer may increase up to 70% in the coming two decades (WHO, 2017).

One of the most crucial and enormously difficult challenge for modern science is the fight against neoplastic disease. However, cancer can be treated by a number of ways but the treatment strategy primarily depends upon the type of cancer and its advancing pattern. The main types of cancer treatment strategies include surgery, radiation therapy, chemotherapy, immunotherapy, hormone therapy, stem cell transplant and precision medicines. Depending upon the type of cancer, these strategies can be used individually or in combination for the treatment of cancer (NCI, 2015). Besides treatment, according to the WHO and Centres for Disease Control and Prevention

(CDC) between 30 to 50% of all cancer types are preventable. Prevention measures offer the long term and most cost effective strategy regarding the control of cancer. Such preventive strategies can be implemented to the society by national policies and programmes which will lead to awareness regarding minimum exposure to cancer risk factors and will provide the required information and support to people so that they can adopt healthy lifestyles. (WHO, 2017; Yang and Colditz, 2014).

1.2. Polyether Antibiotics

Polyethers are quite potent and important antibiotics that belong to a large class of naturally occurring ionophores. The history of polyether antibiotics started in 1951 when nigericin and lasalocid acid were isolated from *Streptomyces* spp. for the first time. Later on, more than 50 microorganisms were identified that produced such carboxyl ionophores, and to date, about 120 compounds have been reported (Dutton et al., 1995). The term polyether reflects the chemical structure of this class of antibiotics having several ether functional groups while the term ionophore is using for these antibiotics due to their ability of transferring/exchanging ions across the lipid bilayer. The term ionophore was used for the first time in 1967 for such compounds due to their ability to bind ions and facilitate the transport of ions across the lipid bilayer in the form of a metal ion complex (Riddell, 2002).

1.2.1. Chemical structure

Primarily the structure of polyether antibiotics consists of multiple tetrahydropyran and tetrahydrofuran rings linked by aliphatic chemical bonds like direct carbon-carbon (CC) bond or Spiro linkages. A terminal carboxylic acid group, several hydroxyl groups, lower alkyl groups and a variety of functional oxygen groups further contribute to the formation of complete chemical structure (Figure 1.1). These groups play crucial roles to form complexes with metal ions (Hilgenfeld and Saenger, 2005). Polyether antibiotics are classified in various groups based on the number of carbon atoms present in their backbone. Among them, the most frequently encountered compounds are the 30-carbon skeletons that account for about 60% of all polyether class antibiotics. A large family of microbial enzymes polyketide synthases (PKSs)

catalyse the biosynthesis of polyether antibiotics by incorporating acetyl-CoA and propyl-CoA as building blocks for the polyketide backbone extension (Seidel, 2006).

The internal face of these compounds is polar due to the presence of many carbonyl groups, ether bridges and hydroxyl groups, which consequently assist the binding of cations during the formation of complex. The external face is hydrophobic making these compounds quite suitable to pass through the lipid bilayer (Dobler, 2004). According to the X-ray studies, these oxygen atoms of the inner face form a cage like structure giving the metals (cation) a binding site (Figure 1.2). Neutral complexes can be formed by polyether antibiotics with different cations i.e salinomycin and monensin form complex with monovalent cations while calcimycin and lasalocid A form complex with divalent cations, as well as with organic bases. Formation of neutral complexes are more favourable than charged complexes due to the deprotonation of terminal carboxylic group at physiological pH. However, recently it has been reported that although ionophores can act like neutral molecules at the protonated state (acidic pH), but still they can transport cations as charged complexes. Typically, the binding pattern of cations during protonated state of ionophores are facilitated by cage like structures (pseudo-cyclic structure) formed by the oxygen atoms in their internal face and terminal hydroxyl group, which is stabilized by head to tail intramolecular hydrogen bonds. This hydrophilic cage is surrounded by the rings of ionophore molecule making the whole complex lipophilic and thus, facilitating the complex to easily cross the lipid bilayer or cell membrane (Rutkowski and Brzezinski, 2013).

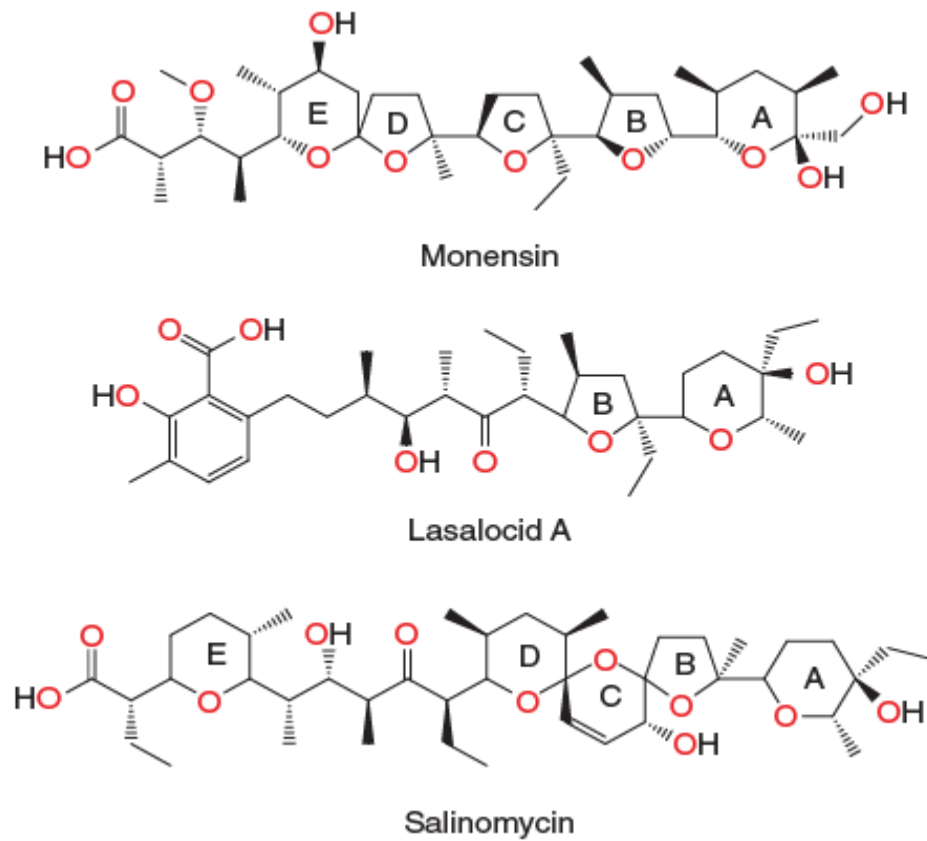


Figure 1.1 Linear chemical structures of some important polyether antibiotics
(Source: Antoszczak et al., 2015)

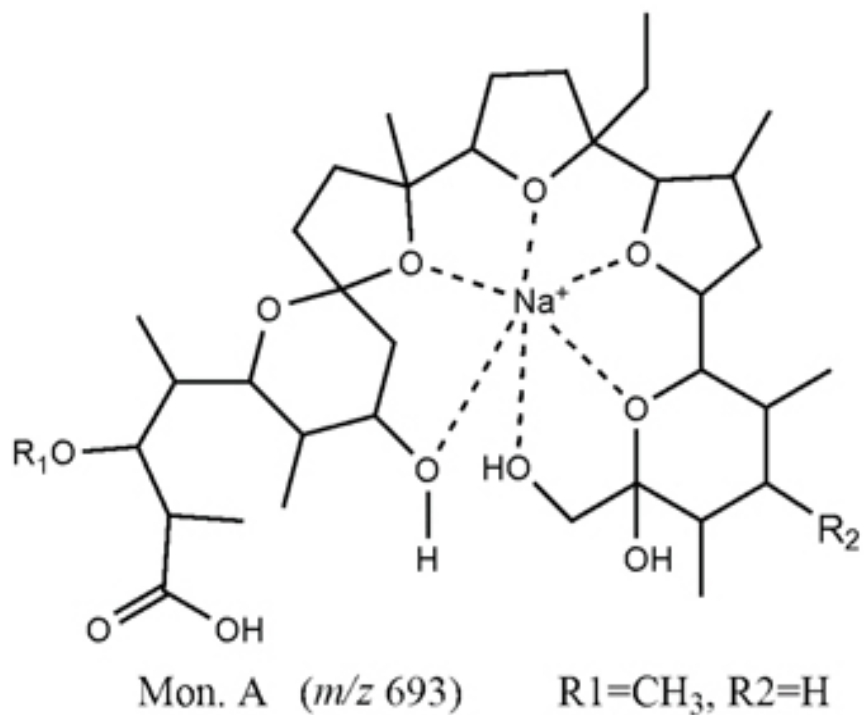


Figure 1.2 Pseudo-cyclic structure of polyether antibiotics – Monensin
(Source: Sousa-Junior et al., 2013)

1.3. Mechanism of Cation Transport by Polyether Antibiotics

Conventionally, it is acceptable that all ionophores are primarily responsible for the transport of cation/proton across biological membranes by different mechanisms. Investigation and better knowledge regarding these different mechanisms followed by each compound lead towards better understanding about their broad spectrum of biological activity. Across the membrane, concentration gradient of cations like high extracellular concentration of Na^+ and high intracellular concentration of K^+ and vice versa is mandatory for normal physiological behaviour of cells (Hildebrandt et al., 1978). Primarily, ionophores lead to the disturbance of this Na^+/K^+ concentration gradient by transporting cation/proton across the lipid bilayer or plasma membrane. Ionophores achieve this by two different mechanisms (Figure 1.3) depending on the surrounding pH of the cell (Riddell, 2002; Gokel, 2004).

1.3.1. Electroneutral mechanism

In neutral pH or slightly alkaline microenvironment, the terminal carboxylic acid group (COOH) of the polyether antibiotics become deprotonated and form carboxylate ion (COO^-). These polyether ionophore anions (I-COO^-) have greater tendency towards cations (M^+) with preference for Na^+ or K^+ ions or proton (H^+) and thus form stable complexes in the form of neutral salt ($\text{I-COO}^-\text{M}^+$) or neutral polyether ionophore in acidic form (I-COOH), respectively. It has been reported that the pseudo-cyclic structure formed by ionophores between the terminal hydroxyl group and inner oxygen atoms have crucial contribution in the stabilization of these salt complexes ($\text{I-COO}^-\text{M}^+$). The permeability of cell membrane only allows uncharged molecules containing metal ion or proton, and in the same way the net charge of these ionophore complexes ($\text{I-COO}^-\text{M}^+$) is zero, and that's why they can easily cross the cell membrane. Due to difference in the electrolyte concentration of the cell across the membrane, these ionophore complexes substitute the cation (M^+) with proton (H^+) on the inner interface of the membrane, and then they come back towards the outer interface of the cell membrane. This cycle is completed within the membrane resulting an exchange of cation (M^+) by proton (H^+), and thus the ionophore acts like a Na^+/H^+ anti-porter. This is the most widely studied mechanism and is known as electroneutral mechanism of ion

transport across the membrane by ionophores. The name given to this mechanism is due to the transfer of same charged or electrically neutral species across the membrane (Mollenhauer et al., 1990; Huczyński, 2012).

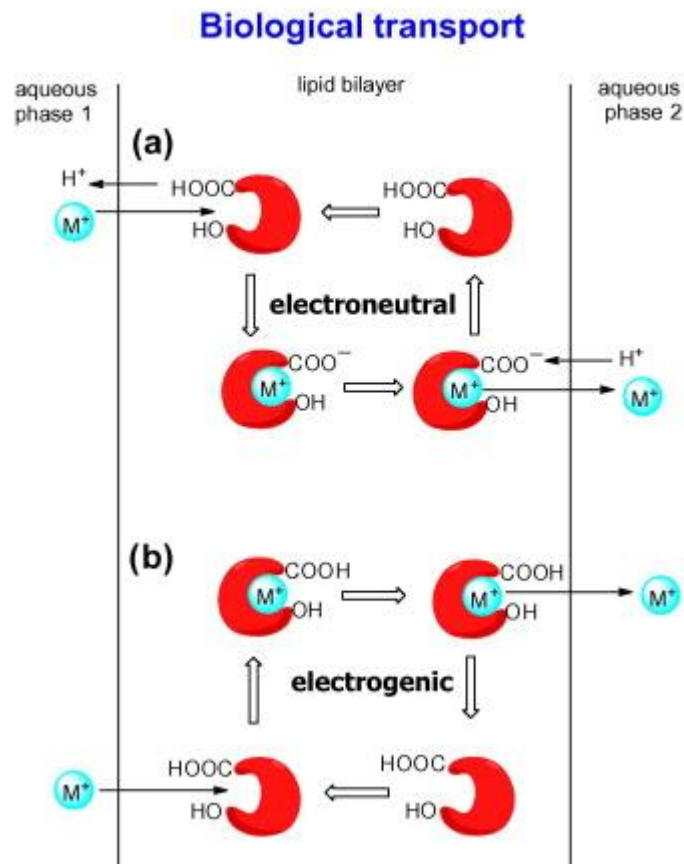


Figure 1.3 Mechanism of ion transport across the membrane (Source: Huczyński, 2012)

1.3.2. Electrogenic mechanism

The microenvironment of tumor cells is significantly acidic compared to healthy cell lines because of an alteration of their metabolic pathways. Tumor cells maintain high glycolytic rate because of the high anabolic demand and consequently, follow the lactic acid production pathway even in the presence of adequate amount of oxygen that leads to decrease in cellular pH, this pathway is known as aerobic glycolysis or Warburg effect (Warburg, 1956; Lazaro, 2008)

In such an acidic microenvironment, the polyether antibiotics follow electrogenic mechanism for the transfer of ions across the cell membrane and show anticancer activity. In this mechanism, the cation binds to the acidic form of polyether

ionophore (I-COOH) at low pH rather than the anionic form (I-COO⁻). The polyether ionophore complex formed under such circumstances is (I-COOH-M⁺), stabilized by the intramolecular hydrogen bonds formed during pseudo-cyclic structure shown by x-ray crystallography studies (Figure 1.2). The conservation of pseudo-cyclic structure of this complex is shown by spectroscopic studies in dichloromethane solution. The molecular electrostatic potential around the supramolecular polyether ionophore complex (I-COOH-M⁺) is completely changed due to the interaction between electronegative oxygen atoms of polyether's acidic form (I-COOH) and metal cation (M⁺). Because of this ability, the polyether antibiotics easily cross the cell membrane in the form of metal ion complex (I-COOH-M⁺). This mechanism is known as electrogenic because the transfer of metal cation (M⁺) by polyether ionophore cause electrical imbalance as well as ionic imbalance across the membrane of the cell (Huczyński et al., 2012b).

1.4. Applications and Biological Activity of Polyether Antibiotics

The major commercial application of polyether antibiotics is to control coccidiosis in poultry farming as well as in ruminants. Along with this, these compounds also target the ruminal bacteria population and that's why it's a controlling agent for ketosis and bloat in ruminants. Therefore, polyethers are used as a growth promoter feed additive in ruminants. In 2003, it was reported that, to increase beef production, the most commonly used antimicrobials were ionophores. (Callawy et al., 2003; Rutkowski and Brzezinski, 2013). Along with this, in biomedical and research laboratories, polyether antibiotics have been used as components in ion-selective electrodes for measurement of transmembrane electrical potential and transport studies (Gabrielli. et al. 2004). Besides this, polyethers are a versatile class of highly active compounds and well known for their broad spectrum of biological activity against bacteria especially to Gram-positive ones, fungus, parasites, viruses and cancer cell lines. The primary mechanism of the vast range of bioactivities is the ability of these compounds to modulate the cation concentration gradient across the membrane, leading to intracellular pH change, cell swelling, vacuolization, mitochondrial injury and at last induction of cell death (Antoszczak et al., 2015).

1.4.1. Antimicrobial activity

Polyether antibiotics exhibit strong antimicrobial activity against range of microorganisms. Among these, this class of antibiotics are active against both drug sensitive and multidrug resistant (MDR) bacterial strains; however, comparatively this activity is reported more in Gram-positive bacteria than Gram-negative. The lower activity of these compounds against Gram-negative bacteria is due to the complex composition of the cell wall, which is not permeable for such hydrophobic molecules or their complexes (Guyot et al., 1993). It has been reported that polyether antibiotics like monensin and salinomycin have strong bactericidal activity against MRSA (methicillin resistant *Staphylococcus aureus*) and VRE (Vancomycin resistant *Enterococci*) that are highly antibiotic resistant Gram-positive bacterial strains causing serious blood, bone and joint infections (Huczyński et al., 2008; Huczyński et al., 2012a). Recently, it has been shown that polyether antibiotics like monensin have high inhibitory activity against *Mycobacterium tuberculosis*, the causative agent of highly contagious and severe disease like tuberculosis (Mimouni et al., 2014).

Overall, in comparison with their activity against bacteria, polyether antibiotics exhibit lower antifungal activity (Westley 1982; Funayama et al., 1992). However, among these polyether antibiotics monensin and lasalocid acid showed optimum inhibitory activity against non-filamentous fungi like *Candida albicans* by induction of chitin accumulation and inhibition of germination (Poli et al., 1986). Similarly, both compounds had the same inhibitory activity against filamentous fungi like *Fusarium oxysporum* and *Fusarium solani*, that can cause serious plant infections in different plant families (Podila et al., 1995; Mimouni et al., 2014).

Initially, the polyether antibiotics came to familiarity because of their high anti-parasitic activity; however, later on among them monensin, salinomycin and lasalocid acid were found to be the highest active compounds against a number of parasites. Among parasitic diseases, coccidiosis is one of the most dangerous disease regarding breeding in poultry, cattle and rabbits that is caused by protozoa known as *Coccidia* (*Eimeria* genus), and polyether antibiotics exhibit an effective activity against these protozoal species (Westley, 1977). Therefore, the first approved application of these polyether antibiotics were their usage for the prophylactic and therapeutic purpose in poultry (Conway et al., 1993; Cerruti et al., 1996) and growth promoter (Munir et al., 1994 and 2007).

Polyether antibiotics exhibit potent activity against both RNA and DNA viruses that can infect human and bovine. Regarding human health among these, the most dangerous one is human Immunodeficiency virus (HIV), which targets the human immune system. Polyether antibiotics have been reported for their different mechanism of actions against HIV inhibiting the virus at both pre and post-absorption stages of its life cycle (Dewar et al., 1989; Nakamura et al., 1992).

1.4.2. Anticancer activity

Polyether antibiotics are numerously reported for their anticancer activity against a number of cancer cells. Among this class of antibiotics initially monensin was reported for its anti-proliferative activity against human lymphoma, colon (SNU-C1) and myeloma cell lines (NCI-H929). This activity was actually due to the induction of cell cycle arrest in G1 and M phase along with loss of transmembrane potential in mitochondria that resulted in apoptosis (Park et al., 2002; 2003 a and b). In another study, monensin was reported for its potent anti-proliferative activity against prostate cancer. Here in this case, it triggered apoptosis by increasing oxidative stress along with reduction of mRNA especially androgen receptors (Ketola et al., 2010). Furthermore, this antibiotic is well known for its synergistic action along with other compounds against cancer cells. In a study, it was demonstrated that the cytotoxic activity of immunotoxin SWA11 ricin A-chain was increased 100 folds by monensin against clonogenic tumor cells where it amplified the inhibition of protein synthesis two times (Colombatti et al., 1990; Derbyshire et al., 1992). Additionally, its anti-proliferative activity was also observed against KB parent (Derivative of HeLa cell line) and KB/MDR (KB with multidrug resistance) cells alone as well as in combination with doxorubicin where it reduced the efflux of doxorubicin. It has been reported that, in the presence of monensin, the IC₅₀ value of doxorubicin is reduced 5 fold because of an increment in the intracellular concentration of doxorubicin three times in KB/MDR cells (Ling et al., 1993; Wood et al., 1996). Beside this, due to its hydrophobic nature, monensin was used in the form of liposomes in combination with specific immunotoxins for *in vitro* studies against human malignant mesothelioma (H-MESO-1), colorectal carcinoma (LS174T) and glioblastoma (MG-1, U87 and U373) cell lines as well as *in vivo* studies in mice. It was observed that compared to immunotoxin with monensin in buffer, the effectiveness of immunotoxin (ricin-A chain) with liposomal

monensin increased up to 5 fold against H-MESO-1 cell line, 1000 times against U373 cell line and 2200 times against U87 cell line (Griffin et al., 1993).

In 2013, another antibiotic from this class, lasalocid acid was reported for its anticancer activity. This compound was tested against different type of cancer cells like human colon adenocarcinoma (HT-29), human lung microvascular endothelial (HLMEC), human breast adenocarcinoma (MCF-7), human lung adenocarcinoma cell (A-549), murine leukemia (P-388) and murine embryonic fibroblast cell lines (BALB/3T3). It was observed that in some cases this compound had higher cytotoxic activity against cancer cells, and lower activity against normal cell lines compared to cisplatin, a cytostatic drug generally used in chemotherapy. The potent anti-carcinogenic activity of lasalocid acid was demonstrated by the fact that its cytotoxic activity was three fold higher than cisplatin against HT-29, A-549 and HLMEC cell lines (Huczyński et al., 2013 a and b).

Scientists' attention was caught by another polyether antibiotic salinomycin in 2009, when a study revealed that this antibiotic was 100 fold more effective against breast cancer stem cells (CSCs) compared to the generally used cytostatic drug Taxol (Paclitaxel) (Gupta, et al., 2009). These results were supported by another study where it was shown that salinomycin specifically triggered apoptosis in leukemic cells with no side effects towards normal cells (Naujokar et al., 2010). Also, this antibiotic induced apoptosis in MDR leukemic CSCs having high expression of ATP binding cassette (ABC) transporter (Fuchs et al., 2010). In another study, salinomycin showed induction of apoptosis by inhibition of Wnt signalling pathway in chronic lymphocytic leukaemia (Lu et al., 2011). Additionally, this compound has been reported for the induction of caspase 3/7 associated apoptosis, inhibition of metastasis and invasion in human lung cancer cell lines like A-549 and LNM35 (Wang, 2011). Regarding human colon cancer cell lines, salinomycin displayed a remarkable cytotoxic activity compared to the commonly used cytostatic drug oxaliplatin for colon cancer treatment (Dong et al., 2011). In chemo-resistant prostate cancer cell lines (LNCaP, PC-3 and DU-145), this antibiotic caused accumulation of reactive oxygen species (ROS) that resulted in mitochondrial depolarization, cytochrome c release and subsequently apoptosis by activation of caspase 3 (Kim et al., 2011a). Moreover, salinomycin was reported for its activity against resistant CSCs to cisplatin, Taxol (Paclitaxel) and 5-fluorouracil (Kim, et al., 2011b). This antibiotic was also reported for its synergistic effect in combination with gemcitabine against human pancreatic cancer cells (Zhang et al., 2011). In another

study, salinomycin led to the accumulation of ROS, inhibition of Akt and NF- κ B signalling, triggering apoptosis in cisplatin resistant ovarian and colon cancers (Zhou et al., 2013; Parajuli et al., 2013).

Another group investigated the effects of salinomycin, and showed that human breast cancer cell lines, namely T47D, MCF-7 and MDA-MB-231, were susceptible to this antibiotic due to the increment of p21 expression and hyperacetylation of H3 and H4 (Al. Dhaheri et al., 2013). This antibiotic was also reported for its cytotoxic effects against various cancer cell lines by the induction of autophagy and ER stress. (Li et al., 2013).

1.5. Autophagy

Autophagy is the conserved intracellular self-eating process and degradation system in eukaryotes (Mizushima et al., 2011). Conventionally it is long been known as a protein degradation pathway particularly during cellular stress or starvation. In parallel, inside the cell, ubiquitin proteasome system (UPS), the most common degradation pathway responsible for selective degradation of short lived proteins, is known, However, in contrast with UPS, the autophagy is a bulk process having the capability of degrading long lived proteins and even whole organelles like mitochondria, endoplasmic reticulum, nucleus, ribosomes and peroxisomes (Mizushima and Klionsky, 2007; Stolz et al., 2014). Under normal physiological condition, both of these mechanisms are crucial for protein homeostasis and quality control inside the cell and that's why basal autophagy is considered as a housekeeping pathway required for the degradation of dysfunctional protein complexes or organelles. However, during cellular stress or nutrient starvation, autophagy has a leading role in the sustenance of cells. Evidence indicate that autophagy boosts the recycling and salvage of cellular nutrients and thereby enhancing the cell survival during cellular stress or nutrient starvation (Kuma et al., 2004; Hara et al., 2006).

Autophagy is a collection of extensive regulatory catabolic processes in which all the targeted cytoplasmic contents are eventually delivered to lysosome for degradation. That is why it is broadly classified in three groups: macroautophagy, microautophagy and chaperone-mediated autophagy (CMA). Macroautophagy refers to the major class: a double membrane vesicle (autophagosome) surrounds all the targeted cytoplasmic components, and upon delivery to lysosome, they are fused to degrade

these cargos by the help of lysosomal hydrolytic enzymes (Mizushima and Komatsu, 2011). Microautophagy is the intussusception of lysosomal or endosomal membrane that directly engulfs the cytoplasmic contents followed by degradation (Li et al., 2012). Chaperone mediated autophagy is a distinct type characterized by a specific pentapeptide (KFERQ) sequence in the target proteins recognised by cytosolic heat shock cognate 70 kDa protein (HSC70). This complex is translocated to lysosomal lumen by the help of lysosomal associated membrane protein 2A (LAMP2A) receptor followed by degradation of target proteins (Cuervo and Wong, 2014).

Autophagy is responsible for both housekeeping and disorders in the cells due to its dual role in the cellular metabolism and homeostasis (Figure 1.4). Under normal physiological condition, it is required for its housekeeping role in post-mitotic tissues like nerves and muscles, where it is responsible for the turnover of aggregated proteins and prevent the cells from the toxic effects of these aggregates. That is why loss of autophagy in these cells lead to the aggregation of protein complexes conjugated with ubiquitin and inclusion bodies results in neurodegeneration and cardiac hypertrophy (Nakai et al., 2007; Masiero et al., 2009). On other hand, during cellular stress (Oxidative damage, ER stress or genetic mutations), the activation of autophagy lead to the infliction of proteins or organelles damage in order to cope with given challenge for the assurance of cellular survival in that particular circumstances, i.e. nutrient deprivation, infection, hypoxia or growth factor withdrawal (Murrow and Debnath, 2013).

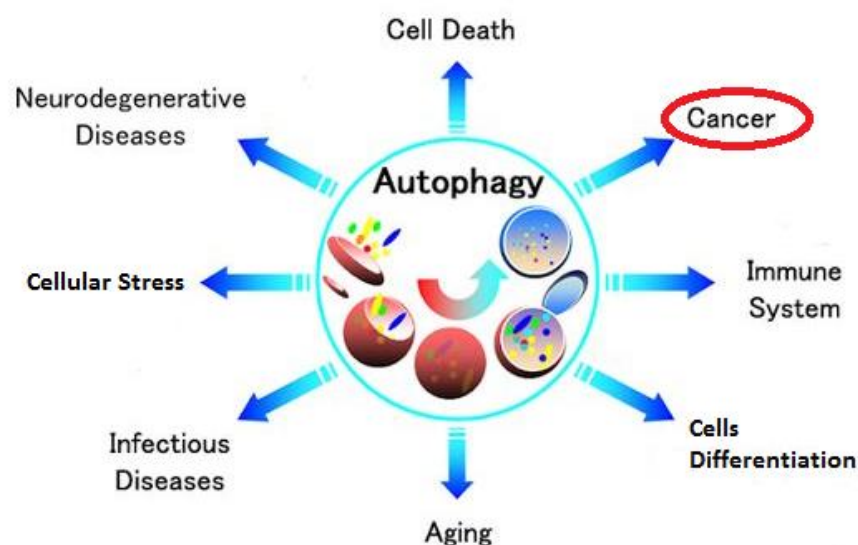


Figure 1.4 Role of autophagy in the cell
(Source: Guo and White, 2016)

Indeed, protein degradation and turnover is the silent feature of autophagy but it has been revealed that in parallel it has an equal contribution for cellular differentiation, aging and turnover of other nutrient stores like carbohydrates, lipids and minerals. Thus, a growing interest towards the role of autophagy in regulation of cellular metabolism in both normal and diseased cells has been arisen. In this track, scientists are trying to elucidate how autophagy modulation influences metabolic disorders and adaptations such as cancer (Kaur and Debnath, 2015).

1.6. Autophagy Signalling Pathway

The process of autophagy is executed by variety of molecular machineries consisting of distinct steps like induction, autophagosome formation, cargo recognition and selection, autophagosome-lysosome fusion and degradation of cargo followed by release of degraded components to cytosol. In each of these steps along with other essential components, different sets of autophagy related proteins (Atg) consist the core molecular machinery for the execution of this proces. (He and Klionsky, 2009).

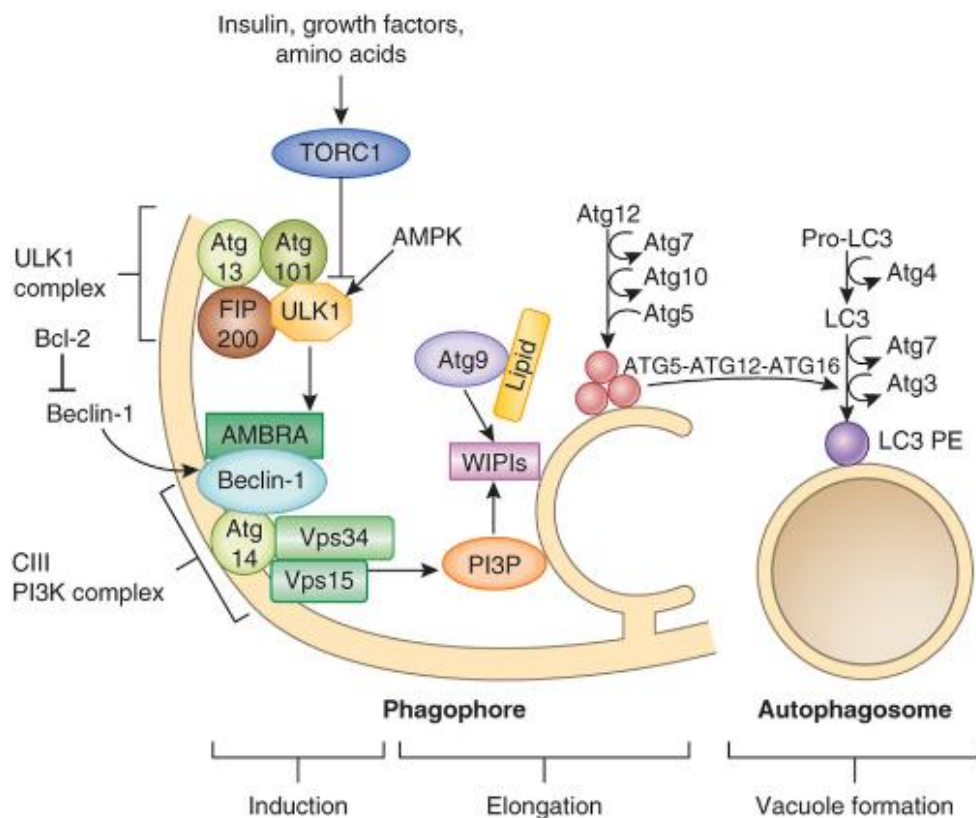


Figure 1.5 Autophagy induction and autophagosome biogenesis
(Source: Nixon, 2013)

1.6.1. Induction of autophagy

Inside the cells under normal physiological condition, basal autophagy is lower; however, in order to cope with certain type of stresses the cell need an efficient autophagy induction mechanism. In this track, a central regulator of autophagy is the serine/threonine protein kinase TOR (target of rapamycin). During normal circumstances and nutrient rich condition, the mTORC1 complex downregulates autophagy by inhibiting another serine/threonine protein kinase (Atg1-yeast homologs) ULK 1/2 (Unc-51 like kinase) (Figure 1.5) (Kamada et al., 2000; Scott et al., 2007; Chang et al., 2009). However, during cellular stress or starvation, the low energy signals (\uparrow AMP/ATP) activate a signalling protein LKB1 that transmits the signal to AMP kinase (Adenosine monophosphate kinase). The activation of AMPK lead to the inhibition of mTORC1 by the activation of Tuberous sclerosis (TSC1/2) (He and Klionsky, 2009). Inhibition of mTORC1 and activation of AMPK resume the kinase activity of ULK1/2 by its auto-phosphorylation and conformational changes, which increase its tendency for the downstream phosphorylation towards its interacting proteins FIP200 (focal adhesion kinase family-interacting protein of 200 kDa) and mammalian Atg13 (Kamada et al., 2000; Hara et al., 2008; Kawamata et al., 2008; Chan, 2009). Interestingly, this ULK1/2 is downregulated by mTORC1 and upregulated by AMPK with phosphorylation at different residues (Kim et al., 2011c; Egan et al., 2011). ULK1 is downregulated by mTORC1 by phosphorylation of serine 757 and 637 (Kim et al., 2011c; Shang et al., 2011; Wong et al., 2015) while, during nutrient starvation, a protein phosphatase 2A (PP2A) dephosphorylate the ULK1 sites especially S637 and allow the ULK1 for interaction with AMPK (Wong et al., 2015). The upregulation of ULK1 by AMPK is the consequence of more complex modification including phosphorylation of ULK1 on at least seven different serine/threonine residues predominantly on Serine 555 (Kim et al., 2011c; Lee et al., 2010a).

It has been reported for mammalian cells that, despite of nutritional condition, these three proteins (ULKs-FIP200-Atg13) form a stable complex that is downregulated by mTORC1 and upregulated by activated ULKs with phosphorylation on different residue on Atg13 (Hosokawa et al., 2009; Jung et al., 2009). These proteins form the initial upstream scaffold, which is further stabilized by the recruitment of Atg101 before localization to membrane initiation site (Mercer et al., 2009).

1.6.2. Early membrane Initiation

Membrane initiation is still the most arguable step of autophagic pathway; however, there are three most commonly accepted mechanisms by which membrane biogenesis may be initiated: 1) Maturation model: The pre-existing cytoplasmic organelles are acting like a platform where the membrane can be predominantly derived from them such as endoplasmic reticulum; 2) Assembly model: The membrane can be primarily derived from different membrane sources; 3) Combination of these both models (Bento et al., 2016). According to the analysis of electron tomography, along with endoplasmic reticulum other organelles like mitochondria, Golgi apparatus, plasma membrane and endosomes made significant contribution in the biogenesis of autophagosome (Biazik, et al., 2015). In preliminary studies, it was reported that the pre-existing membrane, also known as isolation membrane, could be the source of autophagosome initiation because it was formed even during protein inhibition in the cell (Hwang et al., 1974; Ishikawa et al., 1983). However, recently by using electron tomography, it has been revealed that these isolation membranes are being interconnected with ER and being cradled from the subdomain of ER (Hayashi et al., 2009). These results are also supported by the localization of lipids responsible for autophagosome formation, namely phosphatidylinositol 3-phosphate (PI3-P), on this subdomain by using PI3-P binding protein DFCP1 (Axe et al., 2008). Therefore, these results suggest the close relationship between autophagosome initiation and ER; yet to be identified unambiguously.

Additionally, the outer membrane of mitochondria was reported to participate this membrane initiation in the starved cells on the basis of the localization of Atg-5 and LC3 on the punctae of mitochondria (Hailey et al., 2010). Other studies revealed that, in mammalian cells, the contact sites of ER and mitochondria was responsible for the formation of autophagosome. It is being supported by the localization of phagophore markers Atg-5 and Atg-14 on this sites during starvation. Along with this, contact disruption between ER and mitochondria showed dramatically fall in starvation induced autophagy, suggesting that the contribution of these sites in the initiation of the membrane (Hamasaki et al., 2013).

Another study reported the rapid incorporation of plasma membrane during phagophore and autophagosome formation by employing plasma membrane lipid labelling under live cell microscopy (Ravikumar et al., 2010). More recently, it has been

investigated that, ER-Golgi intermediate compartments (ERGIC) buds LC3 lipidation active vesicles during starvation, which may provide a potential source for such membrane initiation (Ge et al., 2013; Ge and Schekman, 2014). Conclusively, the process of membrane initiation towards autophagosome formation is still poorly understood. However, in simplistic way, it is thought that during autophagy, the early membrane is initiated on pre-existing platform (isolation membrane), which is then receiving membrane from other cellular compartments during elongation from phagophore towards autophagosome development (Bento et al., 2016).

1.6.3. Autophagosome formation

Once the activated ULK1 complex localized to the membrane initiation site, it further interact with downstream signalling molecules in a variety of ways in order to induce autophagy. Among these downstream molecules, one of the crucial complexes is Beclin 1-Atg14L-VPS34 complex, phosphorylation of which will lead to the induction of autophagy (Hara et al., 2008; and Chan et al., 2009). During starvation, initially the activated ULK1 complex activate Beclin 1 by phosphorylation on serine 14 (Russell et al., 2013). This interaction and phosphorylation occur at the autophagosome assembly site that is facilitated by Atg-14L making a bridge between ULK1 complex and Beclin 1. In fact, the Atg-13 present in ULK1 complex primarily interact with Atg-14L making it susceptible to phosphorylation on S29 by ULK1 to form a bridge between ULK1 and Beclin 1. These phosphorylations are crucial for the full activation of VPS34 to produce PI3P (Gallagher et al., 2016). VPS34 (PI3K catalytic subunit 3) along with VPS15 (PI3K regulatory subunit 4), Beclin 1 form a part of class III PI3K complex 1 with Atg-14L, and complex 2 with UVRAG (UV radiation resistance associated). This class III PI3K complex is responsible for the production of PI-3P at the site of phagophore initiation (Fig-1.5) (Bento et al., 2016).

These PI-3Ps forming a cluster where its cytosolic surface act like a platform for the recruitment of further required machineries, which consequently influence on the geometry of membrane in terms of membrane tethering, fusion or bending. Eventually, the membrane favours the bending into positive curvature, and that may form the phagophore sculpting. Along with this, the naive PI-3P at phagophore initiation site allow the recruitment of PI-3P binding proteins of the WIPI family, which consequently lead to the autophagosome formation and elongation (Fig-1.5). Among WIPI family

proteins, the WIPI2 recruits Atg-16L1 in a form of complex with other binding partners (Atg5-Atg-12) to the fledgling phagophore in order to extend it further (Dooley et al., 2014). During this extension process, primarily two ubiquitin like conjugation reactions take place. In initial reaction, ubiquitin like protein Atg-12 bind to its substrates like ubiquitin through the carboxylic acid group of glycine at C-terminal. Then, Atg-7, an enzyme like E1, activates the terminal glycine of Atg-12 that is consequently transferred to an intermediate E2 like enzyme Atg-10, and eventually conjugated with Atg-5 (Mizushima et al., 1998). After this, the Atg5-12 conjugate form a supramolecular complex with Atg-16L1, location of which helps in defining the sites of autophagosome formation, and act like E3 enzyme (ubiquitin ligase) for the conjugation reaction of other ubiquitin like proteins (Atg-8 family) with lipids like phosphatidylethanolamine (PE) (Sakoh et al., 2013).

During the second ubiquitin like conjugation reaction, the LC3 (microtubule-associated protein 1 light chain 3), mammalian homologs of Atg-8 containing the terminal arginine residues, are cleaved by Atg-4 cysteine protease leaving glycine on carboxylic terminal (Kirisako et al., 1999). In a similar fashion, Atg-7 activates this terminal glycine also, which is first transferred to an intermediate E2 like enzyme Atg-3, and later on in the presence of E3 like enzyme conjugate (Atg-12-5-16L1) execute the conjugation reaction between LC3 and PE. The resulting naive conjugate is known as LC3-II having the ability of tight binding to the surface of developing autophagosome membrane and make it matured. Along with LC3s, there are other homologs of Atg-8 in human known as GABARAPs and GATE-16, each of these have its distinct contribution during the extension and closure of phagophore edges (Weidberg et al., 2010).

Besides, during this extension process, Atg-9 a multi-membrane spanning protein is postulated for its membrane carrying function due to its interaction with Atg-16L1 leading to both homotypic and heterotypic membrane fusion in different types of SNAREs dependent manner (Orsi et al., 2012; Popovic and Dikic, 2014). Alternatively, the recycling endosomes containing Atg-9 interact with vesicles having Atg-16L1 leading to their fusion in a SNAREs dependent way enabling subsequent phagophore extension (Puri et al., 2013).

Finally, the closure process of autophagosomes are poorly known; however, protein like Atg-2A and Atg-2B are reported for its regulation. It has been shown that Atg-2A targets towards the enrich region of PI-3P at the naïve phagophore formation

site and associate with WIPI1 proteins during starvation (Pfisterer et al., 2014). Overall, despite of poor understanding, these proteins are crucial for the closure of autophagosome because its knockdown leads to the accumulation of opened autophagosomes (Velikkakath et al., 2012).

1.6.4. Cargo recognition and selection

Conventionally it is known that autophagy is the bulk degradation of cytoplasmic contents including organelles that is why based on the type of cargo and contents targeted by autophagy, further classification has been established: Aggrephagy (degradation of aggregated proteins or other metabolites), reticulophagy (Endoplasmic reticulum), mitophagy (mitochondria), ribophagy (ribosomes), pexophagy (peroxisome) and xenophagy (pathogens). The recognition and selection mechanism is varying in each type of autophagy depending on the contents of cargo (Stolz, et al. 2014). During autophagy, this selectivity is achieved by the use of specific autophagy receptors. These receptors particularly recognise the specifically tagged cargos with degradation signals, and facilitate their binding by interaction with their LIR domain (LC3-Interacting region) to the LC3-II located in the developing phagophore (Figure 1.6) (Slobodkin and Elazar, 2013). In mammalian cells, the most predominant degradation signal is the conjugation of ubiquitin to the particular cytoplasmic content (Kirkin et al., 2009a). Thus, majority of the known autophagy receptors up to now harbour both LIR and ubiquitin binding domains (UBA) (Wild et al., 2014).

However, exceptionally during erythrocyte differentiation or hypoxia, there are some autophagy receptors like NIX, BNIP3 and FUNDC1 lacking UBA domain, which are directly attached to the surface of mitochondria in ubiquitin independent manner and bind them to the LC3 by LIR (Liu et al., 2012). Also, it has been reported that NIX and BNIP3 promotes mitochondrial depolarization where only NIX can trigger translocation of E3 ligase Parkin (PTEN-induced putative kinase protein 1) to the mitochondrial surface leading to polyubiquitination and subsequently Ub-p62 mediated mitophagy (Sandoval et al., 2008; Ding et al., 2010).

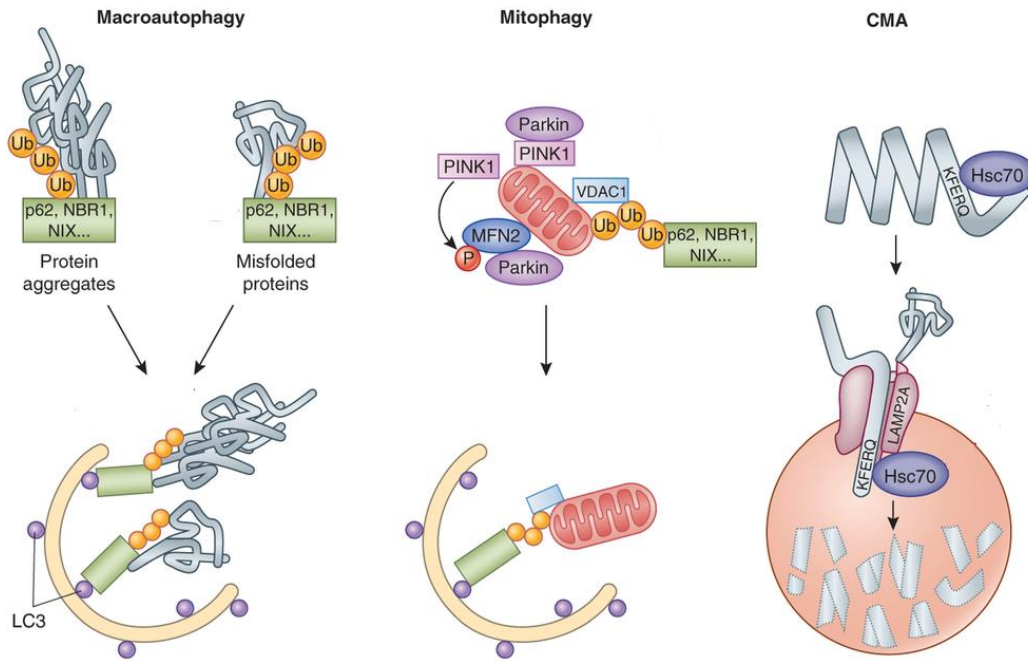


Figure 1.6 Substrate recognition and selective autophagy
(Source: Nixon, 2013)

In mammalian cells, the most predominant autophagic receptor p62 binds to the ubiquitin-tagged cargos by the help of its UBA domain; however, as selective autophagy receptors, it lacks prominent specialization that is why different receptors cooperate with each other during selection of cargos. For example, during p62-dependent selection and sequestration of aggregated proteins, peroxisomes and mid body rings, another autophagy receptor NBR1 cooperates with p62 and plays an essential role during this process (Kirkin et al., 2009b; Deosaran et al., 2013). In another case, during the sequestration of invading bacteria (xenophagy), p62 takes the assistance of other autophagy receptors like OPTN and NDP52 for the successful elimination of given bacteria (Mostowy et al., 2011; Thurston et al., 2012). Each of these proteins has its own crucial role during xenophagy and even it is also reported that the autophagy receptor NDP52 can not only recognize and bind to the bacteria through ubiquitination but also with cytosolic lectin galectin-8 (Cemna et al., 2011; Thurston et al., 2012).

Beside this, one of the most intriguing features of these autophagy receptors is their tendency towards oligomerization and clustering making the cargos more susceptible for sequestration. These cargos become more tangled and form inclusion bodies like structures known as sequestosomes allowing its degradation more conveniently by autophagy (Narendra et al., 2010; Itakura et al., 2011). Regarding the regulation of these autophagy receptors at the post-translational level, it has been reported that

phosphorylation of LIR domain in case of BNIP3 triggers its affinity towards its target LC3s (Zhu et al., 2013). Similarly, specific phosphorylation of p62 and OPTN leads to an increase propensity towards Ub chains and LC3s (Wild et al., 2011; Rogov et al., 2013).

1.6.5. Autophagosome and lysosome fusion

At the terminal stage of autophagy, mature autophagosome become fused with lysosome making an autolysosome to degrade the given cargo by hydrolytic enzymes. This maturation step is quite critical but poorly known; however, it is reported in yeasts that loss of Atg-8 family proteins from the outer surface of autophagosome is a fully maturation signal allowing the attachment of fusion factors (Nair et al., 2012; Yu et al., 2012). In mammalian cells, it is unknown whether the loss of these Atg-8 family protein is required for autophagosome maturation or not. However, the loss of other phagophore initiator complexes such as ULK1 complex and Atg-16L1 absence were observed at the mature autophagosome, suggesting that their loss was compulsory before fusion with lysosome (Bento et al., 2016).

The role of cytoskeleton during autophagosome movement towards lysosome have an equal significance like other cellular trafficking pathways (Figure 1.7). Inside the cells, predominantly the autophagosomes and lysosomes are found in the perinuclear region. Loss of molecular motors like dynein or kinesin impair this fusion process meaning that the autophagosomes are moving toward the lysosomes by the cooperative efforts of these molecular motors on microtubules (Ravikumar et al., 2005; Fass et al., 2006; Jahreiss et al., 2008). Another study investigated the role of histone deacetylase 6 (HDAC6) during this fusion process via actin filaments by myosin motor proteins. It was observed that a protein, namely cortactin, was recruited by HDAC6, which was required for the actin polymerization to the autophagosome. However, loss of these proteins resulted in the blockage of this fusion process, indicating the importance of this protein for the process. Interestingly, this loss was only limited to the fusion of aggrephagy not to starvation induced autophagy, suggesting that the itinerary of the autophagosome was dependent on the type of cargo contained (Lee et al., 2010b; Tumbarello et al., 2012).

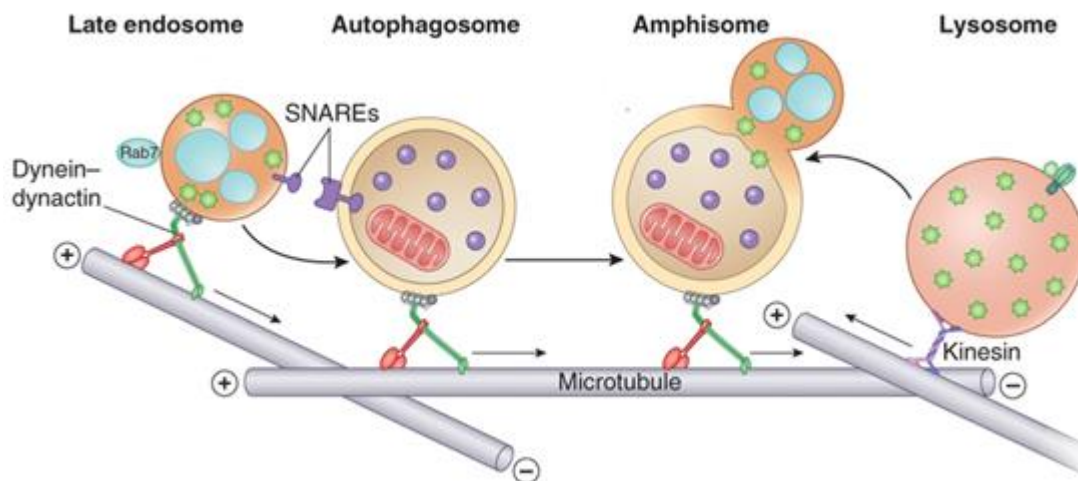


Figure 1.7 Autophagosome and lysosomal fusion
(Source: Nixon, 2013)

As current understanding about the molecular machineries involved in autophagosome-lysosome fusion is relied on general mechanism of intracellular membrane trafficking that primarily depends on three types of protein families. Membrane tethering complexes, Rab GTPases and SNARE proteins (Bento et al., 2016). Among them, Rab7 have multiple roles in this process; however, initially it is localized to the surface of mature autophagosome/endosome, and by the help of its effector protein RILP (Rab interacting lysosomal protein), it recruits dynein to the surface of autophagosome (Jordens et al., 2001). In this regard, lipid signalling has a crucial role in Rab activation and fusion process. The VPS34-UVRAG complex, which is responsible for PI-3P production, have a direct role in the maturation of autophagosome. The UVRAG initially stimulate VPS34 to bind with a subunit of HOPS complex (VPS16). This interaction leads to recruitment of HOPS complex to the surface of autophagosome that subsequently activate Rab7 by its guanine exchange factor subunit (VPS39) (Liang et al., 2008; Poteryaey et al., 2010). This HOPS complex is a multi-subunit complex that acts as a membrane tethering factor responsible for the bridging between the two opposing membrane and stimulation of SNARE complex during fusion (Brocker et al., 2010). Additionally, there are some adaptor proteins reported like PLEKHM1 that directly interacts with HOPS complex as well as autophagosome by its LIR domain, during this fusion process (McEwan et al., 2015). Moreover, HOPS complex and other proteins like TECPR1 (tectonin β -propeller repeat containing protein 1) have been reported for their membrane tethering ability where they bind to PI-3P in a Atg5-12 dependent manner to the mature autophagosome.

Recently, their roles have been investigated revealing that the loss of these proteins leads to accumulation of autophagosomes, implying their importance during autophagosome-lysosome fusion (Chen et al., 2012; Kim et al., 2015).

Finally, during fusion process of autophagosomes-lysosomes, membrane anchored proteins SNAREs have a crucial role. A trans SNARE complex establishes between the R-SNARE of donor membrane (VAMP7 and VAMP8) and Q-SNARE of acceptor membrane (syntaxin 7, syntaxin 8, and Vti1b) during this fusion process (Pryor et al., 2004). Another study revealed that, among SNAREs, the Q-SNARE syntaxin 17 is vital for this fusion process especially in autophagy because its loss led to the accumulation of autophagosomes. This study also demonstrated interaction of this SNARE protein with other proteins, namely Q-SNARE SNAP-29 and R-SNARE VAMP8 (Itakura et al., 2012). Recently, a novel role of Atg-14L has been reported in this regard, which directly bind to syntaxin 17-SNAP29 binary complex on autophagosomal surface making it prominent for VAMP8 interaction, promoting the fusion between autophagosome and lysosome (Diao et al., 2015).

1.7. Role of Autophagy in Cancer

The most significant and primary role of autophagy in the cell is homeostasis in terms of protein and organelles quality control. That is why a low level of basal autophagy is necessary under normal physiological condition to protect the cells from the toxic effects of these damaged contents (Mizushima and Komatsu, 2011). Deregulation of autophagy in autophagy modulated cells/tissues is the most common track for the identification of autophagy associated genes, biological role, target substrates and cell specificity (White, 2015). Some tissues such as brain, liver and muscles are primarily dependent on autophagy for the elimination of defective organelles and protein aggregates along with autophagy substrates like p62/SQSTM1 and ubiquitin (Mizushima and Komatsu, 2011). However, due to impaired autophagy, the accumulation of defective mitochondria leads the cell to oxidative stress (Rabinowitz and White, 2010). Along with this, autophagy also decreases the ER stress; however, its deregulation leads to accumulation of chaperons due to unfolded protein burden on the cell (Hoyer-Hansen and Jaattela, 2007; Mathew et al., 2009). Autophagy is also one of the crucial driving track for the sustenance of cells during cellular stresses as it modulates the metabolic processes in the cells for the provision of required

nutrients to the cell under such circumstances (Guo et al., 2013a; White, 2013). Additionally, the role of autophagy is observed in the pathogenicity of many diseases like liver, heart and neurodegenerative diseases (Levine and Kroemer, 2008). However, its contribution in the case of cancer is quite intriguing because it may promote or inhibit cellular proliferation in cancer cells suggesting that its role may be tumor suppressor or promoter in a context dependent manner (White, 2012).

1.7.1. Autophagy as tumor suppressor

Earlier, it was believed that autophagy involved in the tumor suppression because, in 40% to 75% prostate, breast and ovarian cancers, the primary autophagy responsible genes (ATG6/BECN1) were lost (Aita, et al., 1999; Liang et al., 1999). These finding was further supported by *in-vivo* studies of mice where the *Becn1* heterozygous mutant mouse were observed more prone to the development of lymphoma mass, liver, lung tumors suggesting that suppression of autophagy leads to promotion of cancer (Qu et al., 2003; Yue et al., 2003). However, in contrast, only benign liver tumor was observed in the mice upon the deletion of basic autophagy responsible genes (*Atg5/Atg7*) in liver cells. This study revealed the significance of autophagy during suppression of liver tumor but in parallel it also dictated its role during progression from benign to malignant tumor. This contradictory finding made the scenario more complex regarding the role of autophagy in cancer along with role of BECN1 in autophagy (Takamura et al., 2011). The tumor suppression role of BECN1 was supported by its adjacent location with other known tumor suppressor genes like BRCA1 in breast and ovarian cancer (Laddha et al., 2014). However, beyond expectations the allelic loss of *Becn1* in a genetically engineered mouse model (GEMMs) for breast cancer reduced tumorigenesis by triggering p53 activation (Huo et al., 2013). This study confirmed that BECN1 was not a tumor suppressor, which was further supported by number of studies where consistently loss of BRCA1 was observed in breast cancer but not BECN1 (Laddha et al., 2014). However, in poor characterized cancers at genomic level like hepatomas, mutations in autophagy responsible genes and their deficiencies are responsible for the promotion of cancer (White, 2015).

Another investigation revealed that oxidative stress was developed in the absence of autophagy leading to genomic instability by activation of DNA damage response, establishing the well-known signs of cancer initiation and progression

(Karantza et al., 2007; Mathew et al., 2007; Mathew et al., 2009). In parallel, it was also observed that the key regulator of antioxidant defence erythroid 2 like 2 (NRF2) activation took place due to the developed oxidative stress, which consequently triggered the tumor growth (Strohecker et al., 2013). Along with this, in hepatocellular carcinoma, the loss of autophagy increased the toxicity inside the cells leading to the known drivers of liver cancer like chronic cell death and inflammation of hepatocytes (Sun and Karin, 2013).

1.7.2. Autophagy as tumor promoter

Cancer cells are more dependent on autophagy than normal cells due to their altered microenvironment, increased metabolic and biosynthetic demand inflicted by their deregulated proliferation (White, 2015). It has been concluded from different studies that basal autophagy increases at the hypoxic tumor region making it essential for the tumor cell survival (Degenhardt et al., 2006). In RAS transformed cancer cells, primarily autophagy is upregulated being responsible for the tumorigenesis, tumor cell survival, growth, invasion and metastasis (Lock et al., 2014). RAS driven cancers are believed autophagy addicted due to its susceptibility to stress leading to defective mitochondrial function during autophagy deficiency (Guo et al., 2011 and 2013a). This concept has been further extended to other type of cancers like the growth of mammary cancer that is inhibited due to knock out of FIP200, the principal signalling component during autophagy initiation (Wei et al., 2011).

Further, it was found that loss of Atg7 in KRAS driven tumor cells decreased tumor burden by accumulation of defective mitochondria, premature induction of p53, proliferation arrest and cellular death (Guo et al., 2013a). In fact, this loss of Atg7 alter the fate of tumor from adenoma and carcinoma to rare benign neoplasms oncocytoma, characterised by accumulation of damaged mitochondria (Gasperee et al., 2011). Thus, Atg7 deficient mice with KRAS driving cancer have no life expectancy and die earlier despite of reduced tumor burden and promotion of benign tumor instead of malignant. Besides, due to autophagy defects, the upregulation of p53 arrest the growth of tumor cells and lead them to death (Guo et al., 2013a). However, concurrent deletion of p53 and Atg7 leads to the extension of mouse's life because of reduction in tumor burden, suggesting that p53 is primarily upregulated upon autophagy deficiency arresting the tumor growth (Guo et al., 2013b). In another study, it was demonstrated that Atg7 and

p53 deficiency in RAS driven tumor cells resulted in loss of lipid catabolism, increased glutamine dependency, and the cells did not survive during starvation. These results imply that autophagy is responsible to maintain the proper mitochondrial function for lipid catabolism and to provide the required contents back to the cells after degradation of cargos that can facilitate the tumor cell survival during normal and starvation conditions (Guo et al., 2013a; White, 2015). These results are not only limited to Atg7 deletion in such tumor cells, in a similar fashion, deletion of Atg5 instead of Atg7 provides the same consequences. Hence, it is clear that overall autophagy is primarily required for the tumor promotion (Rao et al., 2014).

Similarly, in RAS driven pancreatic tumor cells, autophagy promotes the tumor growth by suppressing p53 induction. However, here concurrent loss of autophagy and p53 improve the tumor defects suggesting specific cancer cell type dependency on autophagy. Based on these studies, it might be concluded that loss of p53 increases glycolysis and decreases oxidative metabolism in cancer cells, where autophagy alternatively relieves their survival (Rosenfeldt et al., 2013). Moreover, Atg7 loss in a mouse model with BRAF induced lung cancer gave the same results; activation of p53 and proliferative defects indicated the contribution of autophagy in tumor cell survival rather than cause of tumor (Strohecker et al., 2013). In another study, it was shown that human BRAF driven melanomas had more basal autophagy, that was the reason for their more sensitivity to autophagic modulation (Ma et al., 2011).

1.8. Influence of Anticancer Agents on Autophagy

Almost all the anticancer drugs and radiation therapy have effects on autophagy and most of the time induction of autophagy has been reported commonly (Levy and Thorburn, 2011). Among them, variety of results were obtained dependent on number of autophagosomes increasing or decreasing and fluctuation of autophagy flux. (Shen et al., 2011; Ganley et al., 2011). The real fact about the contribution of autophagy in cancer therapy is that all type of anticancer drugs like DNA damaging agents, microtubule targeting inhibitors, receptor agonist, hormonal agents or other signalling molecule inhibitors effects autophagy directly or indirectly. While up to now there is no anticancer agent having no effect on autophagy (Thorburn et al., 2014). For example, drugs like vinblastine inhibit microtubules which consequently lead to the inhibition of autophagosome and lysosome fusion due to unavailability of trafficking route (Köchler et

al., 2006). Another drugs like chloroquine (CQ) and hydroxychloroquine (HCQ) alter the pH of lysosome and lead to the inhibition of autophagy (Amaravadi et al., 2011).

Another type of drug like rapamycin or temsirolimus which target mTOR inhibition and up regulate autophagy from the upstream as mTOR is the negative regulator of autophagy. Beside this, some drugs like ABT737 or sulfonyl benzamide directly targeting autophagy machineries like Bcl-2 family proteins (Oltersdorf et al., 2005). Originally, these drugs were designed for the inhibition of anti-apoptotic protein Bcl-2 family protein for the induction of apoptosis however, in parallel this protein also regulate BECN1 complex which is considered the principal component of autophagy during initiation (Pattingre et al., 2005). Along with this, inhibition of epidermal growth factor receptor (EGFR) by inhibitor like erlotinib which directly regulate BECN1 complex in order to change its state for the induction of autophagy (Wei et al., 2013).

In case of all these anticancer drugs autophagy is inducing while beside these there are other anticancer drugs like DNA damaging agents which have influence on autophagy but their molecular mechanism is not clear up to now. That's why it is most important to come with clear understanding that how different anticancer agents can influence autophagy which will make us more specific during cancer therapy.

1.9. Effects of Autophagy on Cancer Therapy

Numerous studies have reported that the role of autophagy is protective regarding cancer therapy and mostly accepted the track of chemoresistance (Levy and Thorburn, 2011; Maycotte and Thorburn, 2011). Keeping in mind these, recently, clinical trials have been in progress where autophagy inhibitors are used in combination with anticancer agents however, it is not a blanket agreement (Thorburn, et al. 2014). Because this strategy is context dependent, and its efficiency vary relying on the cancer type. During the treatment of lung cancer (EGFR mutant) with EGFR inhibitor erlotinib, autophagy is required for the maximum efficiency of the drug. It exerts that autophagy is not a protective process, but it is required for the drug's antitumor effect in specific cancer type. In contrast to the common concept, here the inhibition of autophagy reduces the tumor cell death and enhanced the tumor growth despite of same therapy (Wei et al., 2013). These type of conflicting results really make this paradox more tangled because how the same process can protect or kill tumor cells?

Another example of this paradox is treatment of estrogen receptor positive breast cancer cells (MCF-7) with standard therapy by using tamoxifen (antiestrogen). Regarding this treatment, initially, it was reported that the drug killed MCF-7 cells by the help of autophagy (Bursch et al., 1996). However, later on, other studies revealed that MCF-7 was acquiring tamoxifen resistance by autophagy suggesting that autophagy was acting against the anticancer agent (Qadir et al., 2008; Samaddar et al., 2008; Cook et al., 2012). Besides, another group reported that, in MCF-7 cell line, a kinase HSPB8 was responsible to overcome tamoxifen resistance by induction of autophagy (Gonzalez-Malerva et al., 2011). These different studies on the same cell line with same antitumor agent concluded that general treatment of MCF-7 with tamoxifen increased autophagy leading to different outcomes. The possible explanation of such type of results is the occurrence of different strains from same type of cell or acquisition of resistance by different mechanism by the cells.

To cope with this paradox, recently, another group investigated effects of autophagy with different apoptosis inducing agents from the same class on the same cell line at the same time. In the given study, in response to known anticancer agents and death receptor agonists, tumor necrosis like apoptosis-inducing ligand (TRAIL) and Fas Ligand (FasL), autophagy was examined. Interestingly, in the same population of cells, apoptosis was induced efficiently by FasL at high autophagy level, while lowered by TRAIL. However, these results are limited to the cell type, as, by changing the tumor cell type, autophagy becomes responsible to inhibit the FasL induced apoptosis. The molecular explanation regarding these results in context dependent manner revealed that, selective degradation of negative regulator [protein phosphatase FAP1 (known as PTPN13)] of FasL induce apoptotic pathway by autophagy, which does not affect the TRAIL induced apoptosis (Gump et al., 2014). On the other hand, protecting role of autophagy is common during cancer therapy having quite less explanation like above. However, it might be possible that autophagy can specifically degrade some required proteins for apoptosis as cargo in order to execute its role. Regarding this, there are very little understanding why autophagy inhibition leads to the promotion of apoptosis (Yonekawa and Thorburn, 2013).

All these are cell autonomous responses where a tumor cell decides to die or survives against anticancer agent through autophagy. However, in parallel, there are non-autonomous responses to the given drugs during cancer treatment. In case of real tumor, each cell cannot behave autonomously, and in the microenvironment of tumor,

both tumor and normal cells have fundamental contribution on the behaviour of tumor as well as in response to cancer therapy (Thorburn et al., 2014). In this regard, a study showed that autophagy had a crucial role in communication of cells that are going to be die within the microenvironment of cancer. In tumor tissue, autophagy is regulated by release of signalling molecule HMGB1 from the dying cells (Thorburn et al., 2009). Extracellular HMGB1 have its own role in the regulation of autophagy by binding to its receptor RAGE and intracellular signalling, which is a track towards chemotherapy resistance by induction of autophagy (Tang et al., 2010 a, b; Liu et al., 2011b). This study suggests that in tumor tissue the presence or absence of autophagy in one cell significantly affects the behaviour and response of other tumor cell through autophagy, depending on release of HMGB1 (Thorburn et al., 2014).

Hence, in conclusion during cancer treatment, autophagy is responsible for protecting the tumor cells or required for the killing effects of anticancer agents in a context dependent manner. This bring us to the significance of studying these underlying mechanisms by which a specific anticancer agent particularly kills the given tumor cells. Along with this, investigation for effective biomarkers to identify different responses of the cells during modulation of autophagy is quite important for the improvement of cancer therapy.

1.10. Polyether Antibiotics Against Autophagy

Carboxylic polyether antibiotics are well known for their transportation or exchange of monovalent/divalent ions with H^+ ions across the biological membrane (Pressman, 1976). Initially, it has been reported that ionophores could inhibit the transport of membrane receptors towards plasma membrane from Golgi apparatus leading to the vesicle formation in Golgi region, and consequently dilation of Golgi apparatus (Tartakoff and Vassalli, 1977). However, further studies revealed that primary role of ionophores in eukaryotic cell was the loss of proton gradient due to its transmembrane exchange of ions in macrophages resulting an increase of pH in lysosomes and blockage of lysosomal degradation (Ohkuma and Poole, 1978). Among polyether antibiotics, monensin and nigericin are the most common antibiotics studied for their effects on autophagy. Initially, monensin was reported for accumulation of autophagic vacuoles inside the cell. In these cells, it was also observed by electron

microscopy that the average size of these vacuoles was two fold in comparison to the normal one consisting of 4-5 small vacuoles (Grinde, 1983).

Further studies confirmed that monensin led to the accumulation of autophagic vacuoles by inhibiting the terminal fusion stage of autophagy pathway, viz., autophagosome and lysosome fusion, and triggering apoptosis in HeLa cell line (Boya et al., 2005). Similarly, another study revealed that, polyether antibiotics monensin and nigericin both showed their inhibitory effects on autophagosome and lysosome fusion in MN9D neuronal cells causing the accumulation of autophagic vacuoles in the cytoplasm. In parallel, Western blotting analysis showed the accumulation of both autophagy flux markers LC3-II and p62 along with cleavage of caspase 3 upon the treatment of these polyether antibiotics (Lim et al., 2012).

Along with this, it was demonstrated that concurrent treatment of monensin with anticancer drugs like rapamycin (mTOR inhibitor) or erlotinib (epidermal growth factor receptor inhibitor) resulted in improved synergistic anticancer activity in lung cancer cell line NCI-H1299. It is well known that due to pro-survival role of autophagy, during cancer treatment, the cells manage to escape from death via autophagy, especially in case of rapamycin treatment that inhibits mTOR, the negative regulator of autophagic pathway. However, in case of concurrent treatment with autophagy inhibitor like monensin leads to high concentration of pro-apoptotic proteins like Bax and apoptosis executors like cleaved caspase 3 and poly (ADP-ribose) polymerase (PARP) while the concentration of anti-apoptotic proteins like bcl-2 and bcl-xL becomes lower. In parallel, both autophagy markers LC3-II and p62 increased in combination treatment suggesting that the apoptotic activity was being triggered by inhibition of autophagy (Choi, et al. 2013). Another study revealed that the polyether antibiotics like monensin, nigericin, salinomycin, narasin and lasalocid overcame tumor necrosis factor-related apoptosis-induced ligand (TRAIL) resistance in malignant glioma cells. These polyether antibiotics restored the sensitivity of these cells towards TRAIL mediated apoptosis by triggering ER stress, CHOP mediated DR5 upregulation and c-FLIP downregulation by proteasomal degradation making them efficient molecules in combination therapy especially in the treatment of resistant cancer cell lines (Yoon et al., 2013).

1.11. Aim of This Work

Autophagy, on one hand protects the cells from the effects of anticancer agent while in contrast it may increase the efficiency of anticancer agents. This diverse and intriguing contribution of autophagy during cancer treatment challenges the scientists to investigate these bidirectional molecular mechanisms of autophagy. In early convenience, it should be investigated that which tumor is efficiently treated with particular agents upon modulation in autophagy (especially autophagy inhibition). Another thing is to find out the best biomarkers from which we can predict about autophagy addiction and dependency of tumors. Additionally, we should come to know that which drug is more efficient for autophagy inhibition during this treatment process. Are the direct acting drugs like mTOR inhibitors better or the indirect acting drugs are more efficient? Can we discover and develop better autophagy inhibitors with less cytotoxicity towards normal cells and more therapeutic effects in tumor cells at low concentrations? Can we apply these studies to clinical setting after getting fruitful results? Prompted by these questions, this study was designed to investigate the effects and molecular mechanism of a new compound (**C2**) and a known compounds **Arenaric acid**, **K41 A** polyether antibiotics on autophagy compared to the previous known modulators (monensin and bafilomycin A1) from this class. To compare the cytotoxicity of these compounds in both cancer as well as in healthy cell lines, a parallel study has undertaken. This study, as a continuation of our efforts, aims to find new chemotherapeutics with established mechanism of actions.

CHAPTER 2

MATERIALS AND METHODS

2.1. Materials

A detailed list of materials, commonly used chemicals, buffers, solutions and their compositions are presented in Appendix A.

2.2. Methods

2.2.1. Monensin isolation and purification

2.2.1.1. Monensin containing product

A commercial animal feeding product “Elancoban 200” was purchased from the veterinary medicine shop, containing 23.6% monensin sodium salt.

2.2.1.2. Extraction and isolation

The granule product (20 g) was extracted with Water: Ethyl acetate (1:1) in a separation funnel. The upper organic layer (EtOAc) was concentrated by rotatory evaporation giving a semisolid pasty residue. This extract was subjected to open column chromatography (Silica gel 60, 120 g) employing Chloroform: MEtOH: Acetone: Glycerol (98:20:40:2) as mobile phase. Fractions from 77 to 92 were pooled together, and after evaporation, it was applied to second open column chromatography (Silica gel 60, 80 g) using ethyl acetate as mobile phase.

2.2.1.3. Thin layer chromatography

In order to compare the chemical composition of each fraction and to decide the required solvent systems for chromatographical separations, TLC analyses were performed. Solvent systems used were as follows: EtOH:MEtOH:Water (20:2:1); Chloroform:MEtOH:Water (90:10:1); Chloroform:MEtOH:Acetone (98:5:10); Chloroform:MEtOH:Acetone (98:5:40) and Ethyl acetate:MEtOH (98:2).

2.2.1.4. Structure confirmation

The pure fractions were pooled together and evaporated in vacuum rotary evaporation system. Then the pure compound was dissolved in chloroform for mass and proton NMR spectrometry analysis to confirm the purity and chemical structure of monensin.

2.2.2. Mammalian cell culture

In this study, five mammalian cell lines were used. Among them three were cancer cell lines, while two were healthy cell lines.

HeLa: Human adenocarcinoma epithelial cell line from cervical cancer

PC-3: Human adenocarcinoma epithelial cell line from prostate cancer (Metastatic site)

CaCo-2: Human colorectal adenocarcinoma epithelial cell line

MRC-5: Human fibroblast cell line from lungs

Vero: Grivet (*Cercopithecus aethiops*) epithelial cell line from kidney

2.2.2.1. Cells maintenance and growth

Cells were grown in 100 x 20 mm culture dishes by using appropriate culture medium with specific percentage (10-20%) of fetal bovine serum (FBS) according to the need of each cell line. For HeLa and PC-3 DMEM with 10% FBS, CaCo-2 EMEM with 20% FBS while for MRC-5 and Vero EMEM with 10% FBS culture media were used. The cells were incubated in cell culture having 5% CO₂ at 37 °C. Cell were allowed to grow and passaged after they were confluent.

2.2.2.2. Cells passaging

First of all, the old medium was removed by using sterile glass pasture pipette connected to vacuum suction pump. In order to increase the action of trypsin and remove the transition metal ions, cell surface was rinsed with 0.05% trypsin. For the detachment purpose, cells were treated with 0.25% trypsin followed by 1-2 minutes' incubation at 37 °C. Cells were then suspended in the appropriate volume of fresh medium according to the concentration of cells and homogenized by the help of sterile pipette. Appropriate volume of fresh medium was added to the new culture dish and inoculated with required volume of cell suspension. Cells were shake quite gently in order to spread equally on the surface of plate and put back to the 5% CO₂ incubator having 37 °C.

2.2.2.3. Cells freezing and thawing

In order to protect the phenotypic and genotypic characteristics of cell line, each cell line have its own maximum passaging number. Also, in some studies a particular passaging number is recommended for specific cell line. That's why cells were frozen and stored as stock in liquid nitrogen while thawed upon requirement by the following procedure.

After cell detachment due to treatment of 0.25% trypsin, cells were collected in freezing buffer containing cryo-protective agent (95% FBS + 5% DMSO). Particular number of cells (2×10^6 cells/ml) were collected in a cryovial and put them in liquid nitrogen for long term storage. When required, the stored cell`s vial was put out from liquid nitrogen and allowed them to thaw for 1-2 minutes in the water bath at 37 °C. The cells in the vial was suspended by gently pipetting and transferred to appropriate fresh medium in new culture dish. The culture dish was gently shake and put in the 5% CO₂ incubator at 37 °C. Next day, the medium of the cells was changed in order to remove the cryo-protective (DMSO).

2.2.2.4. Cells counting

In order to use the required number of cells in particular experiment, cells were counted by using the following procedure. After detachment of cells with 0.25% trypsin, cells were collected in appropriate volume of fresh medium/freezing buffer. A small amount of cells suspension was taken in separate sterilized eppendorf. Cells were mixed with typan blue with dilution factor (1:9 or 1:4) and shake well. 10 ul from this mixture was transferred to each side of hemocytometer covered with cover slip. In each side of hemocytometer cells were counted in 9 big squares under 10X objective of microscope and take the average of counting from both sides.

The following formula was used to find the cells number/ml in the given cell suspension.

$$\text{Cells/ml} = \frac{\text{Cells counted} \times \text{Dilution factor}}{9} \times 10^4$$

2.2.3. Cytotoxicity analysis

2.2.3.1. Cells seeding

Cells were seeded homogenously in 96 well plates with different number for each cell line. HeLa, PC-3 and CaCo-2 were seeded 7000 cells/well, MRC-5 was 10000 cells/well and Vero was 4000 cells/well. During seeding the first three wells of the first row were left empty. All cell lines were incubated for 24 hours except CaCo-2 which was incubated for 48 hours before compounds treatment. Before treatment, the cells were carefully observed under inverted microscope in order to be sure that they are in healthy condition and bear proper morphology.

2.2.3.2. Preparation of compounds solution

The solution of compounds **C2** and Monensin was prepared in absolute EtOH while for **C1 and K41 A** absolute DMSO was used. All the compounds were prepared in 25 mM concentration as stock solution which was used for further dilutions. **C1, C2** and **K41 A** were used in four different concentrations while Monensin and doxorubicin

were used in six different concentrations. These dilutions were prepared 500X more concentrated from the final concentration in which it was applied to the cell lines in the particular well.

2.2.3.3. Application of compounds on the cell lines

Compounds and doxorubicin were added from each dilution in triplicates to the wells containing grown cells in given procedure. Initially, 2 μ l of the compound and doxorubicin solution were mixed with 48 μ l of medium respectively. Then 10 μ l from this mixture was added to each well in triplicate manner that contain cells with 190 μ l medium. Hence in this way, **C1**, **C2** and **K41 A** were applied in a final concentration of 5, 10, 25 and 50 μ M, Monensin 0.5, 1, 2.5, 5, 10, 25 and 50 μ M while doxorubicin was 0.1, 0.5, 1, 2.5, 5 and 10 μ M in each particular well. Doxorubicin was used here as a positive control while EtOH and DMSO were added in same manner to each cell lines as negative controls in cytotoxicity analysis.

After, addition of compounds in respective wells, the plates were gently agitated and put back in 5% CO₂ incubator at 37 °C. After, 24 and 48-hour incubation, morphology and condition of the cells were examined carefully under inverted microscope (Olympus 1X71) and pictures were taken by using CCD camera system.

2.2.3.4. WST-1 assay

After, 48-hours incubation with compounds, medium was taken out from each well and mixture of WST-1 (Water soluble tetrazolium salt) and medium (1:9) were put in each well respectively. Photometric absorbance at wavelength of 440 nm was measured by using multifunctional spectrophotometer (Variscan flash by Thermo Scientific) after incubation for 0.5 hour, 2 hours, 3 hours and 4-hours incubation time points at 37 °C.

2.2.3.5. IC₅₀ value Calculation

Spectrophotometric data were analysed manually for IC₅₀ value calculation in the given way by using Microsoft Excel 2013. After blank subtraction, the average of

three wells (triplicate) corresponding to 1 dilution of each compound were calculated. The values of negative controls (EtOH and DMSO) were used for the normalization of values corresponding to **C1**, **C2** and **K41 A** dilutions respectively. Normalization were performed in such a way that the average value of triplicate wells with specific dilution of compound were multiplied by 100 and divided by the average value of its negative control viz., EtOH for **C2**, DMSO for **C1**, **K-41 A** and doxorubicin. Finally, the IC₅₀ values were determined by drawing scatter chart along with polynomial trendline for the normalized values against the concentration of the compounds used.

2.2.4. Western blotting

2.2.4.1. Cells seeding

HeLa, PC-3 and CaCo-2 cell lines were used for the investigation of autophagy modulation by monensin, **C2** and **K41 A**. For each cell line 3×10^5 cells/well were seeded in 6 well plates and incubated in 5% CO₂ incubator at 37 °C. After 24 hours, morphology and condition of the cells were examined under inverted microscope (Olympus 1X71). PC-3 and HeLa cell line were incubated for 24 hours however; CaCo-2 cell line was incubated for 48 hours before compounds treatment.

2.2.4.2. Compounds treatment

For each cell line the specific compound were added to each designated well at their particular time. Three independent experiments were designed base on time course, dose concentration and combine treatment strategy. Each experiment was carried out according to the experimental plan along with both positive and negative controls.

In time course experiment HeLa, CaCo-2 and PC-3 cells were treated with these polyether antibiotics (**C2** and **K41 A**) for different treatment time points according to the following table.

Table. 2.1 Time course treatment experimental design

Gel Serial	Compounds used	Final Concentration	Treatment time (hr)
1	EtOH	Absolute	6
2	DMSO	Absolute	
3	Monensin	10 μ M	
4	C2	32 μ M	
5	K41 A	24 μ M	
6	Bafilomycin A1	100 ng/ml	
7*	Starvation	-----	
8	EtOH	Absolute	24
9	DMSO	Absolute	
10	Monensin	10 μ M	
11	C2	32 μ M	
12	K41 A	24 μ M	

*No compound was added here and the cell were starved by using EBSS medium.

In dose response experiment HeLa cells were treated with different concentration of **C2** and **K41 A** for 24-hour time point according to the following table.

Table. 2.2 Dose response treatment experimental design

Gel Serial	Compound	Final Concentration	Treatment time (hr)
1	EtOH	Absolute	24
2	DMSO	Absolute	
3	Monensin	10 μ M	
4	C2	8 μ M	
5		16 μ M	
6		32 μ M	
7		64 μ M	
8	K41 A	6 μ M	
9		12 μ M	
10		24 μ M	
11		48 μ M	
12	Bafilomycin A1	100 ng/ml	6
13*	Starvation	-----	6

*No compound was added here and the cell were starved by using EBSS medium.

In combine treatment experiment, HeLa cells were treated with polyether antibiotics (**C2**, **K41 A** and Monensin) in the presence and absence of Bafilomycin A1 for 18-hour time point according to the following table.

Table. 2.3 Combine treatment experimental design

Gel Serial	Compound	Concentration	Treatment time (hr)
1	DMSO + EtOH	Absolute	6+18
2	DMSO	Absolute	18
3	EtOH	Absolute	18
4	Monensin	10 μ M	18
5	Baf A1 + Monensin	100 ng/ml + 10 μ M	6+18
6	C2	32 μ M	18
7	Baf A1 + Comp 2	100 ng/ml + 32 μ M	6+18
8	K41 A	24 μ M	18
9	Baf A1 + K41 A	100 ng/ml + 24 μ M	6+18
10	Baf A1	100 ng/ml	6
11*	Starvation	6
12	DMSO	Absolute	6
13	Baf A1	100 ng/ml	24

*No compound was added here and the cell were starved by using EBSS medium.

2.2.4.3. Cell harvesting

After incubation all the cells were harvested at the same time in the following way. Medium was taken away from each well and the cells were briefly washed with 0.05% trypsin solution followed by treatment with 0.25% trypsin. After detachment, cells were collected in 1X PBS (Phosphate buffer solution) solution and centrifuged for 5 minutes at 5000 g. After discarding the excess supernatant, the cells were centrifuged again for 3 minutes at 10000 g. The cells pallets were stored at -80 °C.

2.2.4.4. Cells lysis

Cells were lysed in lysis buffer consisting of 1X PBS, 2X RIPA (1:1 ratio) and 100X PIC (protein inhibitor cocktail). Samples were vortexed rigorously for 5 times after each 5 minutes. Then samples were centrifuged at 14000 g at 4 °C for 10 minutes. Finally, the supernatant was transferred to clean eppendorf and processed further.

2.2.4.5. BCA analysis

Total protein concentration was quantified in a triplicate manner for each sample. Initially, BCA (Bicinchoninic acid assay) reagent was prepared by mixing reagent A and B in 50:1 ratio. For each well, sample, water and reagents were mixed in 1:4:95 ratios in a 96 well plate. The plate was covered with aluminium foil and allowed to incubate on 37 °C for 30 minutes. The plate was read by multifunctional spectrophotometer (Varioskan flash by Thermo Scientific) for photometric absorbance using 562 nm wavelength. Finally, the data was analysed manually using Microsoft Excel and the average concentration of three wells for each sample was used.

2.2.4.6. SDS PAGE

SDS gels 12 % were prepared manually and samples were loaded in the given way. Samples were prepared in such a way that each sample contained equal concentration of total protein. Loading dye was added to the samples with 1X final concentration and the samples were allowed to denature at 95 °C for 5 minutes. After a short spin each sample was loaded in a particular series to the given gel along with protein marker (Spectra by Thermo Scientific). Samples were run at 60 volts for 30 minutes followed by 100 volts for 120 minutes.

2.2.4.7. Membrane transfer

The resolved proteins on the gel were transferred to PVDF (Polyvinylidene difluoride) membrane by using the Bio-Rad Mini Trans-Blot System. A sandwich of membrane and gel was formed between Whatman filter papers in transfer cassette

followed by placing it in the blotting tank filled with 1X transfer buffer. The system was run at 20 mA (milli-ampere) for 16 hours.

2.2.4.8. Blotting

The PVDF membrane was taken gently from the transfer cassette and was washed two times with wash buffer. The membrane was placed in 5% milk (pH 7.4) for 45 minutes followed by 2 times washing with wash buffer. Then, the membrane was treated with the particular primary antibody and then conjugated secondary antibody. The membrane was washed 5 times with wash buffer at each 5-minute interval after each antibody treatment.

2.2.4.9. ECL Imaging

An equal amount of stable peroxide solution and luminol enhancer solution (Pico by Thermo Scientific) were mixed and poured equally on the antibodies treated membranes. The chemiluminescence image of the given membrane was taken by using Vilber Lourmat Fx-7 imaging system at different exposure time points.

2.2.5. Acridine Orange staining

HeLa cells (1.5×10^5 cells/well) were seeded in 12 well plates. After 24-hour incubation cells were treated with given compounds in duplicate manner for particular time. (Table: 2.4) Cells were washed 2 times with 1X PBS followed by incubation with 5ug/ml Acridine orange (AO) in 1X PBS for 20 minutes in 5% CO₂ incubator at 37 °C. Cell were washed three times with 1X PBS and immediately observed under fluorescent microscope (Olympus FX7).

Table. 2.4. AO, MDC staining and Fluorometry experimental compounds treatment

Sample serial	Compound	Final Concentration	Treatment time (hr)
1	EtOH	Absolute	24
2	DMSO	Absolute	
3	Monensin	10 μ M	
4	C2	32 μ M	
5	K41 A	24 μ M	
6	Baf A1	100 ng/ml	6
7*	Starvation	6

*No compound was added here and the cell were starved by using EBSS medium.

2.2.6. Monodansylcadaverine staining

HeLa cells (1.5×10^5 cells/well) were seeded in 12 well plate. After 24-hour incubation cells were treated with given compounds in duplicate manner for particular time. (Table: 2.4) Cells were washed 2 times with 1X PBS followed by incubation with 50 μ M monodansylcadaverine (MDC) in 1X PBS for 10 minutes at 37 $^{\circ}$ C and 5% CO₂. Cell were washed three times with 1X PBS and immediately observed under fluorescent microscope (Olympus FX7).

2.2.7. MDC Fluorometry Analysis

HeLa cells (7000 cells/well) were seeded in 96 wells black plate. After 24-hour incubation cells were treated with given compounds in triplicate manner for particular time (Table: 2.4). Cells were washed 2 times with 1X PBS followed by incubation with 50 μ M monodansylcadaverine (MDC) in 1X PBS for 10 minutes at 37 $^{\circ}$ C. Cell were washed three times with 1X PBS and immediately intensity of MDC fluorescence was read by multiplate reader (Variscan flash by Thermo Scientific) using excitation/emission maxima 365nm/525nm. After reading the plate, cells were treated with 0.02% Triton-1X PBS for 10 minutes at room temperature. Then cells were incubated with 100 μ g/ml Propidium Iodide (PI) for 15 minutes at room temperature. Finally, the plate was read again by multiplate reader (Variscan flash by Thermo Scientific) using excitation/emission maxima 535nm/617nm. After blank subtraction,

MDC values were normalized with PI values and the relative MDC specific activity was determined in each sample was compared to the control groups (EtOH and DMSO).

2.2.8. Statistical Analysis

Fluorometric analysis of MDC experiments were performed in triplicates and quantitative data was presented as mean +/- standard error of mean (s.e.m). Data was analysed by one-way analysis of variance (ANOVA) followed by Turkey's *post-hoc* test. Statistical analysis was performed using Origin Pro (V8, OriginLab) software.

CHAPTER 3

RESULTS

3.1 Polyether Antibiotics Isolation and Purification

Polyether antibiotic compounds **1**, **2** and **3** onward indicated as **C1**, **C2** and **C3** (**K 41 A**), were isolated from marine actinomycete *Streptomyces cacaoi* followed by structure elucidation by NMR and MS spectroscopy, which were already reported in the doctoral thesis of our previous lab colleague (Semih, 2014; Özcan, 2013). Among these compounds, **C1** and **C3** are known compounds, namely arenaric acid (Ebata et al., 1975) and **K41 A** respectively (Tsuji et al., 1979; Dirlam et al., 1992; Carter et al., 1994), whereas **C2** is a new natural polyether antibiotic. The chemical structures and formulae of these compounds are given below (Figure 3.1).

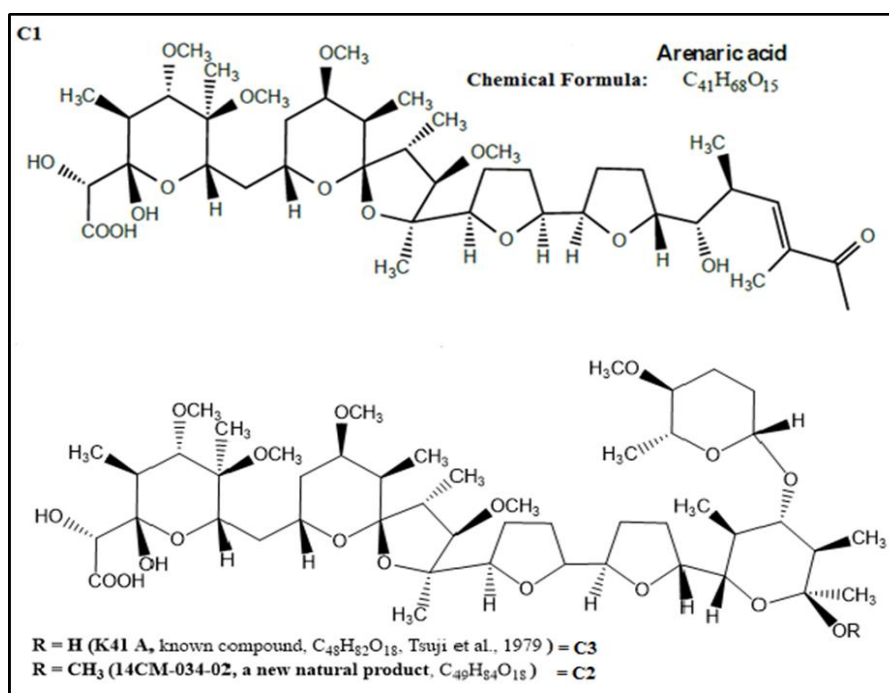


Figure 3.1 Chemical structures of the polyether antibiotics (**C1**, **C2** and **C3**).

This new polyether antibiotic **C2** was synthesized early in 1970`s from **K41 A** (**C3**) by Eli Lilly company and registered under US Patent No: 4.303.647 and 4.331.658

for its potent anti-coccidiosis and anti-dysenteric activity. However, **C2** in this study, is a new natural product isolated for the first time from a natural source (*Actinomyces cacaoi*).

3.2. Monensin Isolation and Purification

3.2.1. Monensin isolation

Initially, a mixture of compounds was obtained from the commercial monensin-containing animal feed product through solid-liquid extraction. The mixture was analysed by thin layer chromatography (TLC), and the spots were visualized by spraying 30% sulphuric acid solution followed by heating on a hot plate. The profile of the mixture is shown below. Mobile phase used for TLC development was Chloroform: MEtOH: Acetone (98:5:40) (Figure 3.2).

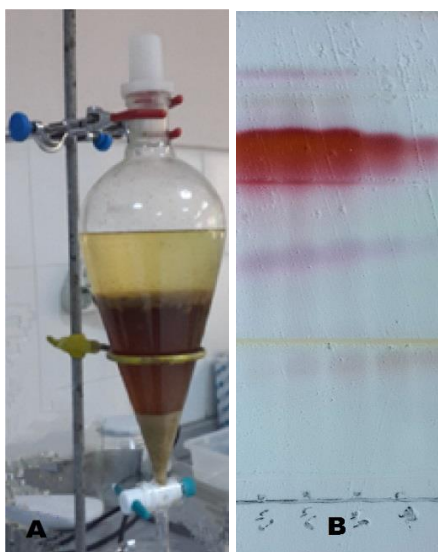


Figure 3.2. A. Solid liquid extraction system (Monensin). B. TLC profile of the obtained mixture

3.2.2. Monensin purification

The mixture was then purified by silica gel column as shown below (Figure 3.3) followed by TLC analysis. Mobile phase used was Ethyl acetate: MEtOH (98:2).

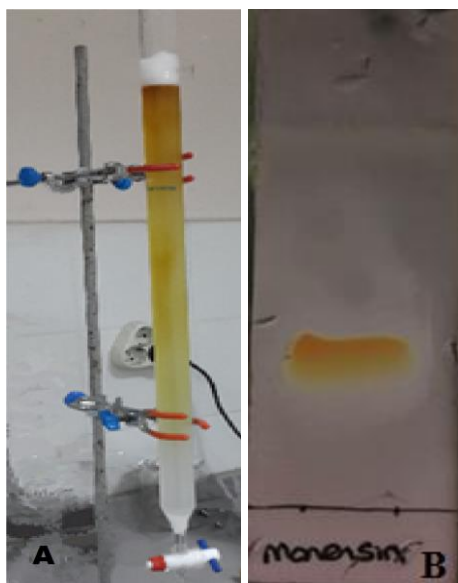


Figure 3.3 A. Silica gel open column chromatography system (Monensin). B. Chromatogram of the purified monensin with the reference of chemical mixture.

3.2.3. Structure confirmation of Monensin

The pure fractions observed on TLC were pooled together, and then the combined samples were evaporated in vacuum by rotary evaporator. After that, a lyophilisation process took place to afford an amorphous compound followed by a mass spectrometry (MS) and Proton Nuclear Magnetic Resonance analyses ($^1\text{H-NMR}$) (Figure 3.4 and 3.5). A solution of the purified compound was prepared in chloroform for MS analysis and analysed by LC-ESI-MS system at FABAL Research Laboratory of Ege University, Izmir. In Figure 3.4, the major ion peak with m/z 693 value corresponds to the sodiated form of monensin $[\text{M} + \text{Na}]^+$. Fifteen mg of the sample was dissolved in CDCl_3 , and run on 400 MHz NMR spectrometer (Varian at Chemistry department, Izmir Institute of Technology). The obtained proton NMR spectral data was completely superimposable with the reference monensin data (Ajaz and Robinson, 1987), confirming identity of the isolated compound. Moreover, no impurity signal was observed on the $^1\text{H-NMR}$ spectrum, verifying the high purity of the compound.

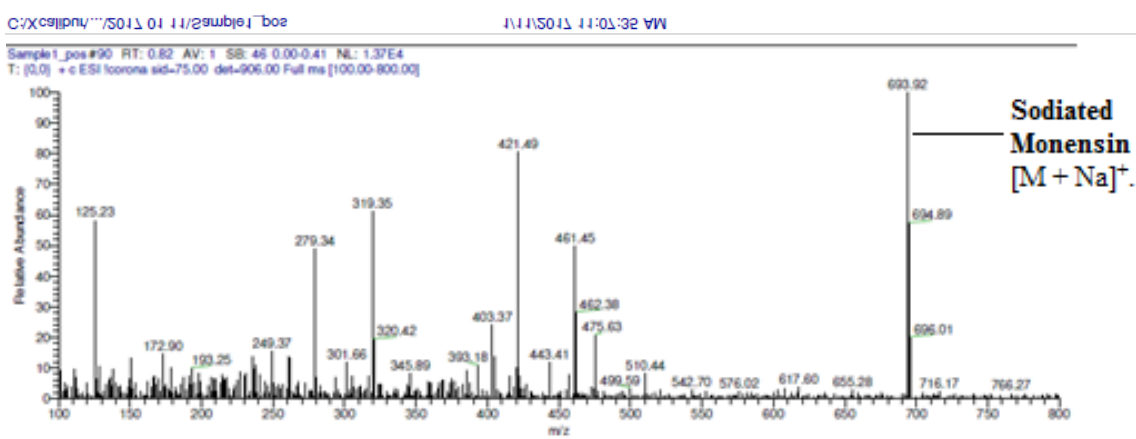
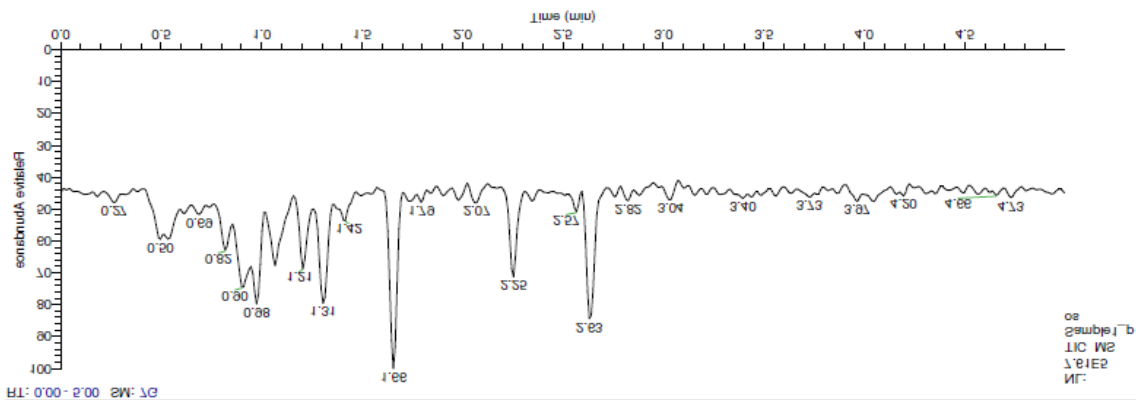


Figure 3.4 LC-ESI-MS spectrum of Monensin

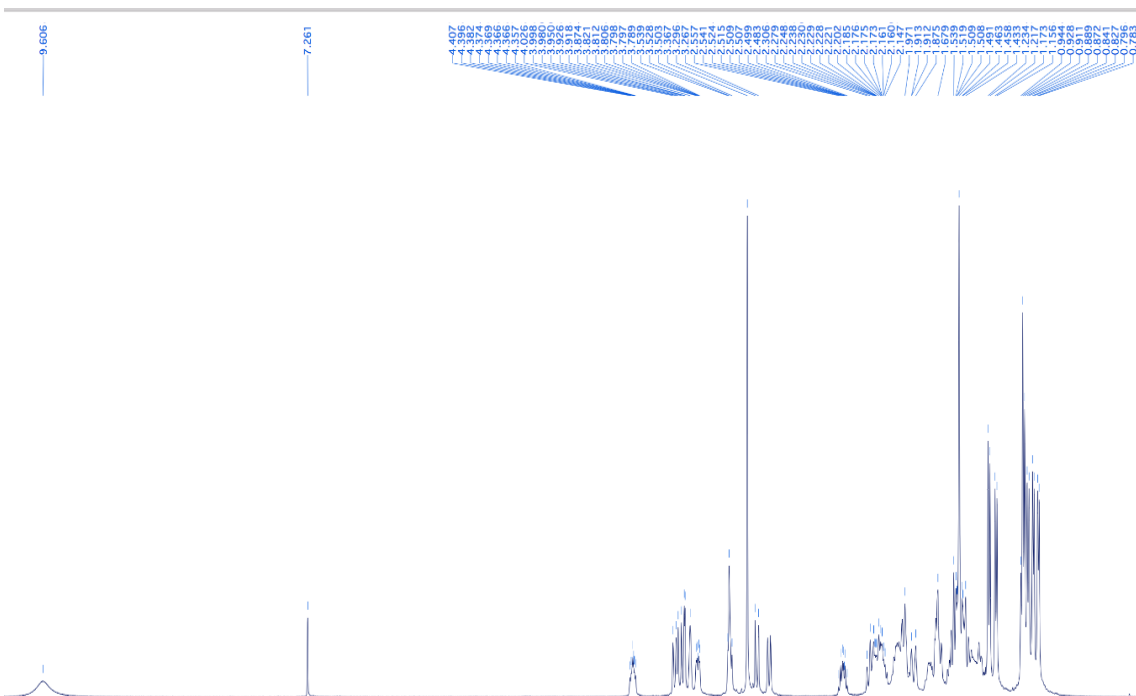


Figure 3.5 ¹H NMR Spectrum of Monensin

3.3. Polyether Antibiotics Activity Against Cancer Cell lines

Among these polyether ionophores, **C1** did not show significant cytotoxicity towards the cancer cell lines, and it was dropped out from this study. However, it was observed that **C2** and **K41 A** were active towards prostate cancer cell line (PC3), then colorectal cancer cell line (CaCo-2) and lastly towards cervical cancer cell line (HeLa) as shown in table (3.1). The table shows the IC₅₀ values of the compounds against these cancer cell lines, where doxorubicin was used as positive control. These IC₅₀ values were calculated from spectrometric data after performing WST-1 assay. It was found that cancer cells were susceptible to the tested polyether antibiotics; however, the activity varied according to the cell line.

Table 3.1 IC₅₀ values (μM) of polyether antibiotics against cancer and healthy cell lines

Cell line	C2	K41 A	Monensin	Doxorubicin
PC3	23.86 ± 1.84	11.76 ± 0.59	8.4 ± 1.5	1.7 ± 0.31
CaCo-2	27.89 ± 0.48	7.43 ± 0.25	9.4 ± 1.1	8.76 ± 0.29
HeLa	32.6 ± 0.1	23.7 ± 0.3	11.9 ± 0.2	1.2 ± 0.2
MRC-5	39.9 ± 0.8	35.2 ± 0.9	---	>5
Vero	39.7 ± 0.4	23.3 ± 0.6	---	> 5

Before starting WST-1 assay, cells were observed microscopically and pictures of the cells were taken for each compound's test concentration applied during cytotoxicity analyses. The pictures are shown in the figures (3.6-8).

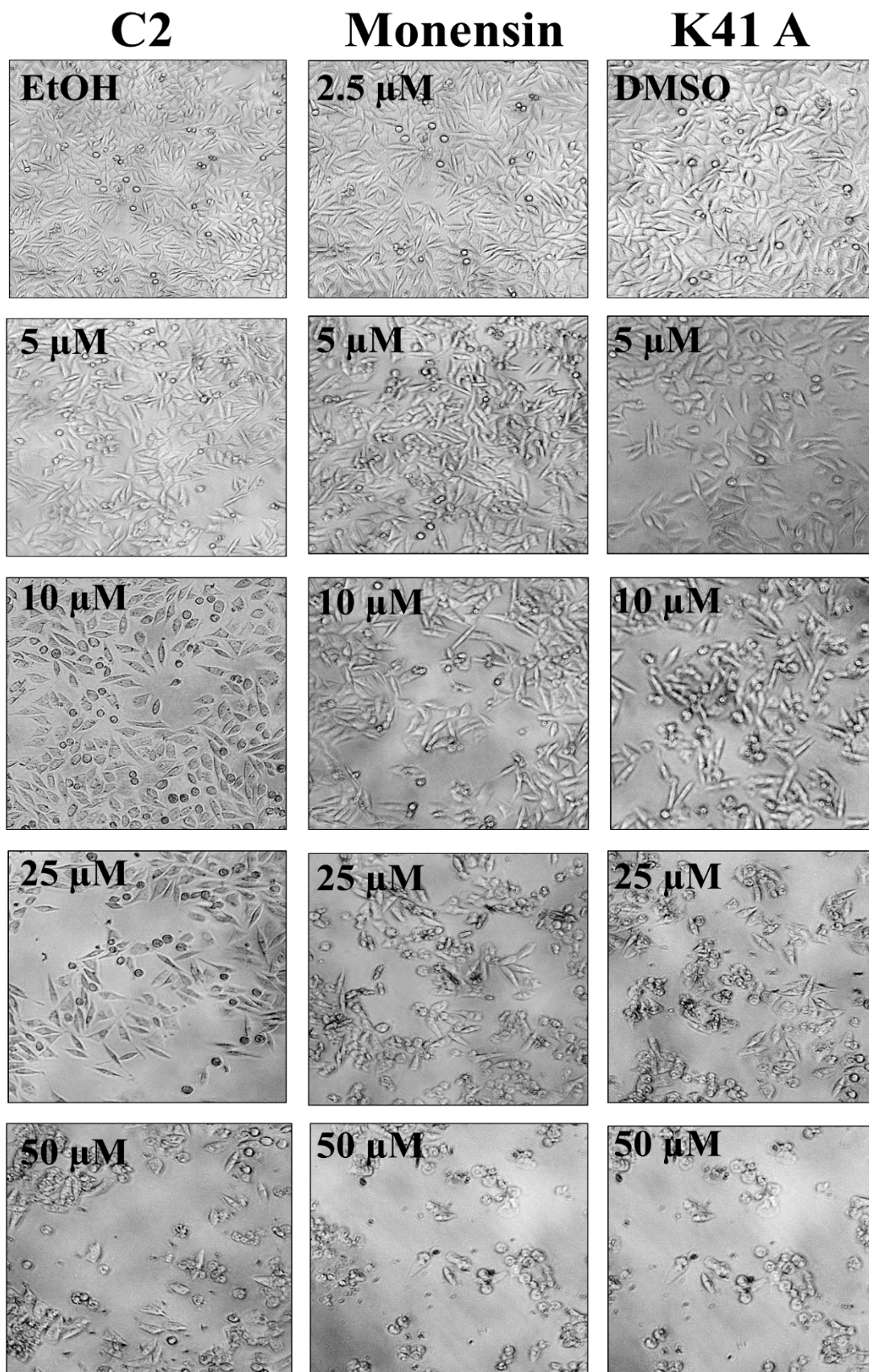


Figure 3.6 Microscopic pictures of PC-3 cell line. EtOH is the control sample for Monensin and C2 while DMSO for K41 A. (Scale bar: 200 μm)

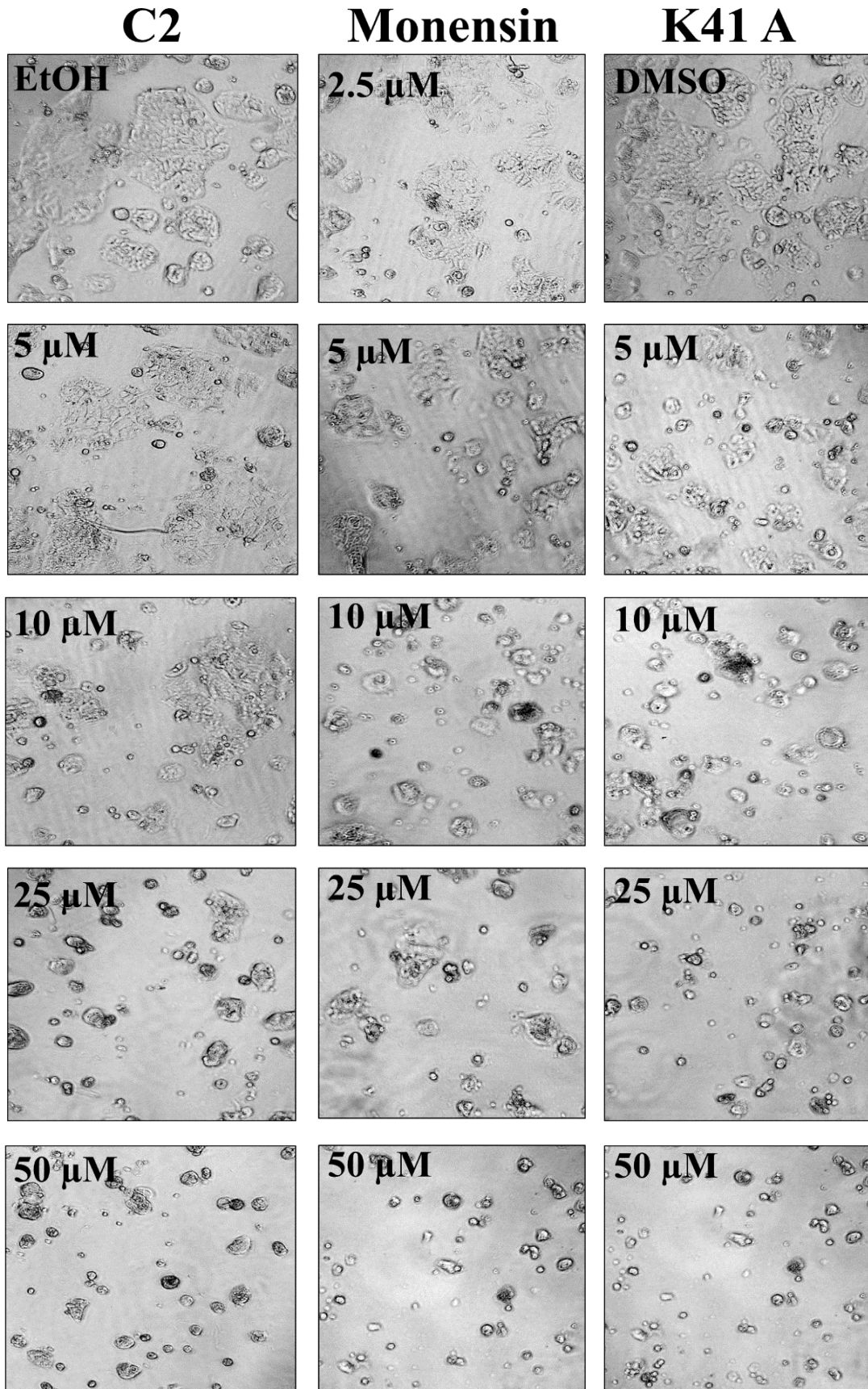


Figure 3.7 Microscopic pictures of CaCo-2 cell line. EtOH is the control sample for Monensin and C2 while DMSO for K41 A. (Scale bar: 200 μm)

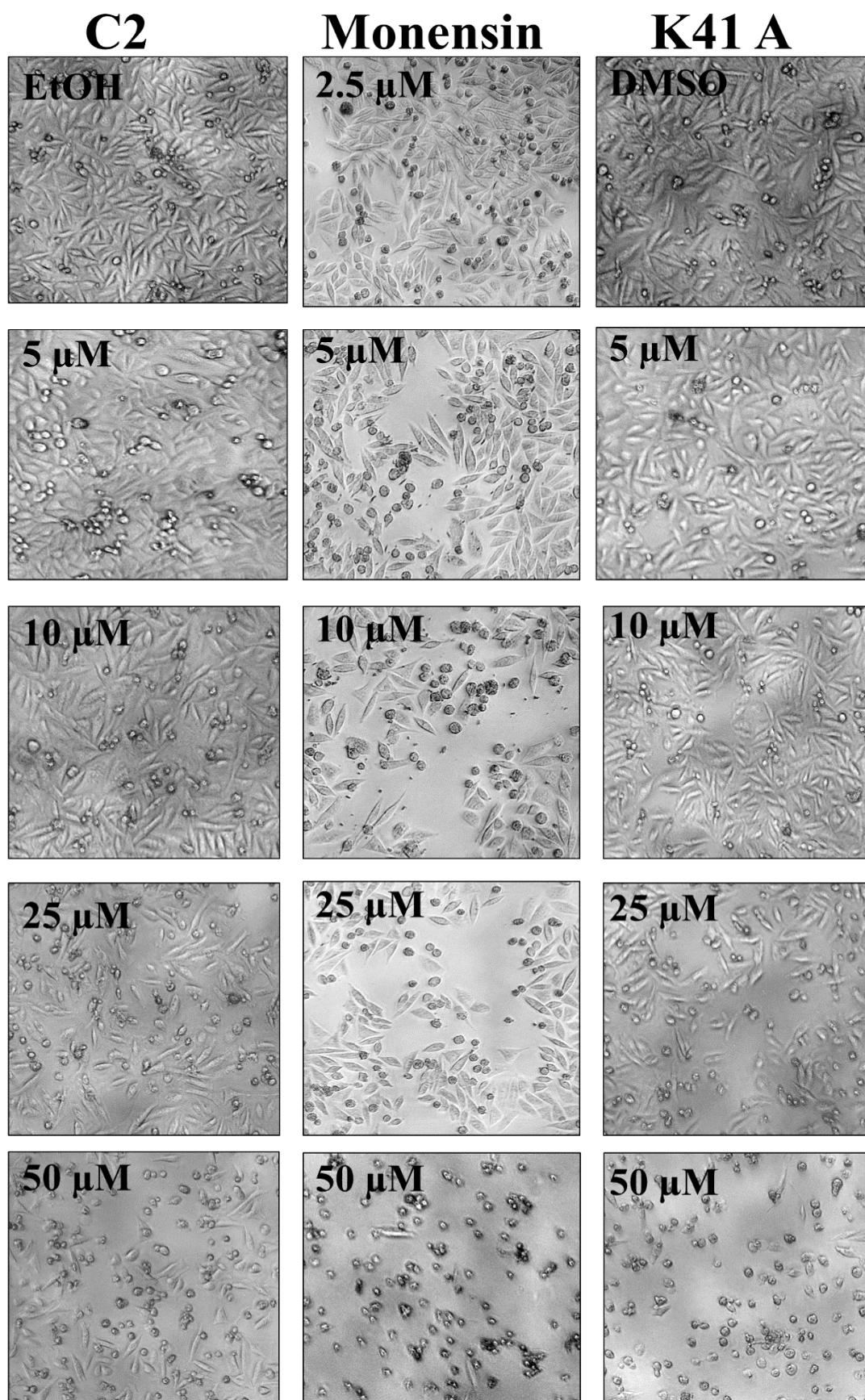


Figure 3.8 Microscopic pictures of HeLa cell line. EtOH is the control sample for Monensin and C2 while DMSO for K41 A. (Scale bar: 200 μm)

After calculation of IC₅₀ values for these compounds, microscopical observation were cross checked with their IC₅₀ values and the images correlated well for these cell lines. It was found that among these compounds, monensin have the lowest IC₅₀ value followed by **K41 A** and then **C2**.

3.4. Polyether Antibiotics Activity Against Healthy Cell lines

The activity of these compounds were also studied against healthy cell lines like human lung fibroblast cell line (MRC-5) and Grivet (*Cercopithecus aethiops*) kidney epithelial cell line. It was found that these polyether antibiotics also have activity against these cell lines. (Table 3.1) shows the IC₅₀ values of these antibiotics against MRC-5 and Vero cell lines. These calculated IC₅₀ values also matched with their microscopical observations of each cell line which are shown below in figure (3.9).

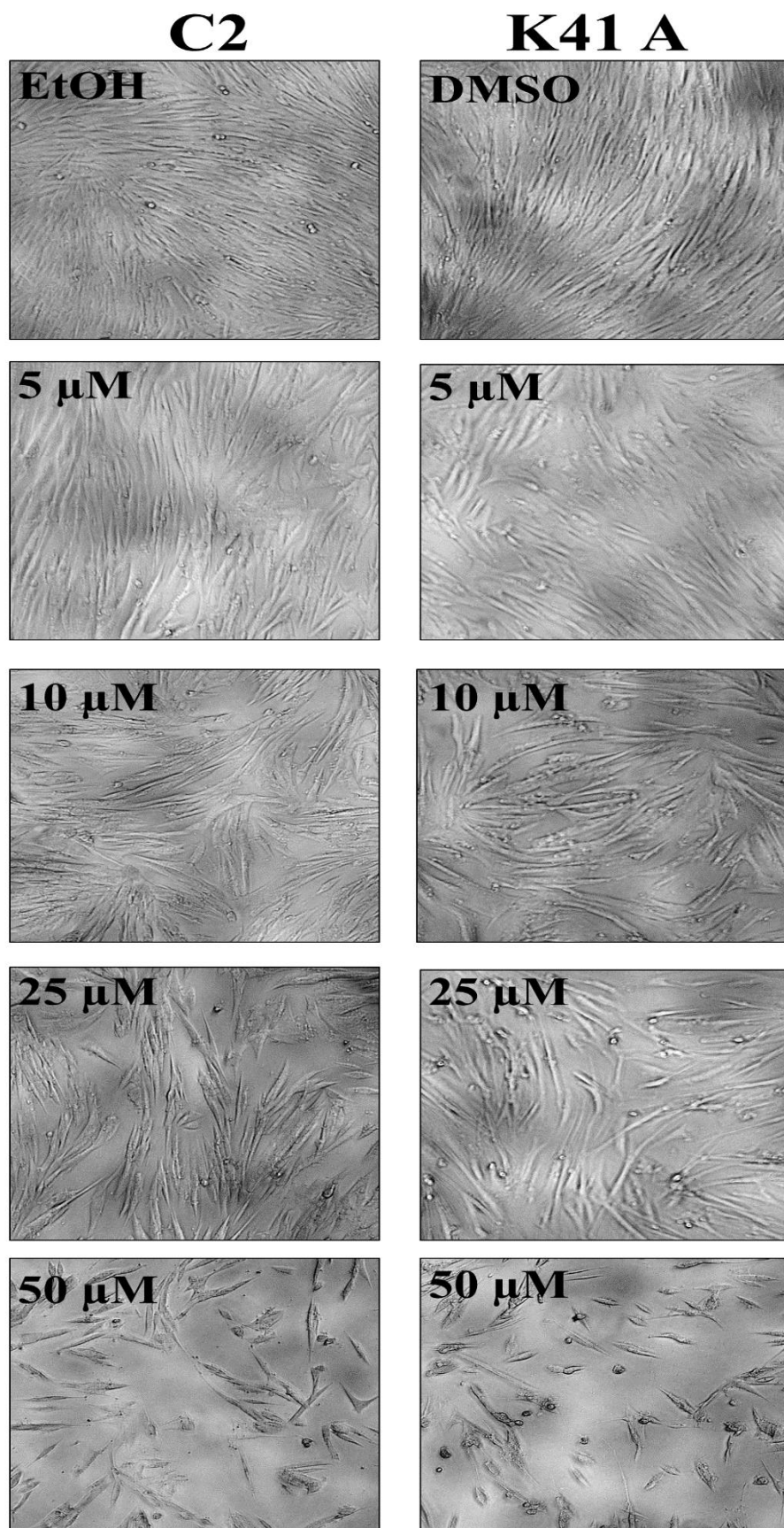


Figure. 3.9 Microscopic pictures of MRC-5 cell line. EtOH is the control sample for Monensin and C2 while DMSO for K41 A. (Scale bar: 200 μ m)

3.5. Polyether Antibiotics Increases the Expression Levels of Autophagy Markers

Primarily, autophagy was measured by investigation of basic autophagy markers with Western blotting technique; LC3-II was used as autophagosome maturation and flux marker, while p62 was used as autophagy flux marker (Figure 3.10-12). It was found that, in all three cancer cell lines, these antibiotics (monensin, **C2** and **K41 A**) increased autophagy markers.

In all experiments bafilomycin A1 was used as autophagy inhibition control, while starvation was used to induce autophagy. In all cancer cells, when compared to negative controls (EtOH and DMSO) and inhibition controls (bafilomycin A1), LC3-II and p62 protein levels were increased in a time dependent manner at concentrations equivalent to their IC₅₀ values. According to the recent guidelines for monitoring autophagy, LC3-II is supposed to be compared with the housekeeping protein (actin) in order to measure the autophagy flux in each sample (Klionsky et al., 2016).

In the case of CaCo-2 cell line, the expression levels of autophagy marker proteins were directly proportional to the treatment time points as shown (Figure 3.10). It was observed that these antibiotics altered the level of autophagy marker proteins dramatically along the treatment time. At 6-hour time point monensin had the highest elevated LC3-II and p62 level, while at 24-hour time point **K41 A** showed highest activity followed by **C2** and then monensin. Here, it was interesting to see loss of monensin's activity over treatment time in regards to LC3-II accumulation. However, in contrast, accumulation of LC3-II was increased in the case of **C2** and **K41 A**. Along with this, accumulation of other autophagy marker p62 was also increased over time by the treatment of all three antibiotics compared to the inhibition control bafilomycin A1. Besides, when this cell line was starved to induce autophagy, LC3-II levels decreased while the level of p62 did not changed significantly compared to negative controls (EtOH and DMSO).

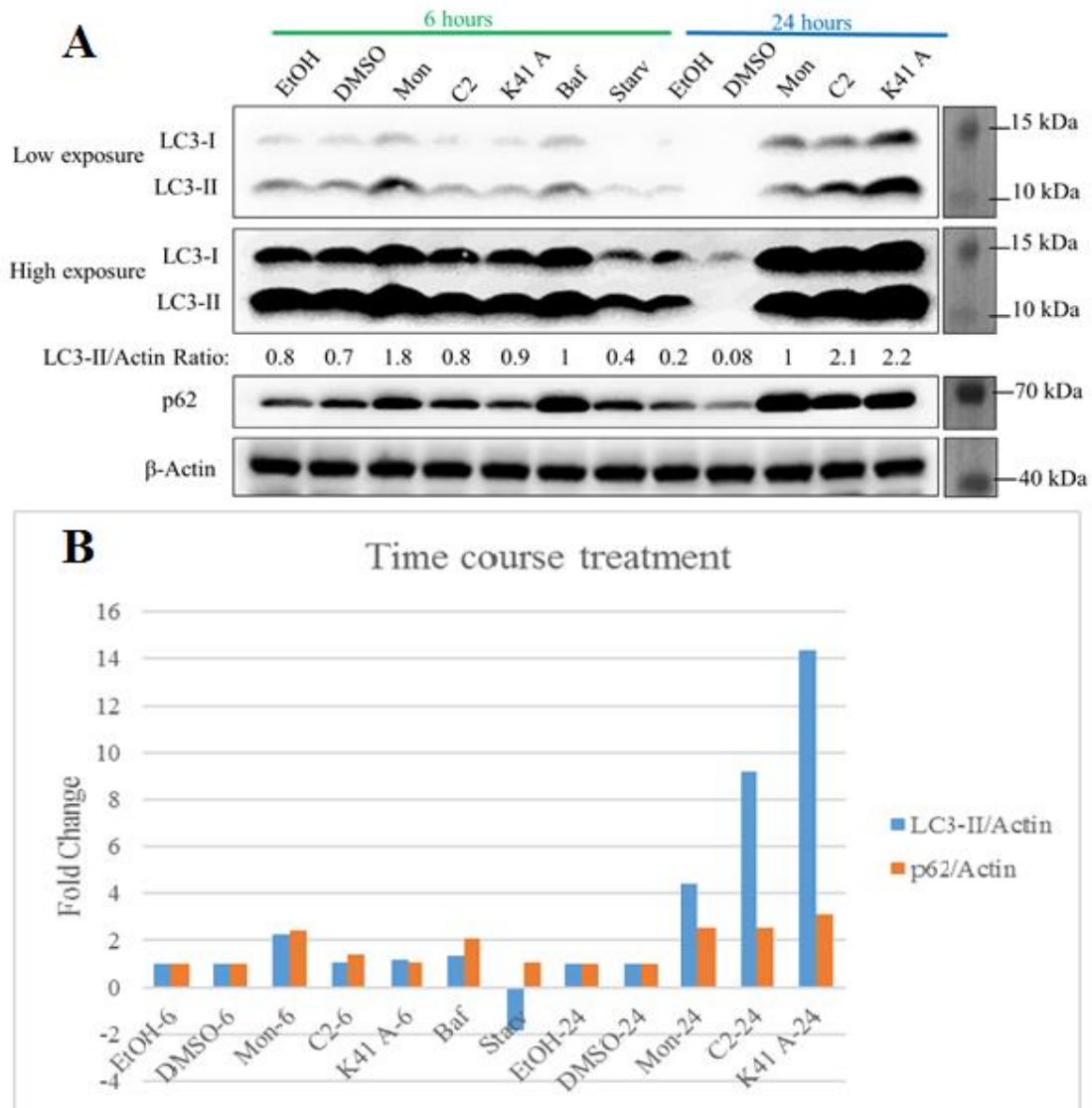


Figure 3.10 A: Western blot images of LC3 and p62, B: Graphical representation of fold change of LC3-II/actin and p62/actin among the samples of CaCo-2 cell line in time course study. EtOH and DMSO: Negative controls of polyether antibiotics. Bafilomycin A1 and Monensin: Autophagy inhibition controls. Starvation: Autophagy induction control. Concentration of the C2 and K41 A: IC₅₀ value, Bafilomycin A1: 100 ng/ml.

Similar to CaCo-2, the expression level of autophagy markers increased with over time with dominant activity of monensin both in HeLa and PC3 cell lines (Figures 3.11 and 3.12). In contrast in case of HeLa, when the cells were starved, both autophagy flux markers were decreased due to the induction of autophagy.

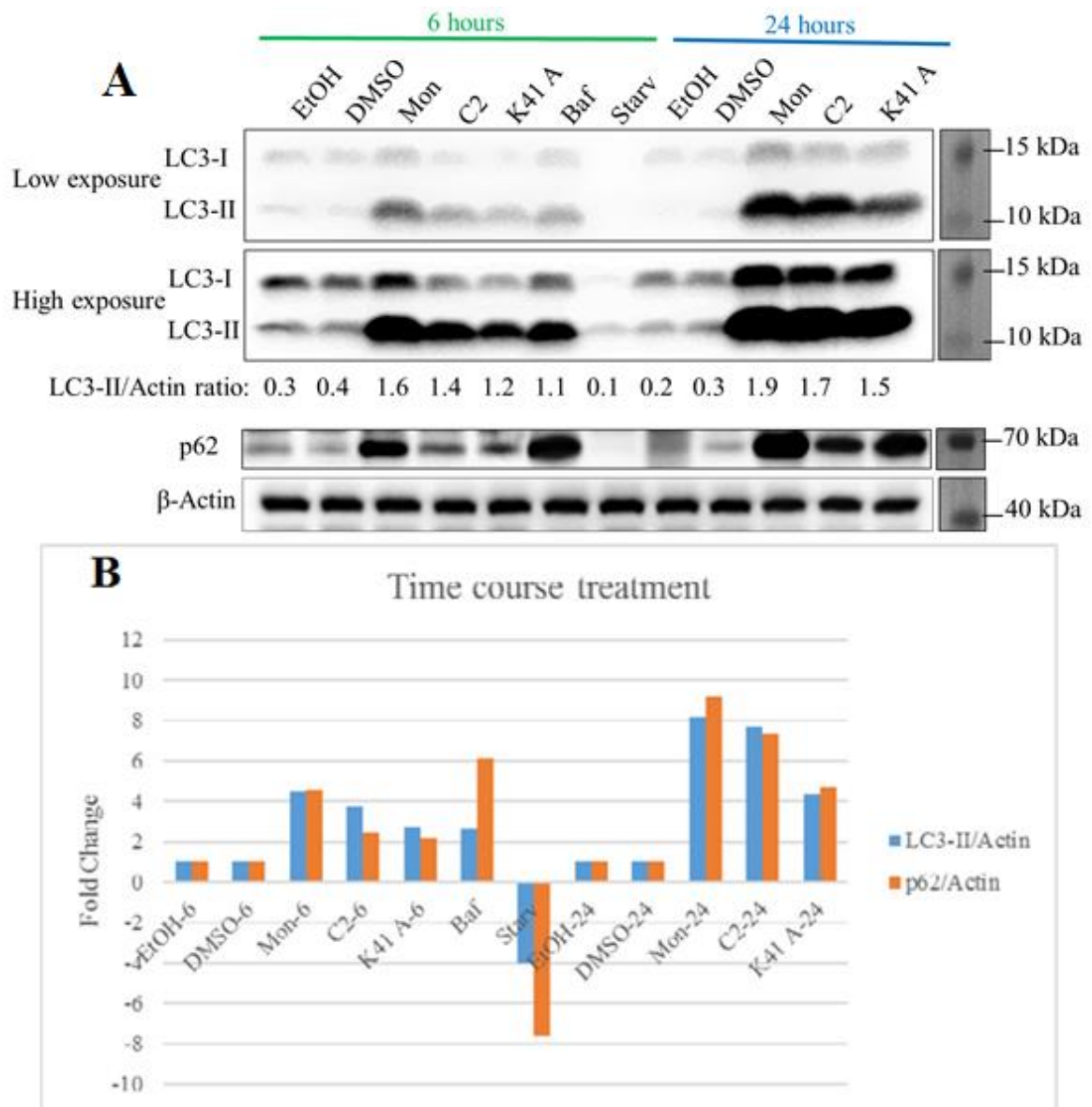


Figure 3.11 A: Western blot images of LC3 and p62, B: Graphical representation of fold change of LC3-II/actin and p62/actin among the samples of HeLa cell line in time course study. EtOH and DMSO: Negative controls of polyether antibiotics. Bafilomycin A1 and Monensin: Autophagy inhibition controls. Starvation: Autophagy induction control. Concentration of the **C2** and **K41 A**: IC₅₀ value, Bafilomycin A1: 100 ng/ml.

In PC3 cell line, the administered polyether antibiotics increased autophagy flux markers (LC3-II and p62) as the time passed (Figure 3.12). Similar to the other two cell lines, each antibiotic showed different action in terms of autophagy marker proteins accumulation. Monensin showed highest LC3-II and p62 accumulation followed by **C2** and then **K41 A**. Interestingly, in this cell line, p62 levels increased as LC3-II levels decreased during starvation.

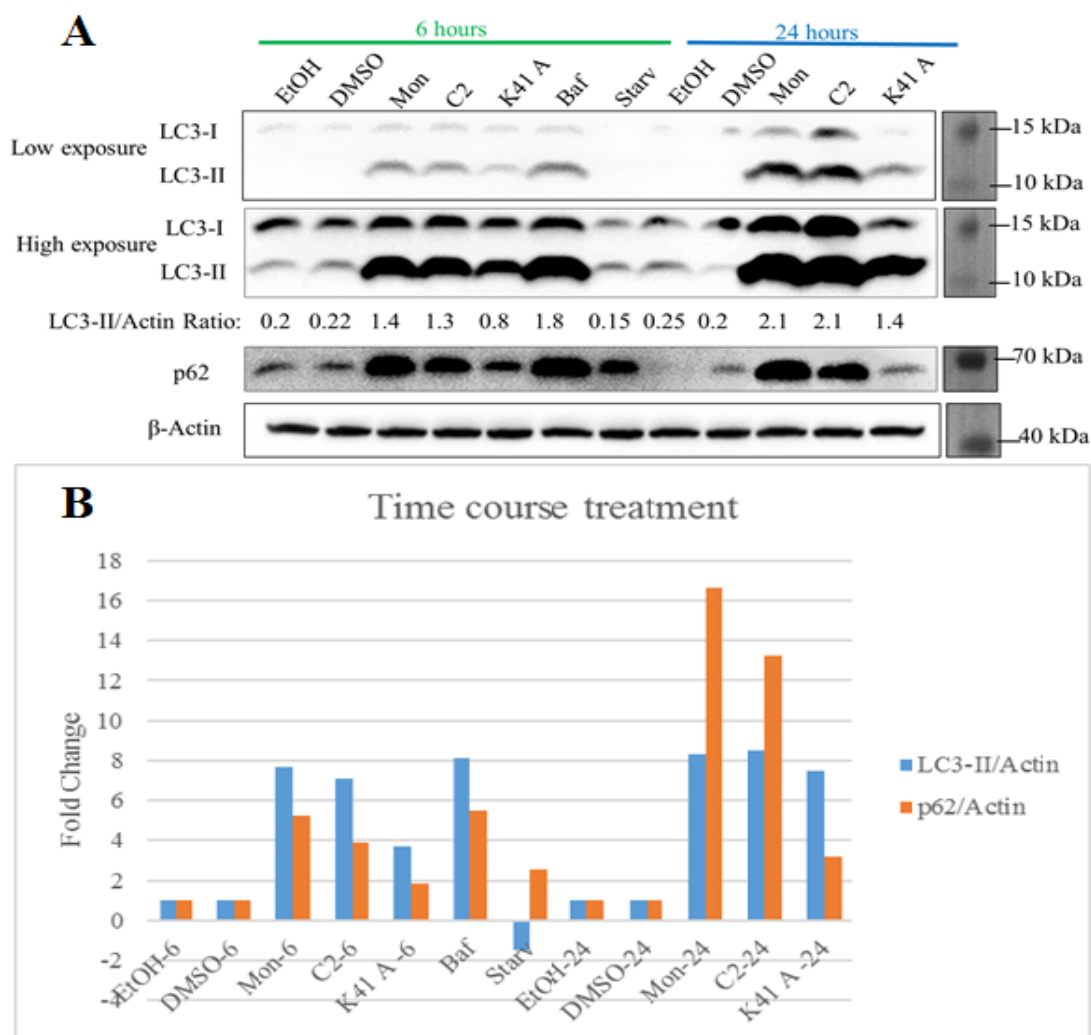


Figure 3.12 A: Western blot images of LC3 and p62, B: Graphical representation of fold change of LC3-II/actin and p62/actin among the samples of PC-3 cell line in time course study. EtOH and DMSO: Negative controls of polyether antibiotics. Bafilomycin A1 and Monensin: Autophagy inhibition controls. Starvation: Autophagy induction control. Concentration of the C2 and K41 A: IC₅₀ value, Bafilomycin A1: 100 ng/ml..

3.6. Autophagy Markers Accumulation Depend on Polyether Antibiotics Concentration

In a dose response experiment, HeLa cells were treated for 24-hours with different concentrations of polyether antibiotics (C2 and K41 A). Each compound was used at four different concentrations; a quarter, half, one and 2 times of its IC₅₀ value. It was observed in parallel with time course experiment that monensin was the one with highest ability to accumulate autophagy markers in HeLa cell line (Figure 3.13). Interestingly, in the case of C2 and K41 A, a consistent fall was observed in level of

autophagic markers LC3-I, LC3-II and p62 as the concentration of these polyether antibiotics increased. Taken together, it was observed that, at higher concentrations of both compounds ($2 \times IC_{50}$), these autophagy markers decreased dramatically; however, they were still high than negative controls (EtOH and DMSO). This decrease in autophagy proteins at higher doses than IC_{50} values might be due to the high cytotoxic activity of these compounds at this concentration or switching an alternative pathway for the induction of cellular death in this cell line. However, further studies are required for clear understanding of this inverse relationship between concentrations (**C2** and **K41 A**) and autophagy markers.

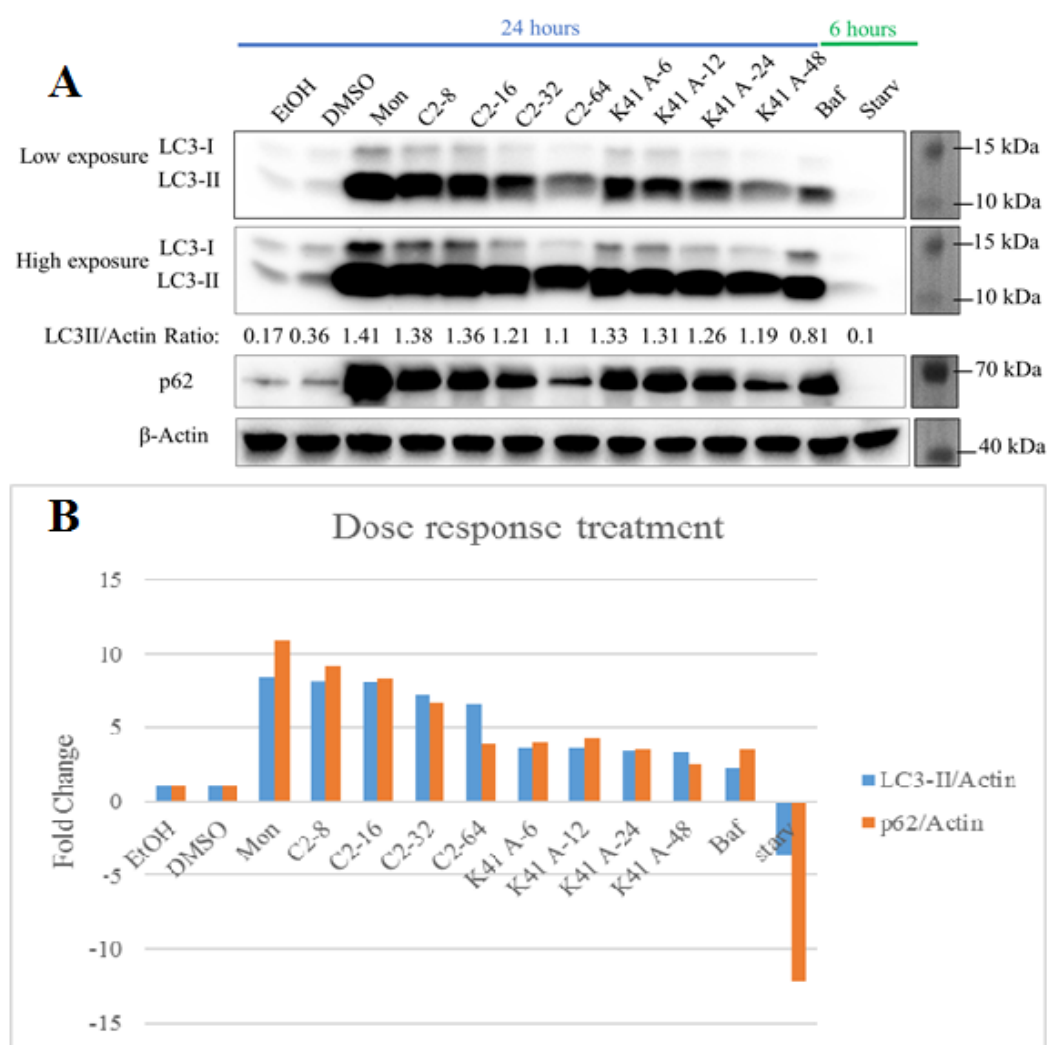


Figure 3.13 **A**: Western blot images of LC3 and p62, **B**: Graphical representation of fold change of LC3-II/actin and p62/actin among the samples of HeLa cell line in dose response study. EtOH and DMSO: Negative controls of polyether antibiotics. Bafilomycin A1 and Monensin: Autophagy inhibition controls. Starvation: Autophagy induction control. Concentration of the **C2** and **K41 A**: $\frac{1}{4}$, $\frac{1}{2}$, 1X and 2X of IC_{50} value, Bafilomycin A1: 100 ng/ml.

3.7. Polyether Antibiotics Increases the Synthesis of Autophagic Vacuoles

Lysosomal acidic pH is regulated by the action of H⁺ ion pump Vacuolar type H⁺ ATPase (V-ATPase) present in the membrane of lysosomes. Bafilomycin A1 is a well-known inhibitor of this ion pump, which eventually demolishes the acidic pH of lysosomes. Treatment of cells with bafilomycin A1 for 6 hours followed by treating with polyether antibiotics (monensin, **C2** and **K41 A**) caused higher accumulation of LC3-II and p62 levels in comparison to single treatment of these polyether antibiotics and autophagy inhibition control (bafilomycin A1). According to the recent guidelines of monitoring autophagy (Klionsky et al., 2016), these results suggest that these polyether antibiotics increases the synthesis of autophagy vacuoles and membrane as shown in Figure 3.14. Along with this, it was also stated in these guidelines that, autophagy carrier flux can be measured from LC3II level in comparison of single treatment of bafilomycin A1, single treatment of compound and bafilomycin A1 followed by compound treatment. The results obtained based on the abovementioned guidelines (Figure 3.14) indicated that the autophagy carrier flux meaning autophagy flux was blocked in the stage of cargo delivery to lysosomes.

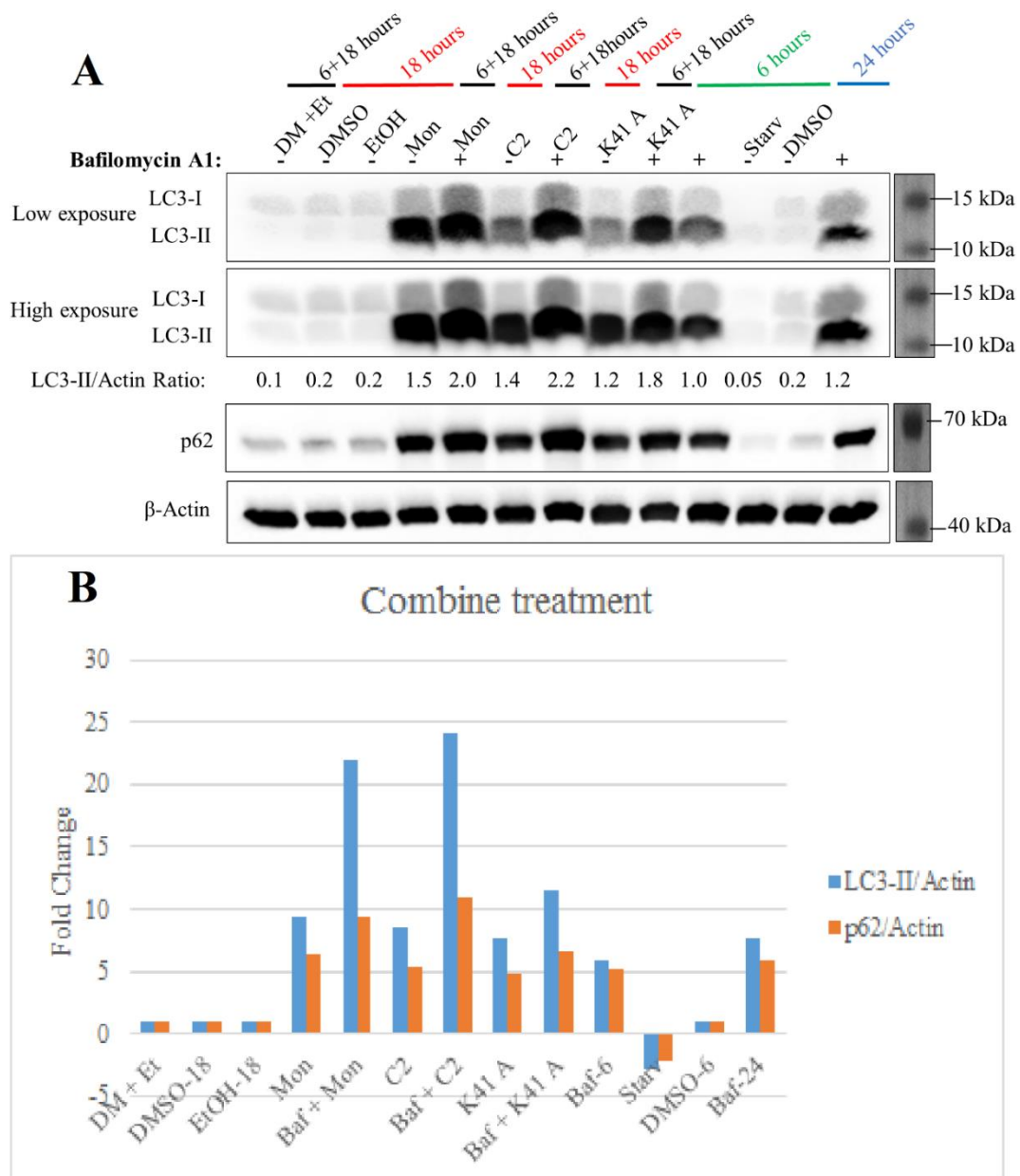


Figure 3.14 **A**: Western blot images of LC3 and p62, **B**: Graphical representation of fold change of LC3-II/actin and p62/actin among the samples of HeLa cell line in combine treatment study with bafilomycin A1. EtOH and DMSO: Negative controls of polyether antibiotics. Bafilomycin A1 and Monensin: Autophagy inhibition controls. Starvation: Autophagy induction control. Concentration of the **C2** and **K41 A**: IC₅₀ value, Bafilomycin A1: 100 ng/ml.

3.8. The Effects on Beclin-1 and Other Autophagy Related Genes (Atgs) Over Time

HeLa and CaCo-2 cell lines were treated with the compounds (Monensin, **C2** and **K41 A**) for 6 and 24-hour at concentrations equivalent to their IC₅₀ values, and Atgs

proteins like Atg-3, Atg-5, Atg-7, Atg-16-L1 and beclin-1 were examined. In HeLa cell line, **C2** and **K41 A** treatment showed different effects on these proteins over time (Figure 3.15). It was found that, both of these antibiotics (**C2** and **K41 A**) downregulated beclin-1, Atg-3 and Atg-16L1 over the time, while no significant effects on Atg-7 in the case of **C2**, and Atg-5 and Atg-7 for **K41 A** at 6-hour time point was noted. However, at 24-hour time point, all these Atgs along with beclin-1 were decreased by both of these compounds (**C2** and **K41 A**), and even this rate of downregulation was increased over time. In contrast, monensin did not show any significant effect on beclin-1 and the Atg proteins over time except Atg-3 and Atg-7, which were decreased at 24-hour time point.

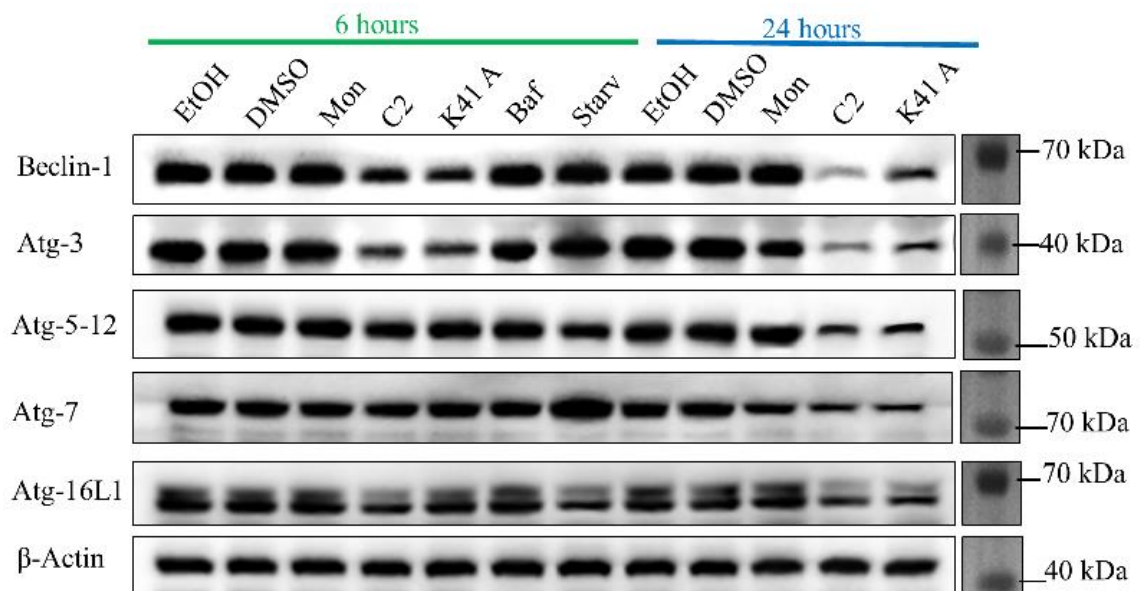


Figure. 3.15 Western blot images of beclin-1, Atg-3, Atg5-12, Atg-7 and Atg-16L1 for HeLa cell line in time course study. EtOH and DMSO: Negative controls of polyether antibiotics. Bafilomycin A1 and Monensin: Autophagy inhibition controls. Starvation: Autophagy induction control. Concentration of the **C2** and **K41 A**: IC₅₀ value, Bafilomycin A1: 100 ng/ml.

When CaCo-2 cells were treated with **C2** and **K41 A**, beclin-1 and other Atg proteins like Atg-5 and Atg-7 decreased over time. In starvation, these proteins were increased due to the induction of autophagy (Figure 3.16). Monensin showed no significant effect on beclin-1, while it downregulated Atg-5 and 7. However, this effect was comparatively less than **C2** and **K41 A** downregulation, especially at 24-hour time point.

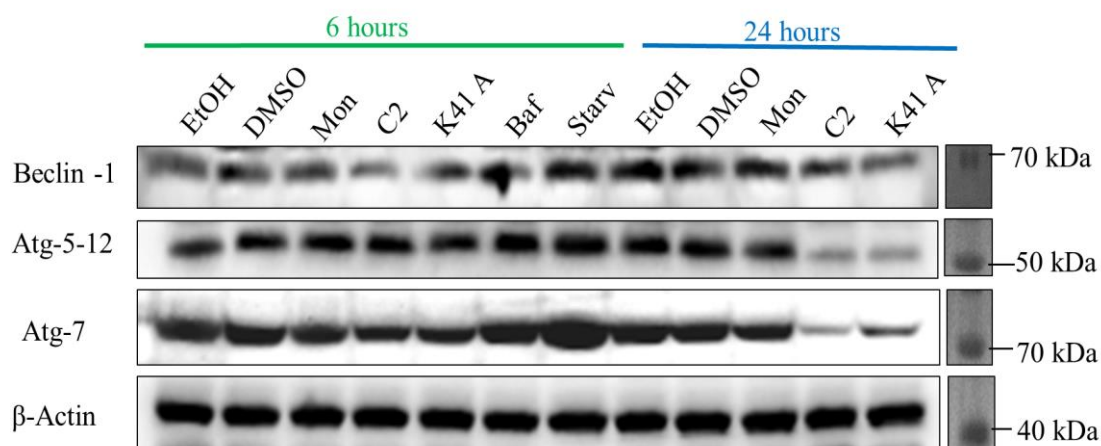


Figure 3.16 Western blot images of beclin-1, Atg5-12 and Atg-7 for CaCo-2 cell line in time course study. EtOH and DMSO: Negative controls of polyether antibiotics. Bafilomycin A1 and Monensin: Autophagy inhibition controls. Starvation: Autophagy induction control. Concentration of the **C2** and **K41 A**: IC₅₀ value, Bafilomycin A1: 100 ng/ml.

Overall, it was clear that these polyether antibiotics also target various autophagy related genes (Atg) like Atg-3, Atg-5, Atg-7, Atg16L1 and core autophagy regulatory protein beclin-1. The level of these Atg proteins decreased over time in HeLa and CaCo-2 cell lines by the treatment with **C2** and **K41 A** especially at 24-hour treatment. However, this pattern is predominantly context dependent and vary depending on the cell type. Interestingly, monensin belongs from the same class of these polyether antibiotics (**C2** and **K41 A**), showed highest accumulation of autophagy markers (LC3-II and p62) especially in HeLa and PC-3 cell lines. However, in comparison to **C2** and **K41 A** effects, monensin did not show any significant effect on beclin-1 in both cell lines (HeLa and CaCo-2). Regarding the effect on other Atgs by monensin, it was found that this compound had context dependent effect as observed in both cell lines; reduced Atg-7 levels were observed in both cell lines, but Atg-5/12 level only decreased in CaCo-2 cell line.

3.9. The Effect on Beclin-1 and Atgs are Directly Proportional to Polyether Antibiotics Concentration

In parallel with time course experiments, it was seen that, during 24-hour treatment, the downregulation of beclin-1 and Atg proteins (Atg-3, Atg-5, Atg-7 and Atg-16L1) increased as the concentration of **C2** and **K41 A** risen (Figure 3.17). Among

the compounds, **C2** had collectively the highest potential for the downregulation of these proteins in a concentration dependent manner. However, among the observed proteins, Atg-3 was the one with the highest downregulation in case of both compounds tested. As observed in time course experiments, monensin showed the same results here also; where only two of these proteins Atg-3 and Atg-7 were decreased while no effect on other proteins (beclin-1, Atg-5 and Atg-16L1) was detected. Along with this, bafilomycin A1 and starvation results were in parallel to the observed results in time course experiment.

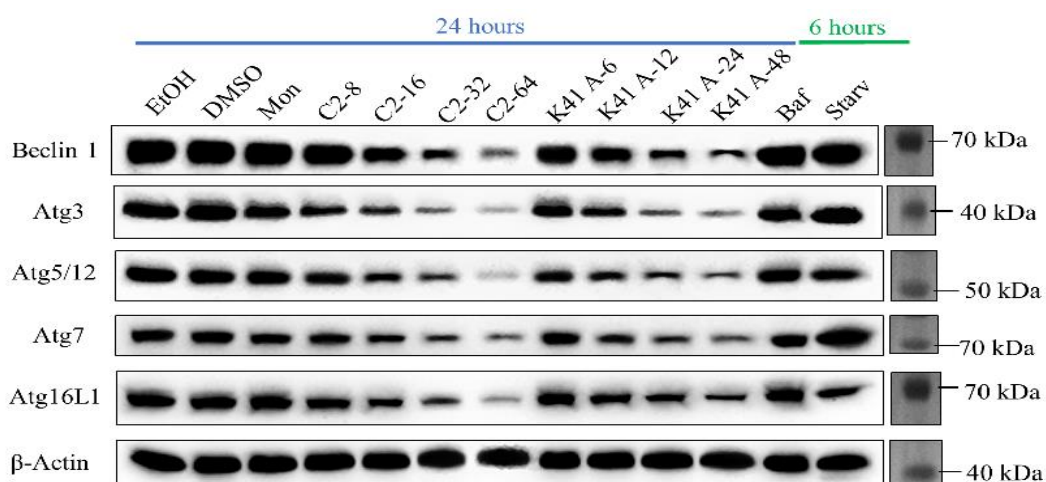


Figure 3.17 Western blot images of beclin-1, Atg-3, Atg5-12, Atg-7 and Atg-16L1 for HeLa cell line in dose response study. EtOH and DMSO: Negative controls of polyether antibiotics. Bafilomycin A1 and Monensin: Autophagy inhibition controls. Starvation: Autophagy induction control. Concentration of the **C2** and **K41 A**: $\frac{1}{4}$, $\frac{1}{2}$, 1X and 2X of IC_{50} value, Bafilomycin A1: 100 ng/ml.

3.10. Effects of Polyether Antibiotics on Acidic Compartments in Cytosol

The polyether antibiotics **C2** and **K41 A** increased the accumulation of acidic compartments suggesting that they were inhibiting autophagy. It was observed that in case of **C2** and **K41 A**, acidotropic dyes like AO (Figure 3.18) and MDC (Figure 3.19) were able to stain these accumulated acidic vacuoles. However, in contrast, monensin possessing the same or even higher activity regarding autophagy flux markers (LC3-II and p62) accumulations showed completely opposite results during both AO and MDC staining. This could be due the action of monensin abolishing acidic pH of these acidic compartments and leading to the inhibition of autophagosome and lysosomal fusion.

However, further studies are warranted to interpret the results of monensin and **C2** and **K41 A**. Regarding bafilomycin A1 which is known for its demolishing effect on acidic pH of lysosome, these acidotropic dyes were incapable for staining the vacuoles having alkaline pH. In the case of starvation, where autophagy induced, high number of autophagic vacuoles were observed during both stainings. According to these staining results, during autophagy inhibition monensin and bafilomycin A1 show similar results, where **C2** and **K41 A** demonstrated parallel results with each other; however, further studies are recommended to investigate the molecular mechanism of this inhibition pattern especially for our compounds **C2** and **K41 A**.

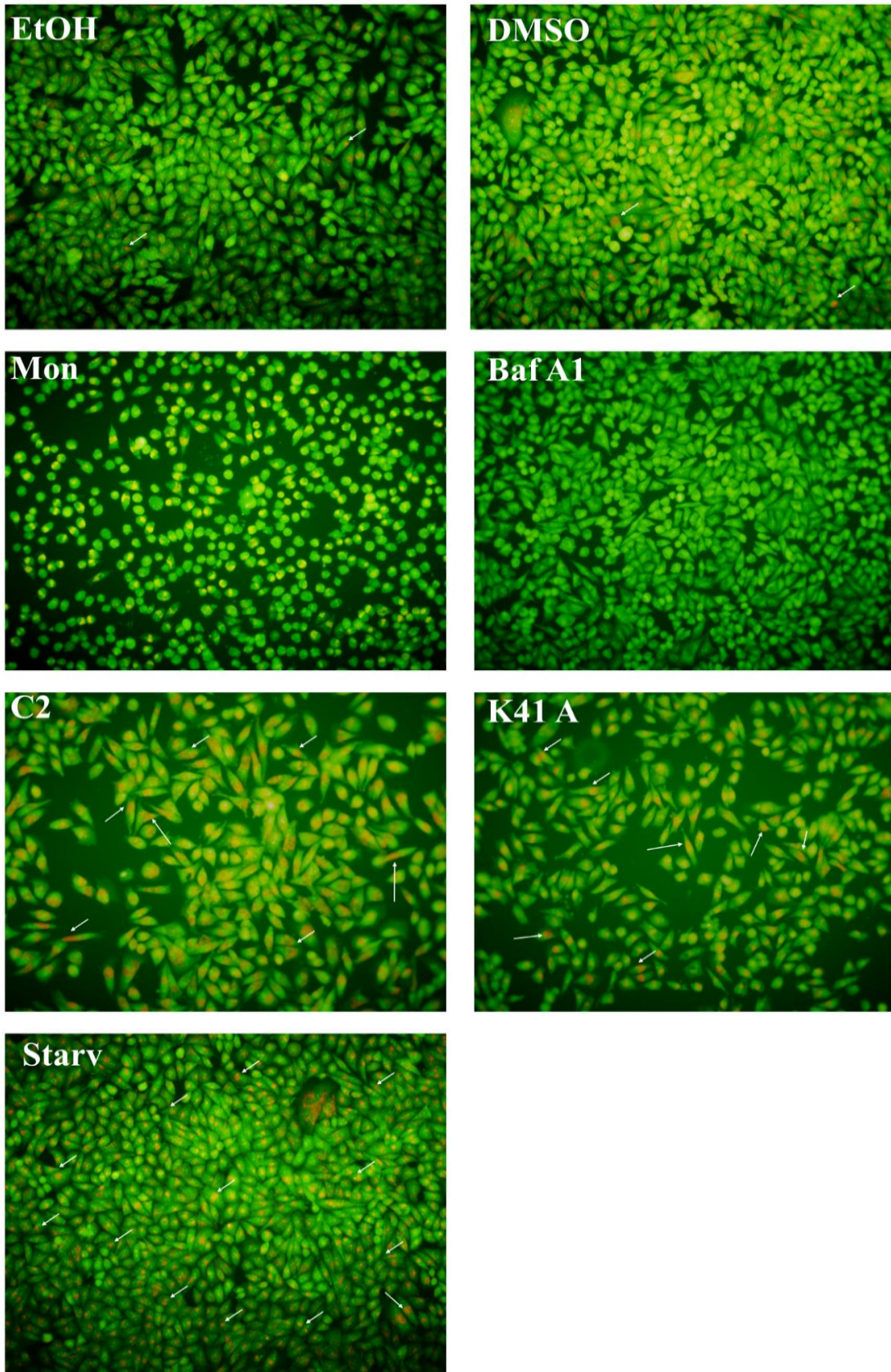


Figure 3.18 Acridine Orange staining of HeLa cell line. EtOH and DMSO: Negative controls of polyether antibiotics. Bafilomycin A1 and Monensin: Autophagy inhibition controls. Starvation: Autophagy induction control. Concentration of the C2 and K41 A: IC₅₀ value, Bafilomycin A1: 100 ng/ml.

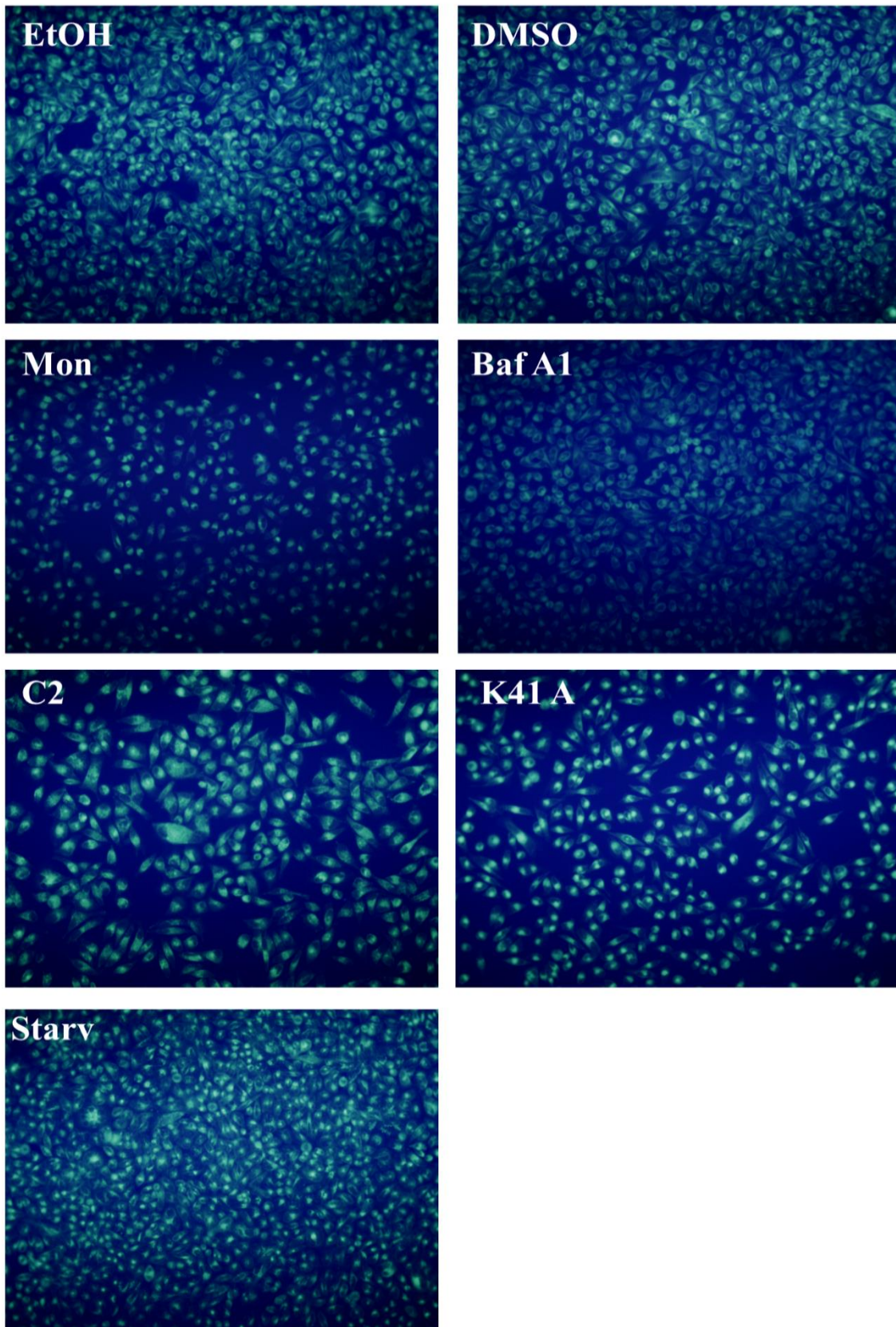


Figure. 3.19 MDC staining of HeLa cell line. EtOH and DMSO: Negative controls of polyether antibiotics. Bafilomycin A1 and Monensin: Autophagy inhibition controls. Starvation: Autophagy induction control. Concentration of the **C2** and **K41 A**: IC₅₀ value, Bafilomycin A1: 100 ng/ml.

3.11. Quantification of Acidic Vacuoles Inside the Cells

Acidic vacuoles inside the cells were quantified from the fluorometry analysis of MDC get trapped in such vacuoles (Figure 3.20). It was observed that in case of polyether antibiotics **C2**, **K41 A** and starvation these acidic compartments get increased compare to their negative controls (EtOH and DMSO). While in case of bafilomycin A1 and monensin these acidic vacuoles become decreased compared to the control groups. Keeping in mind, immunoblotting of autophagy flux markers (LC3-II and p62), MDC and AO staining, these results suggest that, polyether ionophore **C2** and **K41 A** inhibit autophagy at terminal stage however, may not affect the internal pH of these acidic compartments. According to statistical analysis, **C2** and starvation were significantly different from their control. In contrast, regarding monensin and bafilomycin A1 which were known for autophagy inhibition at terminal stage and showed accumulation of autophagy flux markers (LC3-II and p62) by immunoblotting; however, in parallel, they are also known for the demolishing of pH in these acidic compartments which become unable to stain with MDC like acidotropic dyes. That is why in both MDC and AO staining as well as in fluorometry analysis monensin and bafilomycin A1 showed less incorporation of acidotropic dyes. Beside this, during starvation autophagy become induced and consequently number of acidic vacuoles become increased.

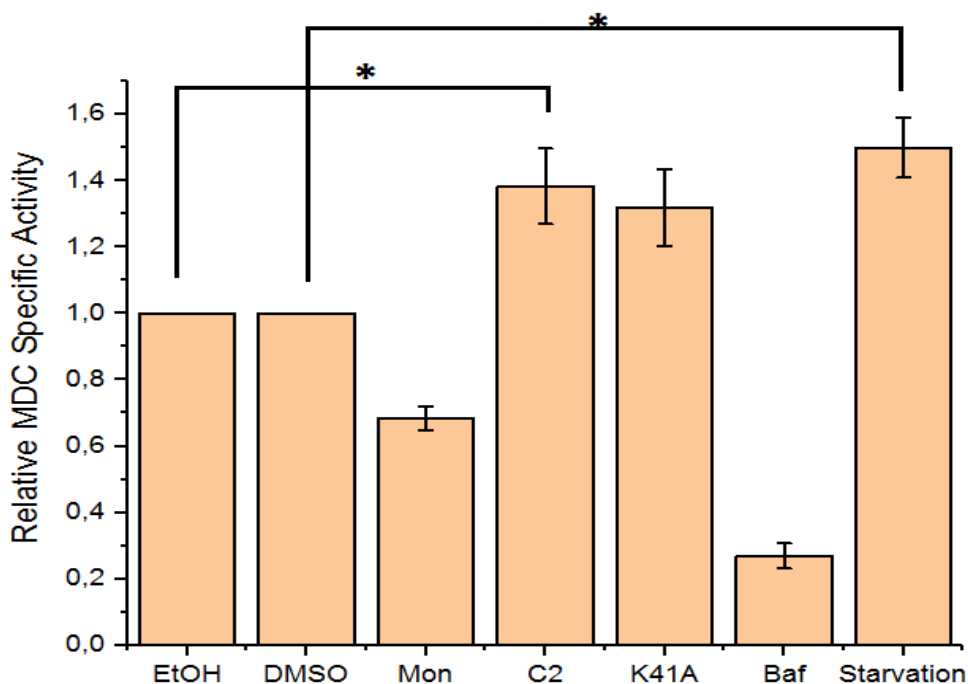


Figure 3.20 Graph showing quantity of acidic vacuoles inside the cells. EtOH and DMSO: Negative controls of polyether antibiotics. Bafilomycin A1 and Monensin: Autophagy inhibition controls. Starvation: Autophagy induction control. Concentration of the **C2** and **K41 A**: IC₅₀ value, Bafilomycin A1: 100 ng/ml. One-way ANOVA with Tukey *post-hoc* analysis. Error bars represents s.e.m. *:p < 0.05.

3.12. Polyether Antibiotics Activate Apoptosis

The polyether antibiotics (**C2**, **K41 A** and monensin) were cytotoxic and inhibit autophagy in all these three cancer cell lines; however, in this study, it was also observed that these antibiotics induced apoptosis in HeLa, CaCo-2 and PC-3 cell lines. In PC-3 cell line, none of the apoptotic markers blotting including caspase or PARP were detected in several trials. Therefore, further studies are required with different techniques to understand and confirm the induction of apoptosis in PC-3 cell line by these polyether antibiotics. As shown in the cytotoxicity results, these antibiotics were cytotoxic toward cancer cell lines where it activated apoptotic pathway. In the case of HeLa cell line, as shown in (Figure 3.21), all of the compounds induced apoptosis by the activation of predominant apoptosis executor caspases at 24-hour treatment at IC₅₀ concentrations. In time course experiment, it was also shown that, among the antibiotics, monensin and **C2** were able to activate apoptosis even at 6-hour treatment at the same concentration. However, in the dose-response experiment, it was found that the concentration of both **C2** and **K41 A** was directly proportional to the induction of

apoptosis. Interestingly, it was also observed that even at lower concentration than IC_{50} values, i.e. quarter or half of IC_{50} , the compounds (**C2** and **K41 A**) were still able to induce apoptosis in HeLa cell line.

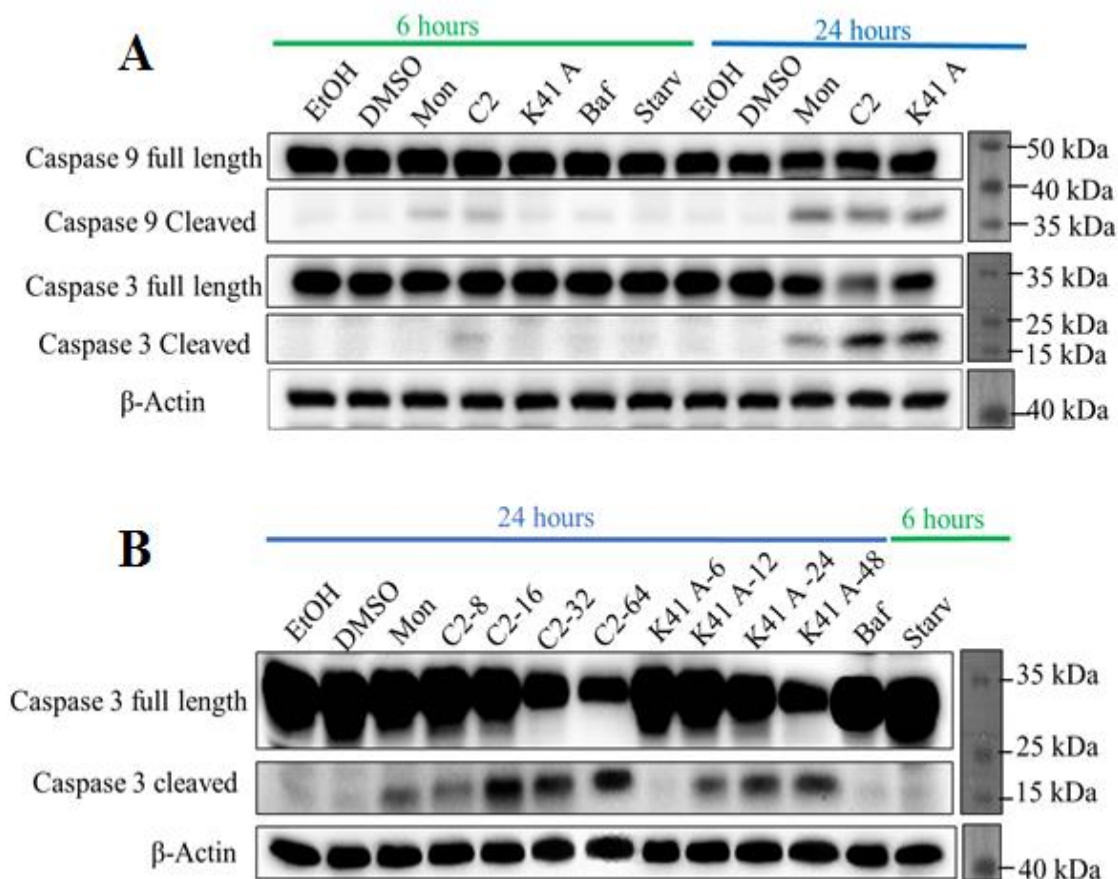


Figure 3.21 A: Western blot images of Caspase 9 and 3 for HeLa cell line in time course study. Concentration of the **C2** and **K41 A**: IC_{50} value, Bafilomycin A1: 100 ng/ml. B: Western blot images of Caspase 3 for HeLa cell line in dose response study. EtOH and DMSO: Negative controls of polyether antibiotics. Bafilomycin A1 and Monensin: Autophagy inhibition controls. Starvation: Autophagy induction control. Concentration of the **C2** and **K41 A**: $\frac{1}{4}$, $\frac{1}{2}$, 1X and 2X of IC_{50} value, Bafilomycin A1: 100 ng/ml.

In parallel with cleaved caspases 9 and 3, it was also observed that the compounds at applied concentrations (IC_{50} value) led to the cleavage of PARP at 89 kDa at 24-hour time point, which further resulted instability of genome and eventually cell death (Figure 3.22). Similarly, it was demonstrated that cleaving of apoptotic marker PARP at 89 kDa was increased in concentration dependent manner of **C2** and **K41 A** in HeLa cell line (Figure 3.22).

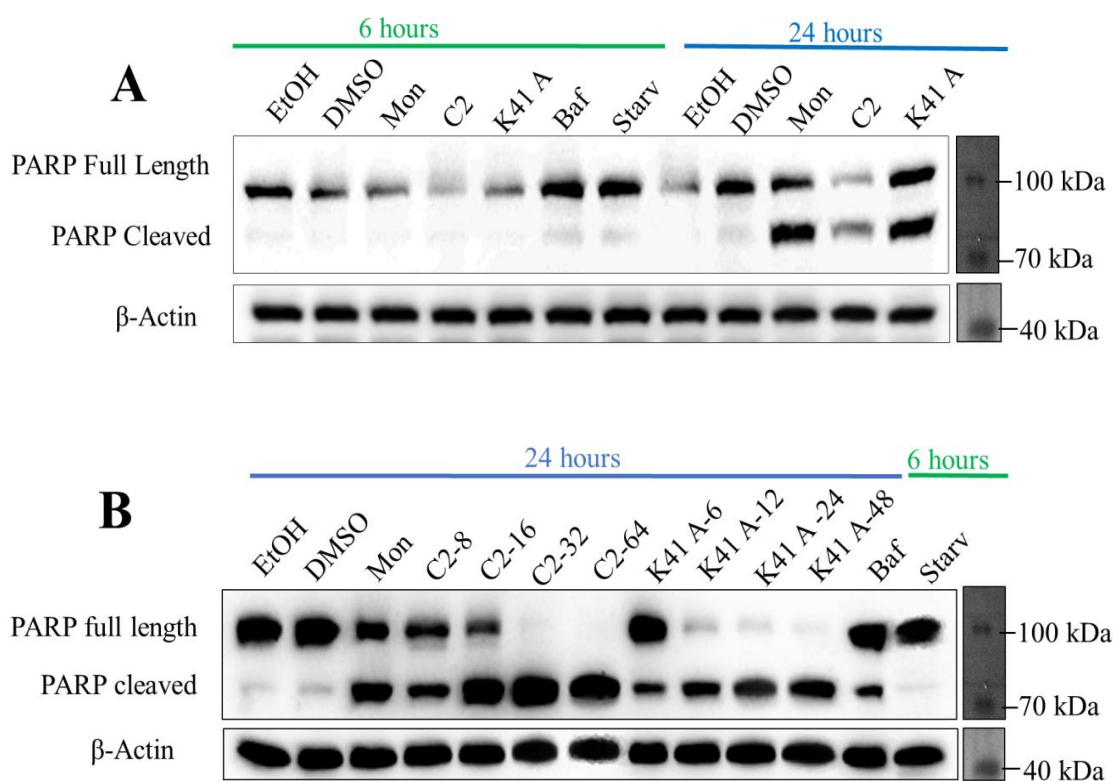


Figure 3.22 A: Western blot images of PARP for HeLa cell line in time course study. Concentration of the **C2** and **K41 A**: IC_{50} value, Bafilomycin A1: 100 ng/ml. B: Western blot images of PARP for HeLa in dose response study. EtOH and DMSO: Negative controls of polyether antibiotics. Bafilomycin A1 and Monensin: Autophagy inhibition controls. Starvation: Autophagy induction control. Concentration of the **C2** and **K41 A**: $\frac{1}{4}$, $\frac{1}{2}$, 1X and 2X of IC_{50} value, Bafilomycin A1: 100 ng/ml.

Similarly, these compounds also cleaved PARP at 89 kDa in CaCo-2 cell line (Figure 3.23) in a time dependent pattern at given concentration (IC_{50} value) resulting genomic instability and eventually cell death.

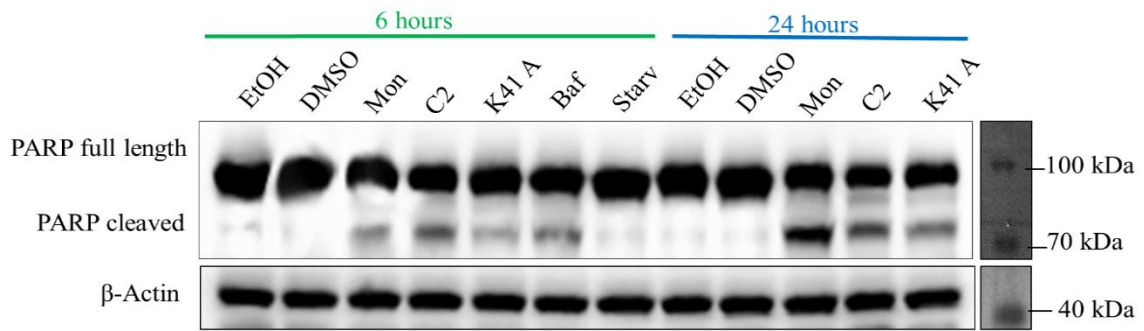


Figure 3.23 Western blot images of PARP for CaCo-2 cell line in time course study. EtOH and DMSO: Negative controls of polyether antibiotics. Bafilomycin A1 and Monensin: Autophagy inhibition controls. Starvation: Autophagy induction control. Concentration of the **C2** and **K41 A**: IC₅₀ value, Bafilomycin A1: 100 ng/ml.

In parallel, it was also seen in this cell line that at 24-hour treatment endoplasmic reticulum (ER) stress increased as shown by the blotting of ER stress markers BIP and CHOP (Figure 3.24). The treatment with these polyether antibiotics resulted in ER stress by upregulation of BIP and CHOP proteins, which might be due to unfolded protein response in this cell line. These results suggest that the treatment time is important for ER stress increasing in time course leading to cellular death at the end. However, further studies are warranted to clear the molecular mechanism of the cytotoxic effect of these polyether antibiotics on studied cancer cell lines.

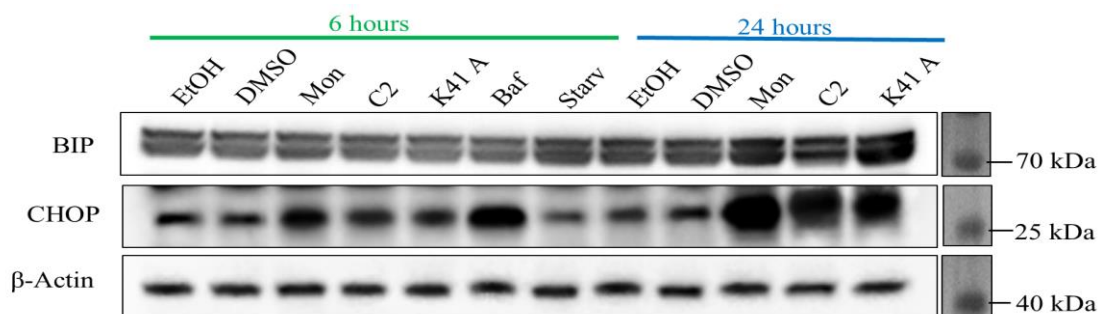


Figure 3.24 Western blot images of ER stress markers (BIP and CHOP) for CaCo-2 cell line in time course study. EtOH and DMSO: Negative controls of polyether antibiotics. Bafilomycin A1 and Monensin: Autophagy inhibition controls. Starvation: Autophagy induction control. Concentration of the **C2** and **K41 A**: IC₅₀ value, Bafilomycin A1: 100 ng/ml.

CHAPTER 4

DISCUSSION

Investigating the biological activity of natural products is a recently blossoming research field, specifically for the development of effective anticancer agents. Majority of these products are purified from microorganisms that have very important role in drug discovery (Huczyński, 2012). Among these natural products, polyether antibiotics are a major class of antibiotics having a broad spectrum of biological activities. These natural products have the ability of forming supramolecular complexes with ions and facilitate the transport of ions across lipid bilayers (Dutton et al., 1995).

Cellular life is compartmentalized with respect to outer environment and even inside the cells. Each compartment has its own concentration of ions for their optimal physiological activity maintained by biological membranes due to its selective transportation control. Variation in this ionic concentration across the membrane leads to cell death (Alfonso and Quesada, 2009). Many research groups have previously reported the anticancer activity of different types of polyether antibiotics against different cancer cell lines in a context dependent manner, like salinomycin, an effective compound against cancer stem cells (Gupta et al., 2009), and monensin active against colon cancer and human lymphoma cells (Park et al., 2002 and 2003a). Similarly, the new polyether antibiotic (**C2**) and the known **K41 A**, used in this study, showed cytotoxic activity against human cancer cell lines like CaCo-2, HeLa, PC-3 cell lines, human healthy cell line like MRC-5 and monkey healthy cell line Vero with different IC₅₀ values as listed in Table 3.1.

Cancer cells are dependent on autophagy more than normal cells due to their altered microenvironment, increased metabolic and biosynthetic demand inflicted by their deregulated proliferation (White, 2015). Autophagy is primarily known for its bulk degradation of cytoplasmic contents by the engulfment in autophagosome structure and their eventual recycling by lysosomal degradation. During this process, autophagy is the target of several pharmacological agents at various steps. In the same track, polyether antibiotics like monensin, nigericin and lasalocid have been reported for their inhibition of lysosomal degradation ability (Grinde, 1983) making them specific autophagy

inhibitors at the terminal stage (Choi et al., 2013). Similarly, polyether antibiotics **C2** and **K41 A** were investigated for their effects on autophagy in cancer cells. In this study, the effect of the compounds were confirmed on autophagy in parallel with previously known inhibitors (monensin and bafilomycin A1), which were used as inhibition controls. Bafilomycin A1 is a macrolide compound that inhibits ATP6V0C/V0 subunit c of V-ATPase H⁺ pump which is responsible for the maintenance of an acidic pH in the lysosomal lumen. In parallel, it also inhibits calcium ATPase Ca-P60A/dSERCA in the ER, responsible for the fusion of autophagosome and lysosome. Due to this dual action of bafilomycin A1, during autophagy, it inhibits both the terminal fusion stage as well the cargo degradation due to inability of lysosomal enzymes at alkaline pH inside lysosomes (Mauvezin and Neufeld, 2015).

For the investigation of autophagy flux, level of both LC3-I and LC3-II proteins were quantified among the samples with respect to actin. LC3-II is one of the reliable marker for mature autophagosome and autophagy flux; however, it is also localized to phagophore. LC3-I or LC3-II only and LC3II/I ratio do not give a complete picture of autophagy flux because of the reduced sensitivity of LC3-I towards LC3 antibodies, degradation of LC3-II over time by lysosomes and different level of LC3-I and II in various cells types. That is why for accurate measurement of autophagy flux, LC3-II/actin ratio should be compared within each sample (Klionsky et al., 2016). Accumulation of LC3-II is the sign of inhibition for autophagosome and lysosome fusion; however, this inhibition can be due to certain reasons, like inhibition of V-ATPase or ATP2A/SERCA Ca²⁺ pump, depolymerisation of microtubules, inhibition of proteins involved during autophagosome and lysosome fusion or rising of the lysosomal pH (Jahreiss et al., 2009).

Similarly, it was observed in this study that the polyether antibiotics **C2** and **K41 A** along with control group monensin led to an increase in the LC3-II/actin ratio over time in all cancer cell lines compared to the inhibition control (bafilomycin A1), suggesting inhibition of autophagy. In parallel, it was also investigated that pattern of LC3-II/actin and p62/actin ratio increased over time in the presence of V-ATPase inhibitor (bafilomycin A1) compared to the single treatment of these polyether antibiotics and bafilomycin A1 alone, suggesting the increase in synthesis of autophagy related membranes and vacuoles over the time and terminal blockage of autophagic flux at the stage of cargo delivery to lysosomes. Besides, during starvation, autophagy

developed, which was characterized by high number of autophagosome formation and fast degradation of LC3-II by lysosomes (Tanida et al., 2005).

Alternatively, p62 (SQSTM1/sequestosome 1) that acts as a selective cargo receptor and binds to LC3-II in developing autophagosome by its LIR domain, can also be measured for the determination of autophagy flux (Bjørkøy et al., 2005). It has been reported that the level of p62 reduces during starvation; while the levels are increased in atg5 deficient mouse fibroblast cells, indicating this protein as an autophagy marker (Nakai et al., 2007). However, due to the versatile role of this protein in many cellular pathways, its expression may also change independent of autophagy, suggesting that autophagy flux can be determined from level of p62 along with other markers (Nakso et al., 2004). Similarly, in this study p62 was also investigated for measuring autophagy flux along with LC3-II in all cancer cell lines. Although, most of the time, p62 accumulation was parallel with LC3-II pattern; however, a few exceptions were also observed especially in the starvation case of CaCo-2 and PC-3 cell lines. Also, in a dose response experiment, its level was consistently decreased as concentration of **C2** and **K41 A** risen, especially at the highest dose where both compounds showed reduction compared to other doses of the test compounds but still higher than the negative controls (EtOH and DMSO) (Figure 3.13). This may be due to the transcriptional regulation of p62 at dose dependent manner or other factors, yet to be elucidated with further studies. Along with this, in parallel with LC3-II accumulation, the combination treatment resulted in increments of p62 levels in the presence of V-ATPase inhibitor bafilomycin A1 (Figure 3.14) suggested the increase in synthesis of autophagic vacuoles and terminal blockage of autophagic flux at the stage of cargo delivery to lysosomes.

Beclin-1 and other Atg proteins are crucial players in the autophagy pathway as shown in Figure 1.5; however, not all of these proteins are essential for the execution of autophagic action. It was demonstrated that under particular circumstances such as treatment of the the cells with pro-apoptotic compounds, some of these proteins could bypass the autophagic pathway (Codogno et al., 2011; Proikas-Cezanne and Codogno, 2011). In HeLa cell line, beclin-1 independent autophagy was reported for compound Z-18 targeting the BH3 binding groove of Bcl-2 protein (Tian et al., 2010). Compounds like etoposide, staurosporine are able to bypass beclin-1, Atg-5, Atg-7, Atg-12 and Atg-16L1 in mouse embryonic fibroblasts and erythroid cells for the formation of autophagosomal structures (Nishida et al., 2009; Honda et al., 2014).

Keeping in mind the significance and bypass of these principal autophagy related proteins, the results observed in this study i:e accumulation of autophagy flux markers LC3-II and p62 and downregulation of beclin-1 and other Atg proteins over time strongly imply the picture of autophagic inhibition. In the case of **C2** and **K41 A**, the autophagic proteins' (beclin-1 and Atgs) downregulation over time may lead to the upstream inhibition of autophagy; however, if they bypass these proteins, still an inhibition of autophagy flux at terminal fusion stage were observed, which was justified by combination treatments here. This flux inhibition can be due to certain factors, like lysosomal malfunction, microtubule destabilization, inhibition of proteins required for autophagosome and lysosomal fusion like membrane tethering complexes, Rab GTPases and SNARE proteins, necessitating further investigations for clear understanding.

Induction of apoptosis by carboxylic polyether antibiotics are known due to their cation transport mechanism across the membrane. These antibiotics are responsible for intracellular Ca^{2+} homeostasis, disruption and loss of mitochondrial membrane potential, which can then lead to oxidative stress by the production of reactive oxygen species (ROS). The resulting ROS activates apoptosis by releasing cytochrome c (cyt c) to the cytosol by outer membrane permeabilization, leading to cleavage of caspases 9, 3 and PARP (Ketola et al., 2010; Kim et al., 2016). Similarly, in this study, it was shown that these polyether antibiotics (monensin, **C2** and **K41 A**) activate apoptosis by the cleaving of caspases 9, 3 and PARP at 89 kilo Dalton (kDa) in both HeLa and CaCo-2 cell lines, giving the picture of apoptosis induction. Additionally, in connection to autophagic inhibition and activation of apoptosis, it is also known that activated caspase 3 degrade various autophagy related proteins like beclin-1 and Atg3 where Atg5 and Atg7 are substrates for activated calpain-1 leading the downregulation of Atg proteins (Cho et al., 2009; Luo and Rubinsztein, 2010; Oral et al., 2012; Pagliarini et al., 2012). Interestingly, the cleaved form of Atg5 is translocated to the mitochondria, and is involved in the induction of apoptosis in an alternative route (Yousefi et al., 2006). Similarly, in this study, it was also observed that as the level of cleaved caspases increased, downregulation of beclin-1 and other Atgs risen during treatment of **C2** and **K41 A** in HeLa cell line, suggesting a direction for the degradation of these proteins (Atgs) by such proteases. However, in this study, measurements of ROS, mitochondrial membrane potential and intracellular Ca^{2+} level were not performed that prevented to make additional comments on this issue.

Consequently, further mechanistic studies are required to connect all the information gained in this study. These forthcoming studies will be valuable in understanding the global molecular mechanism of the polyether antibiotics' cytotoxicity against the cancer cell lines, and their connection between autophagic inhibition and activation of apoptosis.

CHAPTER 5

CONCLUSION

Indeed, treatment of cancer become a challenge for today's scientific world but in parallel it is one of the progressive research field. In this track various natural products are using for their chemotherapeutic purpose. Among these natural products polyether antibiotics were used variously and showed remarkable anticancer activity. Cancer cell lines have increased metabolic demand due to their deregulated proliferation rate. This increased demand become mitigated by upregulation of autophagy pathway in cancer cells. According to previous reported data, some polyether antibiotics like monensin and nigericin are autophagy inhibitors and concurrent treatment of cancer cells with these autophagy inhibitors along with anticancer agents showed efficient anticancer activity. Keeping in mind these findings, this study was performed for the investigation of new polyether antibiotics effects on autophagy. This study revealed that these polyether antibiotics (new one **C2** and known one **K41 A**) were cytotoxic towards three different types of cancer cell lines like HeLa, CaCo-2 and PC-3. Similarly, it was observed that these antibiotics were also active towards human healthy cell line MRC-5 and monkey healthy cell line Vero.

Furthermore, effects of these polyether antibiotics (**C2** and **K41 A**) on autophagy pathway was investigated along with previously known autophagy inhibitor (monensin and bafilomycin A1) on three different cancer cell lines HeLa, CaCo-2 and PC-3. Primarily, this investigation was performed by determining the expression level of autophagy flux markers proteins (LC3-II and p62) along with other autophagy related proteins (Atgs) by using Western blotting technique. It was observed that these polyether antibiotics (**C2** and **K41 A**) have the ability of autophagy flux inhibition due to the accumulation of LC3-II and p62 with respect to housekeeping protein (actin) in comparison with autophagy inhibition control (bafilomycin A1). In parallel, it was also observed that during combine treatment of these antibiotics with known autophagy inhibitor (Bafilomycin A1), increases the synthesis of autophagic vacuoles and block the autophagic flux at the stage of cargo delivery to lysosomes.

Along with this, it was shown that these polyether antibiotics (**C2** and **K41 A**) have a down regulatory effect on beclin-1 and other Atg proteins involved in autophagy pathway. Interestingly, it was observed that monensin which belong from same class of antibiotics didn't show any significant effects on beclin-1 in all cell lines while its effects on other Atgs are context dependent. In parallel, it was observed that, these polyether antibiotics **C2** and **K41 A** led to the accumulation of acidic compartments inside the cells without fluctuating their pH, which become able to stain with acidotropic dyes like MDC and AO. Beside autophagy inhibition, it was also observed that these polyether antibiotics (**C2**, **K41 A** along with monensin) activate apoptosis by cleaving caspase 9, 3 and PARP on 89 kDa in HeLa cell line while cleaving PARP on 89 kDa and induce ER stress in CaCo-2 cell line. This study primarily showed the effects of these polyether antibiotics (**C2** and **K41 A**) on autophagy pathway along with activation of apoptosis in these cancer cell lines. However, further studies should be warranted for understanding the molecular mechanism of action of these polyether antibiotics and crosstalk of autophagy inhibition with apoptosis activation in these cancer cell lines.

REFERENCES

- Aita V.M., Liang X.H., Murty V.V., Pincus D.L., Yu W., Cayanis E., Kalachikov S., Gilliam T.C., Levine B., Cloning and genomic organization of beclin 1, a candidate tumor suppressor gene on chromosome 17q21, *Genomics*, 59 (1999), 59–65.
- Ajaz A.A and Robinson A., Biosynthesis of the Polyether Ionophores Antibiotics Monensin A: Assignment of the Carbon 13 and Proton N.M.R Spectra of Monensin A by two dimensional Spectroscopy. Incorporation of Oxygen 18 labelled Molecular Oxygen, *J. Chem. Soc. Perkin Trans*, 5 (1987), 27 -36.
- Al. Dhaheri Y., Attoub S., Arafat K., Abuqamar S., Eid A., Al. Faresi N., Iratni R., Salinomycin induces apoptosis and senescence in breast cancer: Upregulation of p21, downregulation of surviving and histone H3 and H4 hyperacetylation, *Biochim. Biophys. Acta Gen Subj*, 1830 (2013), 3121–3135.
- Alfonso I. and Quesada R., Biological activity of synthetic ionophores: ion transporters as prospective drugs, *Chem. Sci*, 4, (2009), 3009–3019
- Amaravadi R.K., Yu D., Lum J.J., Bui T., Christophorou M.A., Evan G.I., Thomas T.A., Thompson C.B., Autophagy inhibition enhances therapy-induced apoptosis in a Myc-induced model of lymphoma, *J Clin Invest*, 117 (2007), 326–336.
- Anand P., Kunnumakkara A.B., Sundaram C., Harikumar K.B., Tharakan ST., Lai O.S., Sung B., Aggarwal B.B., Cancer is a preventable disease that requires major lifestyle changes, *Pharmaceutical Research*, 25 (2008), 2097-116.
- Antoszczak M., Rutkowski J., Huczyński A., Structure and Biological Activity of Polyether antibiotics and their Semisynthetic Derivatives, *Bioactive Natural Products: Chemistry and Biology by Wiley-VCH Verlag GmbH & Co. KGaA*, 1 (2015), 107-170.
- Axe E.L., Walker S.A., Manifava M., Chandra P., Roderick H.L., Autophagosome formation from membrane compartments enriched in phosphatidylinositol 3-phosphate and dynamically connected to the endoplasmic reticulum, *J. Cell Biol*, 182 (2008), 685–701.
- Bento C.F., Renna M., Ghislat G., Puri C., Ashkenazi A., Vicinanza M., Menzies F.M., Rubinsztein D.C., Mammalian Autophagy: How Does It Work? *Annu. Rev. Biochem*, 85 (2016), 5.1–5.29
- Biazik J., Yla-Anttila P., Vihinen H., Jokitalo E., Eskelinen E.L., Ultrastructural relationship of the phagophore with surrounding organelles, *Autophagy*, 11 (2015), 439–51.

- Birbrair A., Zhang T., Wang Z.M., Messi M.L., Olson J.D., Mintz A., Delbono O., Type-2 pericytes participate in normal and tumoral angiogenesis, *American Journal of Physiology*, 307 (2014), 25–38.
- Bjørkøy G., Lamark T., Brech A., Outzen H., Perander M., Øvervatn A., Stenmark H., Johansen T., p62/SQSTM1 forms protein aggregates degraded by autophagy and has a protective effect on huntingtin-induced cell death, *J Cell Biol*, 171 (2005), 603-14.
- Boya P., Rosa G.P., Noelia C., Jean L.P., Philippe D., Nathanael L., Didier M., Daniel M., Sylvie S., Tamotsu Y., Ge´rard P., Patrice C., Guido K., Inhibition of Macroautophagy Triggers Apoptosis, *Molecular and cellular biology*, 25 (2005), 1025–1040.
- Brocker C., Engelbrecht-Vandre S., Ungermann C., Multisubunit tethering complexes and their role in membrane fusion, *Curr. Biol*, 20 (2010), 943–52.
- Bursch W., Ellinger A., Kienzl H., Török L., Pandey S., Sikorska M., Walker R., Hermann R.S., Active cell death induced by the anti-estrogens tamoxifen and ICI 164 384 in human mammary carcinoma cells (MCF-7) in culture: the role of autophagy, *Carcinogenesis*, 17 (1996), 1595–1607.
- Callaway T.R., Edringto T.S., Rychlik J.L., Genovese K.J., Poole T.L., Jung Y.S., Bischoff K.M., Anderson R.C., Nisbet D.J., Ionophores: their use as ruminant growth promotants and impact on food safety, *Curr. Issues Intest. Microbiol*, 4 (2003), 43–51.
- Cancer Fact sheet, World Health Organization, (2014), Retrieved 10 June 2014, (Accessed on 20th Mar 2017)
- Cancer Fact sheet, World Health Organization, (2017), Retrieved 12 Feb 2017, (Accessed on 30th Mar 2017).
- Cancer Treatment, National Cancer Institute, <https://www.cancer.gov/about-cancer/treatment/types>, (Accessed on 30th Mar 2017).
- Carter G.T., Schlingmann G., Kenion G.B., Milne L., Allur M.R., Korshalla J.D., Williams D.R., Pinho F., Borders D.B., Martinomycin, a new polyether antibiotic produced by *Streptomyces salvialis*. Part 2, isolation and structure determination, *J Antibiot*, 47 (1994),1549-1553.
- Cemma M., Kim P.K., Brumell J.H., The ubiquitin-binding adaptor proteins p62/SQSTM1 and NDP52 are recruited independently to bacteria-associated microdomains to target *Salmonella* to the autophagy pathway, *Autophagy*, 7 (2011), 341–345.
- Cerruti S.S., Leoni A., Agostini A., Castagnaro M., Efficacy of maduramicin against turkey coccidiosis in battery: a clinical and pathological study, *Schweiz Arch. Tierheilkd*, 138 (1996), 201–206.

- Chan E.Y.W., Longatti A., McKnight N.C., Tooze S.A., Kinase-inactivated ULK proteins inhibit autophagy via their conserved C-terminal domains using an Atg13-independent mechanism, *Mol. Cell. Biol.*, 29 (2009), 157–71.
- Chang Y.Y. and Neufeld T.P., An Atg1/Atg13 complex with multiple roles in TOR-mediated autophagy regulation, *Mol. Biol. Cell.*, 20 (2009). 2004–14.
- Chen D., Fan W., Lu Y., Ding X., Chen S., Zhong Q., A mammalian autophagosome maturation mechanism mediated by TECPR1 and the Atg12-Atg5 conjugate, *Mol. Cell.*, 45 (2012), 629–41.
- Cho D.H., Jo Y.K., Hwang J.J., Lee Y.M., Roh S.A., Kim J.C., Caspase-mediated cleavage of ATG6/Beclin-1 links apoptosis to autophagy in HeLa cells, *Cancer Lett.*, 274 (2009), 95-100.
- Choi H.S., Eun-Hui J., Tae-Gul L., Seo Y.K., Hye-Ryoun K., Cheol, H.K., Autophagy Inhibition with Monensin Enhances Cell Cycle Arrest and Apoptosis Induced by mTOR or Epidermal Growth Factor Receptor Inhibitors in Lung Cancer Cells, *Tuberc Respir Dis (Seoul)*, 75 (2013), 9–17.
- Codogno P., Mehrpour M., Proikas-Cezanne T., Canonical and non-canonical autophagy: variations on a common theme of self-eating, *Nat. Rev. Mol. Cell Biol.*, 13 (2011), 7–12.
- Colombatti M., Dell’Arciprete, L., Chignola R., Tridente G., Carrier protein-monensin conjugates: enhancement of immunotoxin cytotoxicity and potential in tumor treatment, *Cancer Res.*, 50 (1990), 1385–1391.
- Conway D.P., Johnson J.K., Guyonnet V., Long P.L., Smothers C.D., Efficacy of semduramicin and salinomycin against different stages of *Eimeria tenella* and *E. acervulina* in the chicken, *Vet. Parasitol.*, 45 (1993), 215–229.
- Cook K.L., Shajahan A.N., Warri A., Jin L., Hilakivi-Clarke L.A., Clarke R., Glucose regulated protein 78 controls cross-talk between apoptosis and autophagy to determine antiestrogen responsiveness, *Cancer Res.*, 72 (2012), 3337–3349.
- Cuervo A.M. and Wong E., Chaperone-mediated autophagy: roles in disease and aging, *Cell Res.*, 24 (2014), 92–104.
- Degenhardt K., Mathew R., Beaudoin B., Bray K., Anderson D., Chen G., Mukherjee C., Shi Y., Gélinas C., Fan Y., Nelson D.A., Jin S., White E., Autophagy promotes tumor cell survival and restricts necrosis, inflammation, and tumorigenesis, *Cancer Cell.*, 10 (2006), 51–64.
- Deosaran E., Kenneth B., Larsen R.H., Graeme S., Yuqing W., Sarah K., NBR1 acts as an autophagy receptor for peroxisomes, *J. Cell Sci.*, 126 (2013), 939–952.
- Derbyshire E.J., Henry R.V., Stahel R.A., Wawrzynczak E.J., Potent cytotoxic action of the immunotoxin SWA11-ricin A chain against human small cell lung cancer cell lines, *Br. J. Cancer.*, 66 (1992), 444–451.

- Dewar R.L., Vasudevachari M.B., Natarajan V., Salzman N.P., Biosynthesis and processing of human immunodeficiency virus type 1 envelope glycoproteins: Effects of monensin on glycosylation and transport, *J. Virol*, 63 (1989), 2452–2456.
- Diao J., Liu R., Rong Y., Zhao M., Zhang J., ATG14 promotes membrane tethering and fusion of autophagosomes to endolysosomes, *Nature*, 520 (2015), 563–66.
- Ding W.X., Ni H.M., Li M., Liao Y., Chen X., Stolz D.B., Dorn G.W., Yin X.M., Nix is critical to two distinct phases of mitophagy, reactive oxygen species-mediated autophagy induction and Parkin–ubiquitin–p62-mediated mitochondrial priming, *J. Biol. Chem*, 285 (2010), 27879–27890.
- Dirlam J.P., Bordner J., Cullen W.P., Jefferson T., Linabury L.P.J., The structure of CP-96,797, a polyether antibiotic related to K-41A and produced by *Streptomyces* sp, *J Antibiot*, 45 (1992), 1187-1189.
- Dobler M., *Comprehensive Supramolecular Chemistry: Molecular Recognition: Receptors for Cationic Guests*, Pergamon, New York, 1 (2004), 267–313
- Dong T.T., Zhou H.M., Wang L.L., Feng B., Lv B., Zheng M.H., Salinomycin selectively targets ‘CD133+’ cell subpopulations and decreases malignant traits in colorectal cancer lines, *Ann. Surg. Oncol*, 18 (2011), 1797–1804.
- Dooley H.C., Razi M., Polson H.E., Girardin S.E., Wilson M.I., Tooze S.A., WIPI2 links LC3 conjugation with PI3P, autophagosome formation, and pathogen clearance by recruiting Atg12-5-16L1, *Mol. Cell*, 55 (2014), 238–52.
- Dutton C.J., Banks B.J., Cooper C.B., Polyether ionophores, *Natural Product Reports*, 12 (1995), 165–181.
- Ebata E., Kasahara H., Sekine K., Inoue Y., Lysocellin, a new polyether antibiotic. I. Isolation, purification, physico-chemical and biological properties, *J Antibiot*, 28 (1975), 118-121.
- Egan D.F., Shackelford D.B., Mihaylova M.M., Gelino S., Kohnz R.A., Mair, W., Vasquez D.S., Joshi A., Gwinn D.M., Taylor R., Phosphorylation of ULK1 (hATG1) by amp-activated protein kinase connects energy sensing to mitophagy, *Science*, 331 (2011), 456–461.
- Fass E., Shvets E., Degani I., Hirschberg K., Elazar Z., Microtubules support production of starvation induced autophagosomes but not their targeting and fusion with lysosomes, *J. Biol. Chem*, 281 (2006), 6303–16.
- Fuchs D., Daniel V., Sadeghi M., Opelz G., Naujokat, C., Salinomycin overcomes ABC transporter mediated multidrug and apoptosis resistance in human leukemia stem cell-like KG-1a cells, *Biochem. Biophys. Res. Commun*, 394 (2010), 1098–1104.

- Funayama S., Nozoe S., Tronquet C., Anraku Y., Komiyama K., Omura S., Isolation and structure of a new polyether antibiotic, octacyclomycin, *J. Antibiot*, 45 (1992), 1686–1691.
- Gabrielli C., Hemery P., Letellier P., Masure M., Perrot H., Rahmi M.I., Turmine M., Investigation of ion-selective electrodes with neutral ionophores and ionic sites by EIS. II. Application to K⁺ detection, *J. Electroanal. Chem*, 570 (2004), 291–304.
- Gallagher L.E., Williamson L.E., Chan E.Y., Advances in Autophagy Regulatory Mechanisms, *Cell*, 5 (2016), 2-24.
- Ganley I.G., Wong P.M., Gammoh N., Jiang X., Distinct autophagosomal lysosomal fusion mechanism revealed by thapsigargin-induced autophagy arrest, *Mol Cell*, 42 (2011), 731–743.
- Gasparre G., Romeo G., Rugolo M., Porcelli A.M., Learning from oncocytic tumors: why choose inefficient mitochondria, *Biochim Biophys Acta*, 1807, (2011), 633–642.
- Ge L., Melville D., Zhang M., Schekman R., The ER-Golgi intermediate compartment is a key membrane source for the LC3 lipidation step of autophagosome biogenesis, *eLife*, 2 (2013), e00947.
- Ge L., Zhang M., Schekman R., Phosphatidylinositol 3-kinase and COPII generate LC3 lipidation vesicles from the ER-Golgi intermediate compartment, *eLife*, 3 (2014), e04135.
- Gokel G.W., *Comprehensive Supramolecular Chemistry Molecular Recognition Receptors for Cationic Guests*, Pergamon, New York, 1 (2004), 267–313.
- Gonzalez-Malerva L., Park J., Zou L., Hu Y., Moradpour Z., Pearlberg J., Sawyer J., Stevens H., Harlow E., LaBaer J., High-throughput ectopic expression screen for tamoxifen resistance identifies an atypical kinase that blocks autophagy, *Proc Natl Acad Sci USA*, 108 (2011), 2058–2063.
- Griffin T., Rybak M.E., Recht L., Singh M., Salimi A., Raso V., Potentiation of antitumor immunotoxins by liposomal monensin, *J. Natl. Cancer Inst*, 85 (1993), 292–298.
- Grinde B., Effect of Carboxylic Ionophores on Lysosomal Protein Degradation in Rat Hepatocytes, *Experimental Cell Research*, 149 (1983), 27-35.
- Gump J.M., Staskiewicz L., Morgan M.J., Bamberg A., Riches D.W.H., Thorburn A., Autophagy variation within a cell population determines cell fate through selective degradation of Fap-1, *Nat Cell Biol*, 16 (2014), 47–54.

- Guo J.Y., Chen H.Y., Mathew R., Fan J., Strohecker A.M., Karsli-Uzunbas G., Kamphorst J.J., Chen G., Lemons J.M., Karantza V., Coller H.A., Dipaola R.S., Activated Ras requires autophagy to maintain oxidative metabolism and tumorigenesis, *Genes Dev*, 25 (2011), 460–470.
- Guo J.Y. and Eileen W., Autophagy, metabolism and cancer, *Cold Spring Harbor Symposia on Quantitative Biology*, (2016), doi: 10.1101/sqb.2016.81.030981.
- Guo J.Y., Gizem K.U., Robin M., Seena C.A., Autophagy suppresses progression of K-ras-induced lung tumors to oncocytomas and maintains lipid homeostasis, *Genes Dev*, 27 (2013-a), 1447–1461.
- Guo J.Y., Xia B., White E., Autophagy mediated tumor promotion, *Cell*, 155 (2013-b), 1216–1219.
- Gupta P.B., Onder T.T., Jiang G., Tao K., Kuperwasser C., Weinberg R.A., Lander E.S., Identification of selective inhibitors of cancer stem cells by high-throughput screening, *Cell*, 138 (2009), 645–659.
- Guyot J., Jeminet G., Prudhomme M., Sancelme M., Meiniel R., Interaction of the calcium ionophore A. 23187 (Calcimycin) with *Bacillus cereus* and *Escherichia coli*, *Lett. Appl. Microbiol*, 16 (1993), 192–195.
- Hailey D.W., Rambold A.S., Satpute-Krishnan P., Mitra K., Sougrat R., Mitochondria supply membranes for autophagosome biogenesis during starvation, *Cell*, 141 (2010), 656–67.
- Hamasaki M., Furuta N., Matsuda A., Nezu A., Yamamoto A., Autophagosomes form at ER mitochondria contact sites, *Nature*, 495 (2013), 389–93.
- Hanahan D. and Robert A.W., Hallmarks of Cancer: The Next Generation, *Cell*, 144 (2011), 646-74.
- Hara T., Nakamura K., Matsui M., Yamamoto A., Nakahara Y., Suzuki-Migishima R., Yokoyama M., Mishima K., Saito I., Okano H., Mizushima N., Suppression of basal autophagy in neural cells causes neurodegenerative disease in mice, *Nature*, 441 (2006), 885–889.
- Hara T., Takamura A., Kishi C., Iemura S., Natsume T., Guan J.L., Mizushima N., FIP200, a ULK-interacting protein, is required for autophagosome formation in mammalian cells, *J. Cell Biol*, 181 (2008), 497–510.
- Hayashi N.M., Fujita N., Noda T., Yamaguchi A., Yoshimori T., Yamamoto A., A subdomain of the endoplasmic reticulum forms a cradle for autophagosome formation, *Nat. Cell Biol*, 11 (2009), 1433–37.
- He C. and Daniel J.K., Regulation mechanisms and signalling pathways of autophagy, *Annu. Rev. Genet*, 43 (2009), 67–93.

- Hildebrandt J., Meingassner J.G., Mieth H., Mode of action of the anti-coccidial agent septamycine, *Zentralbl Veterinarmed*, 25 (1978), 186–193.
- Hilgenfeld, R. and Saenger, W., Structural chemistry of natural and synthetic ionophores and their complexes with cations, *Topics in Current Chemistry*, 1 (2005), 82.
- Honda S., Arakawa S., Nishida Y., Yamaguchi H., Ishii E., Shimizu S., Ulk1-mediated Atg5-independent macroautophagy mediates elimination of mitochondria from embryonic reticulocytes, *Nat. Commun*, 5 (2014), 4004.
- Hosokawa N., Hara T., Kaizuka T., Kishi C., Takamura A., Nutrient-dependent mTORC1 association with the ULK1-Atg13-FIP200 complex required for autophagy, *Mol. Biol. Cell*, 20 (2009), 1981–91.
- Hoyer-Hansen M. and Jaattela M., Connecting endoplasmic reticulum stress to autophagy by unfolded protein response and calcium, *Cell Death Differ*, 14 (2007), 1576–1582.
- Huczyński A., Janczak J., Stefańska J., Antoszczak M., Brzezinski B., Synthesis and antimicrobial activity of amide derivatives of polyether antibiotic – salinomycin, *Bioorg. Med. Chem. Lett*, 22 (2012-a) 4697–4702.
- Huczyński A., Rutkowski J., Borowicz I., Wietrzyk J., Maj E., Brzezinski B., One-pot synthesis and cytotoxicity studies of new Mannich base derivatives of polyether antibiotic–lasalocid acid, *Bioorg. Med. Chem. Lett*, 23 (2013-a), 5053–5056.
- Huczyński A., Rutkowski J., Brzezinski B., Bartl F., Synthesis, FTIR, ¹H, ¹³C NMR, ESI MS and PM5 studies of a new Mannich base of polyether antibiotic – lasalocid acid and its complexes with Li⁺, Na⁺ and K⁺ cations, *Spectrochim. Acta, Part A*, 104 (2013-b). 497–504.
- Huczyński A., Stefańska J., Przybylski P., Brzezinski B., Bartl F., Synthesis and antimicrobial properties of Monensin A esters, *Bioorg Med Chem Lett*, 18 (2008), 2585–2589.
- Huczyński A., Polyether ionophores—promising bioactive molecules for cancer therapy, *Bioorganic and Medicinal Chemistry Letters*, 22 (2012), 7002–10.
- Huczyński A., Jan J., Daniel Ł., Bogumil B., Monensin A acid complexes as a model of electrogenic transport of sodium cation, *Biochimica et Biophysica Acta*, 1818 (2012-b), 2108–2119.
- Huo Y., Cai H., Teplova I., Bowman-Colin C., Chen G., Price S., Barnard N., Ganesan S., Karantza V., White E., Xia B., Autophagy opposes p53-mediated tumor barrier to facilitate tumorigenesis in a model of PALB2-associated hereditary breast cancer, *Cancer Discov*, 3 (2013), 894–907.

- Hwang K.M., Yang L.C., Carrico C.K., Schulz R.A., Schenkman J.B., Sartorelli A.C., Production of membrane whorls in rat liver by some inhibitors of protein synthesis, *J. Cell Biol*, 62 (1974), 20–31.
- Ishikawa T., Furuno K, Kato K., Ultrastructural studies on autolysosomes in rat hepatocytes after leupeptin treatment, *Exp. Cell Res*, 144 (1983), 15–24.
- Itakura E., Kishi-Itakura C., Mizushima N., The hairpin-type tail-anchored SNARE syntaxin 17 targets to autophagosomes for fusion with endosomes/lysosomes, *Cell*, 151 (2012), 1256–69.
- Itakura E. and Mizushima N., p62 Targeting to the autophagosome formation site requires self-oligomerization but not LC3 binding, *J. Cell Biol*, 192 (2011), 17–27.
- Jahreiss L., Menzies F.M., Rubinsztein D.C., The itinerary of autophagosomes: from peripheral formation to kiss-and-run fusion with lysosomes, *Traffic*, 9 (2008), 574–87.
- Jahreiss L., Renna M., Bittman R., Arthur G., Rubinsztein D.C., 1-OHexadecyl-2-O-methyl-3-O-(2-acetamido-2-deoxy-b-D-glucopyranosyl)-sn-glycerol (Gln) induces cell death with more autophagosomes which is autophagy-independent, *Autophagy*, 5 (2009), 835-846.
- Jordens I., Fernandez-Borja M., Marsman M., Dusseljee S., Janssen L., The Rab7 effector protein RILP controls lysosomal transport by inducing the recruitment of dynein-dynactin motors, *Curr. Biol*, 11 (2001), 1680–85.
- Jung C.H., Jun C.B., Ro S.H., Kim Y.M., Otto N.M., ULK-Atg13-FIP200 complexes mediate mTOR signalling to the autophagy machinery, *Mol. Biol. Cell*, 20 (2009), 1992–2003.
- Kamada Y., Funakoshi T., Shintani T, Nagano K, Ohsumi M, Ohsumi Y., Tor-mediated induction of autophagy via an Apg1 protein kinase complex, *J. Cell Biol*, 150 (2000), 1507–13.
- Karantza W.V., Patel S., Kravchuk O., Chen G., Mathew R., Jin S., White E., Autophagy mitigates metabolic stress and genome damage in mammary tumorigenesis, *Genes Dev*, 21 (2007), 1621–1635.
- Kaur J. and Debnath J., Autophagy at the crossroads of catabolism and anabolism, *Nature Reviews Molecular Cell Biology*, (2015), doi:10.1038/nrm4024.
- Kawamata T., Kamada Y., Kabeya Y., Sekito T., Ohsumi Y., Organization of the pre-autophagosomal structure responsible for autophagosome formation, *Mol. Biol. Cell*, 19 (2008), 2039–50.
- Ketola K., Paula V., Vidal F., Olli K., Kristiina I., Monensin is a potent inducer of oxidative stress and inhibitor of androgen signaling leading to apoptosis in prostate cancer cells, *Mol. Cancer Ther*, 9 (2010), 3175–3185.

- Kim J., Kundu M., Viollet B., Guan K.L., AMPK and MTOR regulate autophagy through direct phosphorylation of ULK1, *Nat. Cell Biol*, 13 (2011-c), 132–141.
- Kim J.H., Chae M.J., Kim W.K., Kim Y.J., Kang H.S., Kim H.S., Yoon S., Salinomycin sensitizes cancer cells to the effects of doxorubicin and etoposide treatment by increasing DNA damage and reducing p21 protein, *Br. J. Pharmacol*, 162 (2011-b), 773–784.
- Kim J.H., Hong S.B., Lee J.K., Han S., Roh K.H., Insights into autophagosome maturation revealed by the structures of ATG5 with its interacting partners, *Autophagy*, 11 (2015), 75–87.
- Kim K.Y., Yu S.N., Lee S.Y., Chun S.S., Choi Y.L., Park Y.M., Song C.S., Chatterjee B., Ahn S.C., Salinomycin-induced apoptosis of human prostate cancer cells due to accumulated reactive oxygenspecies and mitochondrial membrane depolarization, *Biochem. Biophys. Res. Commun*, 413 (2011-a), 80–86.
- Kim S.H., Kwang Y.K., Sun-nyoung Y., Sul-gi P., Hak-sun Y., Young-kyo S., Soon-cheol A., Monensin Induces PC-3 Prostate Cancer Cell Apoptosis via ROS Production and Ca²⁺Homeostasis Disruption, *Anticancer Research*, 36 (2016), 5835-5844.
- Kirisako T., Baba M., Ishihara N., Miyazawa K., Ohsumi M., Formation process of autophagosome is traced with Apg8/Aut7p in yeast, *J. Cell Biol*, 147 (1999), 435–46.
- Kirkin V., Lamark T., Sou Y.S., Bjørkøy G., Nunn J.L., Bruun J.A., Shvets E., McEwan D.G., Clausen T.H., Wild P., Bilusic I., Theurillat J.P., Øvervatn A., Ishii T., Elazar Z., Komatsu M., Dikic I., Johansen T., A role for NBR1 in autophagosomal degradation of ubiquitinated substrates, *Mol. Cell*, 33 (2009-b), 505–516.
- Kirkin V., McEwan D.G., Novak I., Dikic I., A role for ubiquitin in selective autophagy, *Mol. Cell*, 34 (2009-a), 259–269.
- Klionsky D.J. et al., Guidelines for the use and interpretation of assays for monitoring autophagy (3rd edition), *Autophagy*, 12 (2016), 1–222
- Köchl R., Hu X.W., Chan E.Y.W., Tooze S.A., Microtubules facilitate autophagosome formation and fusion of autophagosomes with endosomes, *Traffic*, 7 (2006), 129–145.
- Kuma A., Masahiko H., Makoto M., Akitsugu Y., Haruaki N., Tamotsu Y., Yoshinori O., Takeshi T., Noboru M., The role of autophagy during the early neonatal starvation period, *Nature*, 432 (2004), 1032–1036.
- Laddha S.V., Ganesan S., Chan C.S., White E., Mutational landscape of the essential autophagy gene BECN1 in human cancers, *Mol Cancer Res*, 12 (2014), 485–490.

- Lazaro L.M., The Warburg Effect: Why and How Do Cancer Cells Activate Glycolysis in the Presence of Oxygen, *Anti-Cancer Agents in Medicinal Chemistry*, 8 (2008), 305-312.
- Lee J.W., Park S., Takahashi Y., Wang H.G., The association of ampk with ULK1 regulates autophagy, *PLoS ONE*, 5 (2008), e15394.
- Lee J.Y., Koga H., Kawaguchi Y., Tang W., Wong E., HDAC6 controls autophagosome maturation essential for ubiquitin-selective quality-control autophagy, *EMBO J*, 29 (2010-b), 969–80.
- Levine B. and Kroemer G., Autophagy in the pathogenesis of disease, *Cell*, 132 (2008), 1, 27–42.
- Levy J.M. and Thorburn A., Targeting autophagy during cancer therapy to improve clinical outcomes, *Pharmacol Ther*, 131 (2011), 130–141.
- Li T., Su L., Zhong N., Hao X., Zhong D., Singhal S., Liu X., Salinomycin induces cell death with autophagy through activation of endoplasmic reticulum stress in human cancer cells, *Autophagy*, 9 (2013-a), 1057–1068.
- Li W.W., Li J., Bao J.K., Microautophagy: lesser known self-eating, *Cell. Mol. Life Sci*, 69 (2012), 1125–1136.
- Liang C., Lee J.S., Inn K.S., Gack M.U., Li Q., Beclin1-binding UVRAG targets the class C Vps complex to coordinate autophagosome maturation and endocytic trafficking, *Nat. Cell Biol*, 10 (2008), 776–87.
- Liang X.H., Jackson S., Seaman M., Brown K., Kempkes B., Hibshoosh H., Levine B., Induction of autophagy and inhibition of tumorigenesis by beclin 1, *Nature*, 402 (1999), 672–676.
- Lim J., Yunsu L., Hyun-Wook K., Im J.R., Myung S.O., Moussa B.H.Y., Zhenyu Y., Young J.O., Nigericin-induced Impairment of Autophagic Flux in Neuronal Cells Is Inhibited by Overexpression of Bak, *J Biol Chem*, 287 (2012), 23271–23282.
- Ling Y., Priebe W., Perezsoler R., Intrinsic cytotoxicity and reversal of multidrug-resistance by monensin in KB parent and MDR cells, *Int. J. Oncol*, 3 (1993), 971–977.
- Liu L., Feng D., Chen G., Chen M., Zheng Q., Song P., Ma Q., Zhu C., Wang R., Qi W., Huang L., Xue P., Li B., Wang X., Jin H., Wang J., Yang F., Liu P., Zhu Y., Sui S., Chen Q., Mitochondrial outer-membrane protein FUNDC1 mediates hypoxia-induced mitophagy in mammalian cells, *Nat. Cell Biol*, 14 (2012), 177–185.
- Liu L., Yang M., Kang R., Wang Z., Zhao Y., Yu Y., Xie M., Yin X., Livesey K.M., Lotze M.T., HMGB1-induced autophagy promotes chemotherapy resistance in leukemia cells, *Leukemia*, 25 (2011), 23–31.

- Lock R., Kenific C.M., Leidal A.M., Salas E., Debnath J., Autophagy-dependent production of secreted factors facilitates oncogenic RAS-driven invasion, *Cancer Discov*, 4 (2014), 4, 466–479.
- Lu D., Choi M.Y., Yu J., Castro J.E., Kipps T.J., Carson D.A., Salinomycin inhibits Wnt signaling and selectively induces apoptosis in chronic lymphocytic leukemia cells, *Proc. Natl. Acad. Sci. U.S.A*, 108 (2011), 13253–13257.
- Luo S. and Rubinsztein D.C., Apoptosis blocks Beclin 1-dependent autophagosome synthesis: an effect rescued by Bcl-xL, *Cell Death Differ*, 17 (2010), 268–277.
- Ma X.H., Piao S., Wang D., McAfee Q.W., Nathanson K.L., Lum J.J., Li L.Z., Amaravadi R.K., Measurements of tumor cell autophagy predict invasiveness, resistance to chemotherapy, and survival in melanoma, *Clin Cancer Res*, 17 (2011), 3478–3489.
- Masiero E., Agatea L., Mammucari C., Blaauw B., Loro E., Komatsu M., Metzger D., Reggiani C., Schiaffino S., Sandri M., Autophagy is required to maintain muscle mass, *Cell Metab*, 10 (2009), 507–515.
- Mathew R., Karp C.M., Beaudoin B., Vuong N., Chen G., Chen H.Y., Bray K., Reddy A., Bhanot G., Gelinas C., Dipaola R.S., Karantza-Wadsworth V., White E., Autophagy suppresses tumorigenesis through elimination of p62, *Cell*, 137 (2009), 1062–1075.
- Mathew R., Kongara S., Beaudoin B., Karp C.M., Bray K., Degenhardt K., Chen G., Jin S., White E., Autophagy suppresses tumor progression by limiting chromosomal instability, *Genes Dev*, 21 (2007), 1367–1381.
- Mauvezin C. and Neufeld T.P., Bafilomycin A1 disrupts autophagic flux by inhibiting both V-ATPase-dependent acidification and Ca-P60A/SERCA-dependent autophagosome-lysosome fusion, *Autophagy*, 11 (2015), 1437–1438.
- Maycotte P. and Thorburn A., Autophagy and cancer therapy, *Cancer Biol Ther*, 11 (2011), 127–137.
- McEwan D.G., Popovic D., Gubas A., Terawaki S., Suzuki H., PLEKHM1 regulates autophagosome-lysosome fusion through HOPS complex and LC3/GABARAP proteins, *Mol. Cell*, 57 (2015), 39–54.
- Mercer C.A., Kaliappan A., Dennis P.B., A novel, human Atg13 binding protein, Atg101, interacts with ULK1 and is essential for macroautophagy, *Autophagy*, 5 (2009), 649–662.
- Mimouni M., Khardli F.Z., Warad I., Ahmad M., Mubarak M.S., Sultana S., Hadda, T.B., Antimicrobial activity of naturally occurring antibiotics monensin, lasalocid and their metal complexes, *J. Mater. Environ. Sci*, 5 (2014), 207–214.

- Mizushima N. and Klionsky D.J., Protein turnover via autophagy: implications for metabolism, *Annu. Rev. Nutr.*, 27 (2007), 19–40.
- Mizushima N. and Komatsu M., Autophagy: renovation of cells and tissues, *Cell*, 147 (2011), 728–741
- Mizushima N., Noda T., Yoshimori T., Tanaka Y., Ishii T., A protein conjugation system essential for autophagy, *Nature*, 395 (1998), 395–98.
- Mizushima N., Yoshimori T., Ohsumi Y., The role of Atg proteins in autophagosome formation, *Annu. Rev. Cell Dev. Biol.*, 27 (2011), 107–32.
- Mollenhauer H.H., Morr  D.J., Rowe L.D., Alteration of intracellular traffic by monensin; mechanism, specificity and relationship to toxicity, *Biochim Biophys Acta*, 1031 (1990), 225-46.
- Mostowy S., Vanessa S.S., M lanie A.H., Roxane S., Roland B., Terje J., Pascale C., p62 and NDP52 proteins target intracytosolic Shigella and Listeria to different autophagy pathways, *J. Biol. Chem.*, 286 (2011), 26987–26995.
- Munir K., Muneer M.A., Khan M.Z., Immunomodulatory effects of salinomycin sodium in broiler chickens, *Pakistan Vet. J.*, 14 (1994), 171–179.
- Murrow L. and Debnath J., Autophagy as a stress-response and quality-control mechanism implications for cell injury and human disease, *Annu Rev Pathol*, 8 (2013), 105–137.
- Nair U., Yen W.L., Mari M., Cao Y., Xie Z., A role for Atg8-PE de-conjugation in autophagosome biogenesis, *Autophagy*, 8 (2012), 780–93.
- Nakai A., Yamaguchi O., Takeda T., Higuchi Y., Hikoso S., Taniike M., Omiya S., Mizote I., Matsumura Y., Asahi M., Nishida K., Hori M., Mizushima N., Otsu K., The role of autophagy in cardiomyocytes in the basal state and in response to hemodynamic stress, *Nat Med*, 13 (2007), 619-24.
- Nakamura M., Kunimoto S., Takahashi Y., Naganawa H., Sakaue M., Inoue S., Ohno T., Takeuchi T., Inhibitory effects of polyethers on human immunodeficiency virus replication, *Antimicrob. Agents Chemother*, 36 (1992), 492–494.
- Nakaso K., Yoshimoto Y., Nakano T., Takeshima T., Fukuhara Y., Yasui K., Araga S., Yanagawa T., Ishii T., Nakashima K., Transcriptional activation of p62/A170/ZIP during the formation of the aggregates: Possible mechanisms and the role in Lewy body formation in Parkinson’s disease, *Brain Res*, 1012 (2004), 42-51.
- Narendra D., Kane L.A., Hauser D.N., Fearnley I. M., Youle R.J., p62/SQSTM1 is required for Parkin-induced mitochondrial clustering but not mitophagy; VDAC1 is dispensable for both, *Autophagy*, 6 (2010), 1090–1106.

- Naujokat C., Fuchs D., Opelz G., Salinomycin in cancer: a new mission for an old agent, *Mol. Med. Rep*, 3 (2010), 555–559.
- Nishida Y., Arakawa S., Fujitani K., Yamaguchi H., Mizuta T., Kanaseki T., Komatsu, M., Otsu K., Tsujimoto Y., Shimizu S., Discovery of Atg5/Atg7-independent alternative macroautophagy, *Nature*, 461 (2009), 654–658.
- Nixon R.A., The role of autophagy in neurodegenerative disease, *Nature Medicine*, 19 (2013), 983–997.
- Ohkuma S. and Poole B., Fluorescence probe measurement of the intralysosomal pH in living cells and the perturbation of pH by various agents, *Proc natl acad sci*, 75 (1978), 3327.
- Oltersdorf T., Elmore S.W., Shoemaker A.R., Armstrong R.C., Augeri D.J., Belli B.A., Bruncko M., Deckwerth T.L., Dinges J., Hajduk P.J., An inhibitor of Bcl-2 family proteins induces regression of solid tumors, *Nature*, 435 (2005), 677–681.
- Oral O., Oz-Arslan D., Itah Z., Naghavi A., Deveci R., Karacali S., Gozuacik D., Cleavage of Atg3 protein by caspase-8 regulates autophagy during receptor-activated cell death, *Apoptosis*, 17 (2012), 810-820.
- Orsi A., Razi M., Dooley H.C., Robinson D., Weston A.E., Dynamic and transient interactions of Atg9 with autophagosomes, but not membrane integration, are required for autophagy, *Mol. Biol. Cell*, 23 (2012), 1860–73.
- Özcan K., Semiha Ç.A., Kalkan A.U., Hames K., Erdal B., Diversity and antibiotic-producing potential of cultivable marine-derived actinomycetes from coastal sediments of Turkey, *Journal of soil and sediments*, 13 (2013), 1493–1501.
- Parajuli B., Lee H.G., Kwon S.H., Cha S.D., Shin S.J., Lee G.H., Bae I., Cho C.H., Salinomycin inhibits Akt/NF-KB and induces apoptosis in cisplatin resistant ovarian cancer cells, *Cancer Epidemiol*, 37 (2013), 512–517.
- Park W.H., Kim E.S., Jung C.W., Kim B.K., Lee Y.Y., Monensin mediated growth inhibition of SNU-C1 colon cancer cells via cell cycle and apoptosis, *Int. J. Oncol*, 22 (2003-a), 377–382.
- Park W.H., Kim E.S., Kim B.K., Lee Y.Y., Monensin-mediated growth inhibition in NCI-H929 myeloma cells via cell cycle arrest and apoptosis, *Int. J. Oncol*, 23 (2003-b), 197–204.
- Park W.H., Seol J.G., Kim E.S., Kang W.K., Im Y.H., Jung C.W., Kim B.K., Lee, Y.Y., Monensin mediated growth inhibition in human lymphoma cells through cell cycle arrest and apoptosis, *Br. J. Haematol*, 119 (2002), 400–407.
- Pattingre S., Tassa A., Qu X., Garuti R., Liang X.H., Mizushima N., Packer M., Schneider M.D., Levine B., Bcl-2 antiapoptotic proteins inhibit Beclin 1-dependent autophagy, *Cell*, 122 (2005), 927–939.

- Pfisterer S.G., Bakula D., Frickey T., Cezanne A., Brigger D., Lipid droplet and early autophagosomal membrane targeting of Atg2A and Atg14L in human tumor cells, *J. Lipid Res*, 55 (2005), 1267–78.
- Podila G.K., Rosen E., San Francisco M.J.D., Kolattukudy P.E., Targeted secretion of cutinase in *Fusarium solani* f.sp. pisi and *Colletotrichum gloeosporioides*, *Phytopathology*, 85 (1995), 238–242.
- Poli F., Pancaldi S., Vannini G.L., The effect of monensin on chitin synthesis in *Candida albicans* blastospores, *Eur. J. Cell Biol*, 42 (1986), 79–83.
- Popovic D. and Dikic I., TBC1D5 and the AP2 complex regulate ATG9 trafficking and initiation of autophagy, *EMBO Rep*, 15 (2014), 392–401.
- Poteryaev D., Datta S., Ackema K., Zerial M., Spang A., Identification of the switch in early-to-late endosome transition, *Cell*, 141 (2010), 497–508.
- Pressman B.C., Biological application of ionophores, *Ann rev biochem*, 45 (1976), 501.
- Proikas-Cezanne, T. and Codogno P., Beclin 1 or not Beclin 1. *Autophagy*, 7 (2011), 671–672.
- Pryor P.R., Mullock B.M., Bright N.A., Lindsay M.R., Gray S.R., Combinatorial SNARE complexes with VAMP7 or VAMP8 define different late endocytic fusion events, *EMBO Rep*, 5 (2004), 590–95.
- Puri C., Renna M., Bento C.F., Moreau K., Rubinsztein D.C., Diverse autophagosome membrane sources coalesce in recycling endosomes, *Cell*, 154 (2013), 1285–99.
- Qadir M.A., Kwok B., Dragowska W.H., To K.H., Le D., Bally M.B., Gorski S.M., Macroautophagy inhibition sensitizes tamoxifen-resistant breast cancer cells and enhances mitochondrial depolarization, *Breast Cancer Res Treat*, 112 (2008), 389–403.
- Qu X., Yu J., Bhagat G., Furuya N., Hibshoosh H., Troxel A., Rosen J., Eskelinen E.L., Mizushima N., Ohsumi Y., Cattoretti G., Levine B., Promotion of tumorigenesis by heterozygous disruption of the beclin 1 autophagy gene, *J Clin Invest*, 112 (2003), 1809–1820.
- Rabinowitz J.D. and White E., Autophagy and metabolism, *Science*, 330 (2010), 1344–1348.
- Rao S., Tortola L., Perlot T., Wirnsberger G., Novatchkova M., Nitsch R., Sykacek P., Frank L., Schramek D., Komnenovic V., Sigl V., Aumayr K., Schmauss G., Fellner N., Handschuh S., Glösmann M., Pasierbek P., Schleder M., Resch G.P., Ma Y., Yang H., Popper H., Kenner L., Kroemer G., Penninger J.M., A dual role for autophagy in a murine model of lung cancer, *Nat Commun*, 5 (2014), 3056.

- Ravikumar B., Acevedo-Arozena A., Imarisio S., Berger Z., Vacher C., Dynein mutations impair autophagic clearance of aggregate-prone proteins, *Nat. Genet.*, 37 (2005), 771–76.
- Ravikumar B., Moreau K., Jahreiss L., Puri C., Rubinsztein D.C., Plasma membrane contributes to the formation of pre-autophagosomal structures, *Nat. Cell Biol.*, 12 (2010), 747–57.
- Riddell F.G., Structure, conformation, and mechanism in the membrane transport of alkali metal ions by ionophoric antibiotics, *Chirality.*, 14 (2002), 121–125.
- Rogov V.V., Hironori S., Evgenij F., Philipp W., Andreas K., Alexis R., Ryuichi K., Masato K., David G.M., Frank L., Peter G U., Ivan D., Soichi W., Volker D., Structural basis for phosphorylation-triggered autophagic clearance of Salmonella, *Biochem. J.*, 454 (2013), 459–466.
- Rosenfeldt M.T., O'Prey J., Morton J.P., Nixon C., MacKay G., Mrowinska A., Au A., Rai T.S., Zheng L., Ridgway R., Adams P.D., Anderson K.I., Gottlieb E., Sansom O.J., Ryan K.M., p53 status determines the role of autophagy in pancreatic tumor development, *Nature*, 504 (2013), 296–300.
- Russell R.C., Tian, Y., Yuan H., Park H.W., Chang Y.Y., Kim J., Kim H, Neufeld T.P., Dillin A., Guan K.L., ULK1 induces autophagy by phosphorylating beclin-1 and activating VPS34 lipid kinase, *Nat. Cell Biol.*, 15 (2013), 741–750.
- Rutkowski J. and Brzezinski B., Structures and Properties of Naturally Occurring Polyether Antibiotics, *BioMed Research International*, (2013), Article ID 162513, 31 pages.
- Sakoh N.M., Matoba K., Asai E., Kirisako H., Ishii J., Atg12-Atg5 conjugate enhances E2 activity of Atg3 by rearranging its catalytic site, *Nat. Struct. Mol. Biol.*, 20 (2013), 433–39.
- Samaddar J.S., Gaddy V.T., Duplantier J., Thandavan S.P., Shah M., Smith M.J., Browning D., Rawson J., Smith S.B., Barrett J.T., A role for macroautophagy in protection against 4-hydroxytamoxifen-induced cell death and the development of antiestrogen resistance, *Mol Cancer Ther.*, 7 (2008), 2977–2987.
- Sandoval H., Thiagarajan P., Dasgupta S.K., Schumacher A., Prchal J.T., Chen M., Wang J., Essential role for Nix in autophagic maturation of erythroid cells, *Nature*, 454 (2008), 232–235.
- Scott R.C., Juhasz G., Neufeld T.P., Direct induction of autophagy by Atg1 inhibits cell growth and induces apoptotic cell death, *Curr. Biol.*, 17 (2007), 1–11.
- Seidel A., In *Kirk-Othmer Encyclopedia of Chemical Technology*, fifth, John Wiley and Sons, United State. (2006), 119-148.

- Semiha Ç.A., Denizel sediment örneklerinden biyoaktif metabolit üretici aktinomisetlerin kültürel ve moleküler yöntemlerle karakterizasyonu ve biyoaktif metabolitlerin saflaştırılması, Doctoral thesis, (2014), Defence; 05.06.2014.
- Shang L., Chen S., Du F., Li S., Zhao L., Wang X., Nutrient starvation elicits an acute autophagic response mediated by ULK1 dephosphorylation and its subsequent dissociation from AMPK, *Proc. Natl. Acad. Sci*, 108 (2011), 4788–4793.
- Shen S., Kepp O., Michaud M., Martins I., Minoux H., Métivier D., Maiuri M.C., Kroemer R.T., Kroemer G., Association and dissociation of autophagy, apoptosis and necrosis by systematic chemical study, *Oncogene*, 30 (2011), 4544–4556.
- Slobodkin M.R. and Elazar Z., The Atg8 family: multifunctional ubiquitin-like key regulators of autophagy, *Essays Biochem*, 55 (2013), 51–64.
- Sousa-Junior J.N., Bruno A.R., Marilda D.A., Ana P.F.P., Luiz A.B.M., Yassuko I., Paul J.G., Anderson R.M.O., Norberto P.L., Biomimetic oxidation studies of monensin A catalyzed by metalloporphyrins: identification of hydroxyl derivative product by electrospray tandem mass spectrometry, *Rev. bras. Farmacogn*, 23 (2013), 4.
- Stolz A., Ernst A., Dikic I., Cargo recognition and trafficking in selective autophagy, *Nat. Cell Biol*, 16 (2014), 495–501.
- Strohecker A.M., Guo J.Y., Karsli-Uzunbas G., Price S.M., Chen G.J., Mathew R., McMahon M., White E., Autophagy sustains mitochondrial glutamine metabolism and growth of BrafV600E-driven lung tumors, *Cancer Discov*, 3 (2013), 1272–1285.
- Sun B. and Karin M., Inflammation and liver tumorigenesis, *Front Med*, 7 (2013), 242–254.
- Takamura A., Komatsu M., Hara T., Sakamoto A., Kishi C., Waguri S., Eishi Y., Hino O., Tanaka K., Mizushima N., Autophagy-deficient mice develop multiple liver tumors. *Genes Dev*, 25 (2011), 795–800.
- Tang D., Kang R., Cheh C.W., Livesey K.M., Liang X., Schapiro N.E., Benschop R., Sparvero L.J., Amoscato A.A., Tracey K.J., HMGB1 release and redox regulates autophagy and apoptosis in cancer cells, *Oncogene*, 29 (2010-a), 5299–5310.
- Tang D., Kang R., Livesey K.M., Cheh C.W., Farkas A., Loughran P., Hoppe G., Bianchi M.E., Tracey K.J., Zeh H.J., Endogenous HMGB1 regulates autophagy, *J Cell Biol*, 190 (2010-b), 881–892.

- Tanida I., Minematsu-Ikeguchi N., Ueno T., Kominami E., Lysosomal turnover, but not a cellular level, of endogenous LC3 is a marker for autophagy, *Autophagy*, 1 (2005), 84-91.
- Tartakoff A. and Vassalli P., Plasma cell immunoglobulin secretion: arrest is accompanied by alterations of the golgi complex, *J exp med*, 146 (1977), 1332.
- Thorburn A., Douglas H.T., Daniel L.G., Autophagy and cancer therapy, *Mol. Pharmacol*, 85 (2014), 830–838.
- Thorburn J., Horita H., Redzic J., Hansen K., Frankel A.E., Thorburn A., Autophagy regulates selective HMGB1 release in tumor cells that are destined to die. *Cell Death Differ*, 16 (2009), 175–183.
- Thurston T.L., Wandel M.P., Von M.N., Foeglein A., Randow F., Galectin 8 targets damaged vesicles for autophagy to defend cells against bacterial invasion, *Nature*, 482 (2012), 414–418.
- Tian S., Lin J., Jun Z.J., Wang X., Li Y., Ren X., Yu W., Zhong W., Xiao J., Sheng F., Chen Y., Jin C., Li S., Zheng Z., Xia B., Beclin 1-independent autophagy induced by a Bcl-XL/Bcl-2 targeting compound, Z18, *Autophagy*, 6 (2010), 1032–1041.
- Tsuji N., Nagashima K., Terui Y., Tori K., Structure of K-41B, a new diglycoside polyether antibiotic, *J Antibiot*, 32 (1979), 169-171.
- Tumbarello, D.A., Waxse B.J., Arden S.D., Bright N.A., Kendrick-Jones J., Buss F., Autophagy receptors link myosin VI to autophagosomes to mediate Tom1-dependent autophagosome maturation and fusion with the lysosome, *Nat Cell Biol*, 14 (2012), 1024–35.
- Velikkakath A.K., Nishimura T., Oita E., Ishihara N., Mizushima N., Mammalian Atg2 proteins are essential for autophagosome formation and important for regulation of size and distribution of lipid droplets, *Mol. Biol. Cell*, 23 (2012), 896–909.
- Wang Y., Effects of Salinomycin on cancer stem cell in human lung adenocarcinoma A549 cells, *Med. Chem*, 7 (2011), 106–111.
- Warburg O., On the origin of cancer cells, *Science*, 123 (1956), 309-14.
- Wei H., Wei S., Gan B., Peng X., Zou W., Guan J.L., Suppression of autophagy by FIP200 deletion inhibits mammary tumorigenesis, *Genes Dev*, 25 (2011), 1510–1527.
- Wei Y., Zou Z., Becker N., Anderson M., Sumpter R., Xiao G., Kinch L., Koduru P., Christudass C.S., Veltri R.W., EGFR-mediated Beclin 1 phosphorylation in autophagy suppression, tumor progression, and tumor chemoresistance, *Cell*, 154 (2013), 1269–1284.

- Weidberg H., Shvets E., Shpilka T., Shimron F., Shinder V., Elazar Z., LC3 and GATE-16/GABARAP subfamilies are both essential yet act differently in autophagosome biogenesis, *EMBO J*, 29 (2010), 792–802.
- Westley J.W., Polyether antibiotics: versatile carboxylic acid ionophores produced by *Streptomyces*, *Adv. Appl Microbiol*, 22 (1977), 177–223.
- Westley J.W., Polyether Antibiotics: Naturally Occurring Acid Ionophores, Marcel Dekker Inc., New York. 1 (1982).
- White E., The role for autophagy in Cancer, *The journal of clinical investigation*, 125 (2015), 42–46.
- White E., De-convoluting the context -dependent role for autophagy in cancer, *Nat Rev Cancer*, 12 (2012), 401–410.
- White E., Exploiting the bad eating habits of Rasdriven cancers, *Genes Dev*, 27 (2013), 2065–2071.
- Wild P., Farhan H., McEwan D.G., Wagner S., Rogov V.V., Brady N.R., Richter B., Korac J., Waidmann O., Choudhary C., Dötsch V., Bumann D., Dikic I., Phosphorylation of the autophagy receptor optineurin restricts Salmonella growth, *Science*, 333 (2011), 228–233.
- Wild P.M., McEwan D., Dikic I., The LC3 interactome at a glance, *J. Cell Sci*, 127 (2014), 3–9.
- Wong P.M., Feng Y., Wang J., Shi R., Jiang X., Regulation of autophagy by coordinated action of MTORC1 and protein phosphatase 2A, *Nat. Commun*, 6 (2015), 8048.
- Wood D.J., Rumsby M.G., Warr J.R., Monensin and verapamil do not alter intracellular localization of daunorubicin in multidrug resistant human KB cells, *Cancer Lett*, 108 (1996), 41–47.
- Yang L. and Colditz G.A., An Active Lifestyle for Cancer Prevention, *J Natl Cancer Inst*, 106 (2014), dju135.
- Yonekawa T. and Thorburn A., Autophagy and cell death, *Essays Biochem*, 55 (2013), 105–117.
- Yoon M.J., You J.K., In Y.K., Eun H.K., Ju A.L., Jun H.L., Taeg K.K., Kyeong S.C., Monensin, a polyether ionophore antibiotic, overcomes TRAIL resistance in glioma cells via endoplasmic reticulum stress, DR5 upregulation and c-FLIP downregulation, *Carcinogenesis*, 34 (2013), 1918-1928.
- Yousefi S., Perozzo R., Schmid I., Ziemiecki A., Schaffner T., Scapozza L., Brunner T., Simon H.U., Calpain-mediated cleavage of Atg5 switches autophagy to apoptosis. *Nat Cell Biol*, 8 (2006), 1124-32.

- Yu Z.Q., Ni T., Hong B., Wang H.Y., Jiang F.J., Dual roles of Atg8-PE de-conjugation by Atg4 in autophagy, *Autophagy*, 8 (2012), 883–92.
- Yue Z., Jin S., Yang C., Levine A.J., Heintz N., Beclin 1, an autophagy gene essential for early embryonic development, is a haploinsufficient tumor suppressor, *Proc Natl Acad Sci*, 100 (2003), 15077–15082.
- Zhang G.N., Liang Y., Zhou L.J., Chen S.P., Chen G., Zhang T.P., Kang T., Zhao Y.P., Combination of salinomycin and gemcitabine eliminates pancreatic cancer cells, *Cancer Lett*, 313 (2011), 137–144.
- Zhou J., Li P., Xue X., He S., Kuang Y., Zhao H., Chen S., Zhi Q., Guo X., Salinomycin induces apoptosis in cisplatin-resistant colorectal cancer cells by accumulation of reactive oxygen species, *Toxicol Lett*, 222 (2013), 139–145.
- Zhu Y., et al., Modulation of serines 17 and 24 in the LC3-interacting region of Bnip3 determines pro-survival mitophagy versus apoptosis, *J. Biol. Chem*, 288 (2013), 1099–1113.

APPENDIX A

MATERIALS AND SOLUTIONS

Monensin Isolation

- Silica gel 60 (Merck KGaA, Darmstadt, Germany)
- TLC silica gel 60 F254 paper
- Rotary evaporator
- Open glass column
- Separating funnel

Cell culture

- Class II biosafety cabinet (Esco, Netherland)
- CO₂ incubator (Sanyo-MCO-18AIC, Japan)
- Olympus inverted Microscope (1X71)
- Fluorescence inverted Microscope (Olympus FX7)
- Cooling centrifuge (Sigma- B6916, USA)
- pH meter (Hanna- HI221, Germany)
- Magnetic mixer (Wisd-MSH20A, Germany)
- 100 x20 mm culture dishes (Greiner Bio-One CELLSTAR, Germany)
- 6 wells culture dishes (Greiner Bio-One CELLSTAR, Germany)
- 2.5- 5- 10 and 25 ml sterile pipettes (Orange, Italy)
- 15 and 50 ml falcon tubes (Jet Biofil, Italy)
- Pipettes tips (VWR, USA)
- Eppendorf tubes (Grainer, Germany)
- Cell medium; DMEM and EMEM (Gibco- 31330, USA)
- Fetal bovine serum (FBS) (Gibco- 10270, USA)
- Trypsin-EDTA (Gibco- 3103382, USA)
- Doxorubicin (Adriblastina, Carlo Erba,7126176)
- DMSO (Merck- K33960212-504, USA)
- EtOH (Merck- K33960212-504, USA)
- Trypan Blue solution 4% (Sigma- T6146, USA)

Western blotting

- Protease inhibitor cocktail (Roche-04693159001, Germany)
- BCA kit (Sigma- 088K6138, Germany)
- Isopropanol (Merck- K35707095 607, USA)
- MEtOH (Merck, K34212908503)
- Acrylamide 30% (Sigma- A9099, Germany)
- Ammonium phosphate solution (% 10) (Sigma- A9164, Germany)
- TEMED (Sigma- T9281, Germany)
- Beta-MercaptoEtOH (Sigma, M3148)
- Anti-rabbit IgG horse radish peroxidase (HRP) (Amersham-NA934, USA)
- Anti-mouse IgG horse radish peroxidase (HRP) (Amersham-NA931, USA)
- Anti-B-Actin antibody (Sigma-A5316, Germany)
- Primary antibodies (CST, USA)
- ECL kit (SuperSignal West Pico by Thermo Scientific, USA)
- Centrifuge (Eppendorf, 5415D ve 5415R, USA)
- Block heater (Grant- QBA2, England)
- Running apparatus (Bio-Rad, USA)
- Transfer apparatus (Bio-Rad, USA)
- Whatman filter paper (Bio-Rad, USA)
- Polyvinylidene fluoride (PVDF) transfer membrane (Roche- 03010040001, Germany)
- 1-10, 20-200 ve 100-1000 µl automatic pipettes (Brand-TransferpetteS, Germany)

Resolving gel with different percentages

Resolving gel (10 ml)	6 %	8 %	10 %	12 %	15 %
dH2O	5.4 ml	4.7 ml	4.1 ml	3.4 ml	2.4 ml
30 % Acrylamide	2.0	2.7	3.3	4.0	5.0
4X separating buffer	2.5	2.5	2.5	2.5	2.5
10 X APS	0.1	0.1	0.1	0.1	0.1
TEMED	0.008	0.006	0.004	0.004	0.004

Stacking gel with different percentages

Stacking gel	10 ml	5ml	2.5 ml
dH ₂ O	5.7	2.85	1.425
30 % Acrylamide	1.7	0.85	0.425
4X stacking buffer	2.5	1.25	0.625
10 X APS	0.1	0.05	0.025
TEMED	0.010	0.005	0.005

Stock Solutions

2 X RIPA solution:

- 10 mM Tris base pH=8.0 (Sigma- T5941, Germany)
- % 0.1 SDS (Sigma- L4390, Germany)
- % 1 triton x-100 (Sigma- T8787, Germany)
- 1 mM EDTA (Sigma- K5134, Germany)
- 1 mM EGTA (Sigma- E3889, Germany)
- 140 mM NaCl (Sigma- S3014, Germany)

4X loading dye

- ○ 40 mM Tris base (pH 8.0) (Sigma- T6066, Germany)
- ○ 0.4 mM EDTA (Sigma- K5134, Germany)
- ○ % 4 SDS (Sigma- L4390, Germany)
- ○ % 20 glycerol (Sigma- G5150, Germany)
- ○ Bromophenol blue 200 µl (Merck- L54971322525, USA)

1L volume SDS-PAGE Gel 10X running buffer (1X was used)

- ○ 30 g Tris base (Sigma- T6066, Germany)
- ○ 144 g Glycine (Biochemika/FLUKA- 50046, Germany)
- ○ 10.0 g SDS (Sigma- L4390, Germany)

1L volume SDS-PAGE Gel 10X transfer buffer (1X was used)

- ○ MEtOH 20 % (Merck- K34212908503, USA)
- ○ 30.0 g Tris base (Sigma- T6066, Germany)
- ○ 144.0 g Glycine (Biochemika/FLUKA- 50046, Germany)

4X resolving buffer for SDS PAGE

- 1.5 M Tris HCL
- 0.4 % SDS w/v

Adjust pH to 8.8 – 9.0

4X separating buffer for SDS PAGE

- 0.5 M Tris HCL
- 0.4 % SDS w/v

Adjust pH to 6.8

10X PBS

- NaCL 87.5 g
- Na₂HPO₄ 11.5 g
- NaH₂PO₄ 2.3 g
- Add H₂O to 1 liter

Adjust pH to 7.4 with NaOH/HCL

Wash Buffer

- 10X PBS 1 liter
- Distilled water 9 liter
- Tween 20 10 ml

Adjust pH to 7.4 with NaOH/HCL

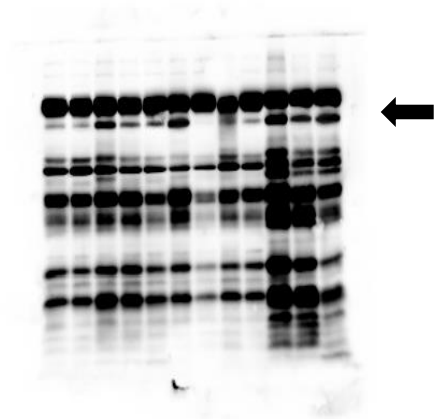
SUPPLEMENTARY INFORMATION

Time course experiment Western blots (Whole membrane images)

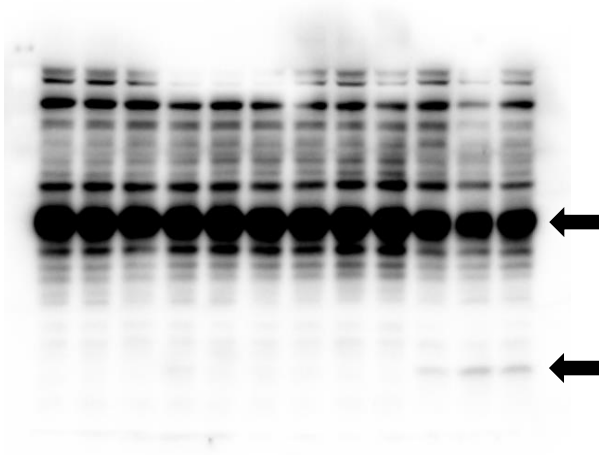
HeLa Cell line



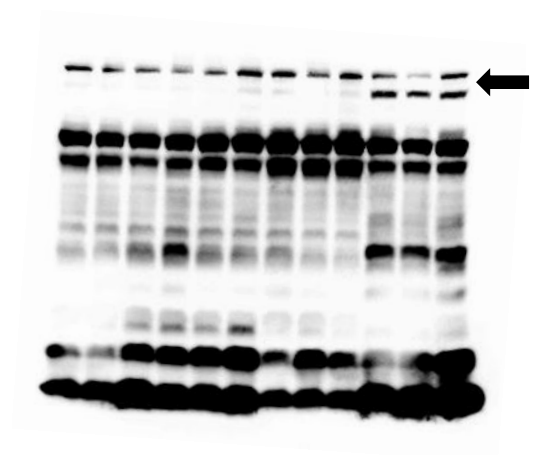
LC3 Western blot image



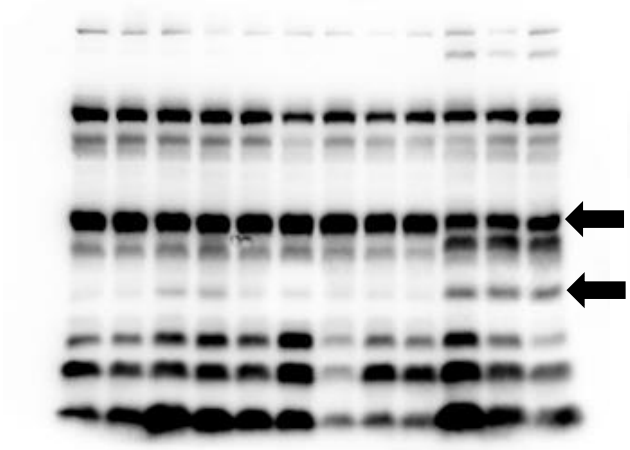
p62 Western blot image



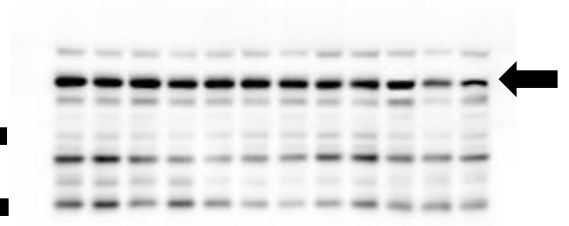
Caspase 3 Western blot image



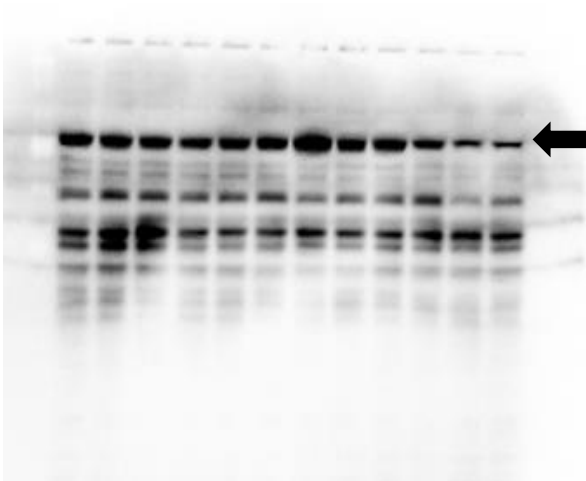
PARP Western blot image



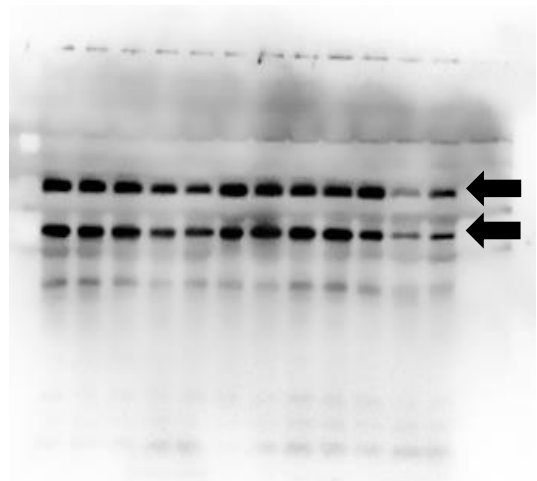
Caspase 9 Western blot image



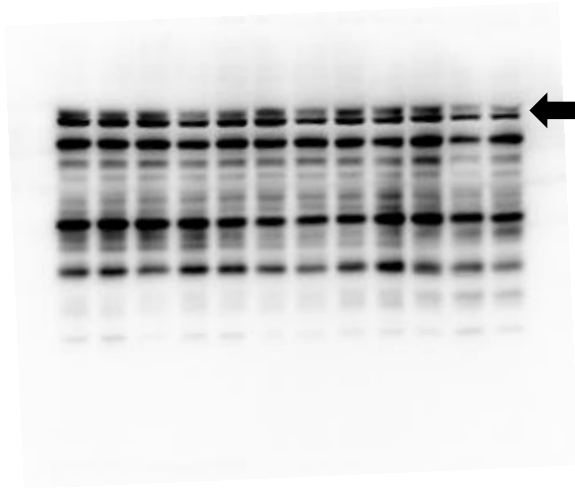
Atg-5/12 Western blot image



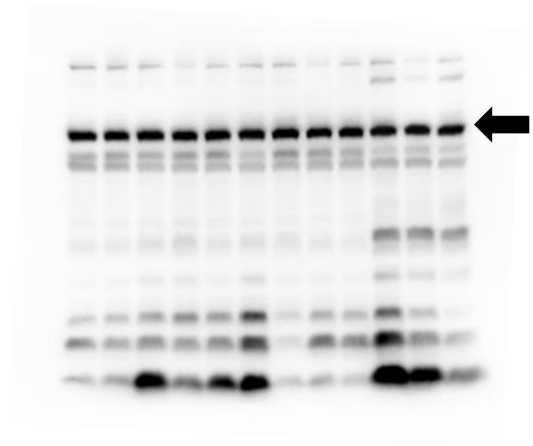
Atg-7 Western blot image



Beclin 1 and Atg-3 Western blot image

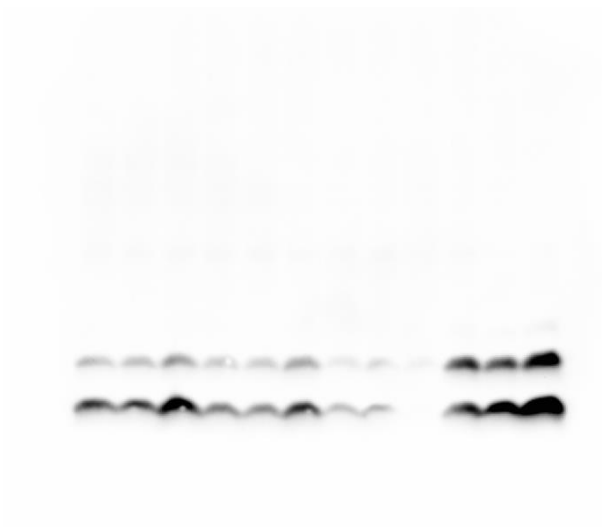


Atg-16L1 Western blot image

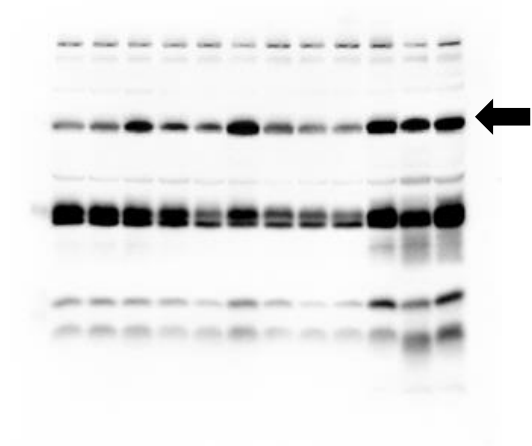


Actin Western blot image

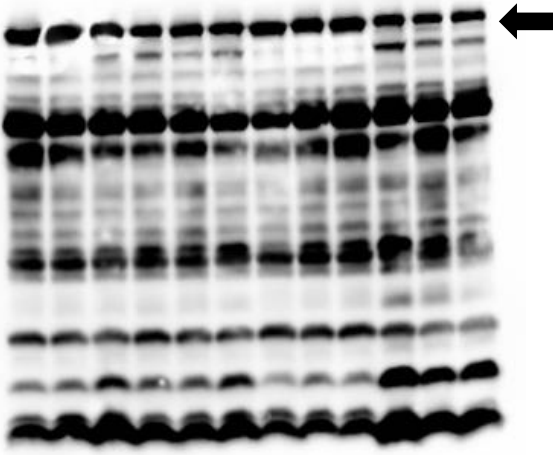
CaCo-2 Cell line



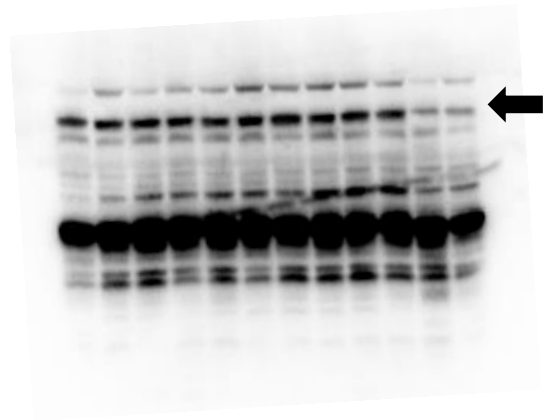
LC3 Western blot image



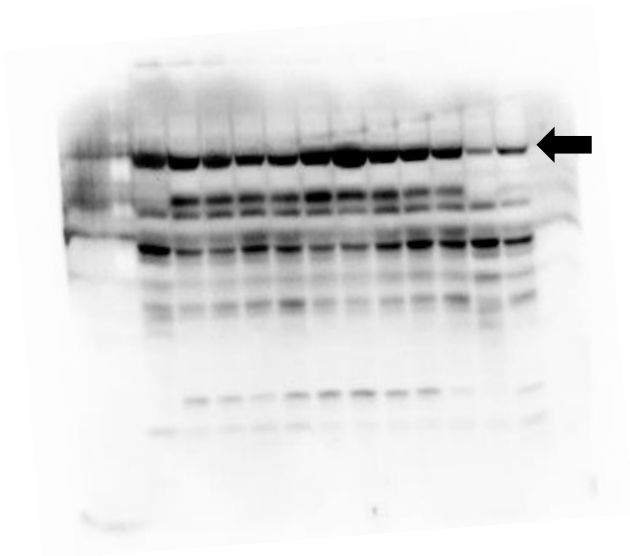
p62 Western blot image



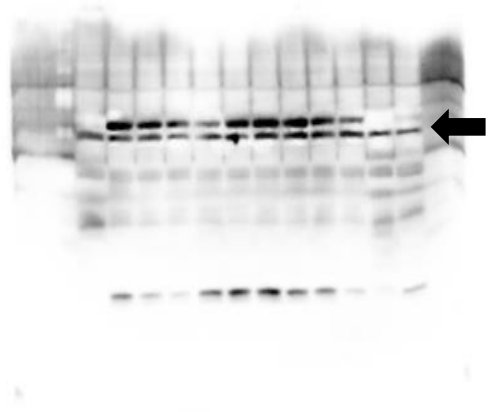
PARP Western blot image



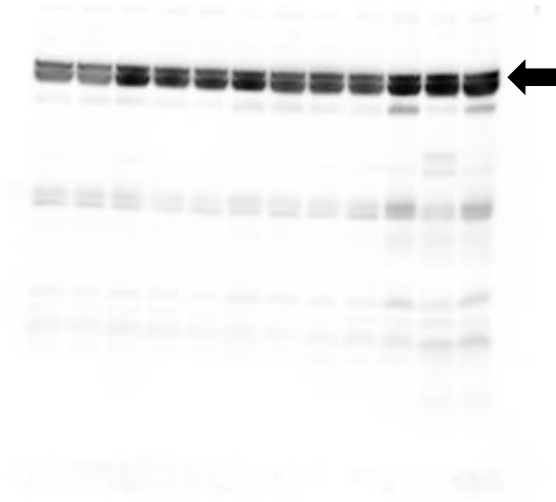
Atg-5/12 Western blot image



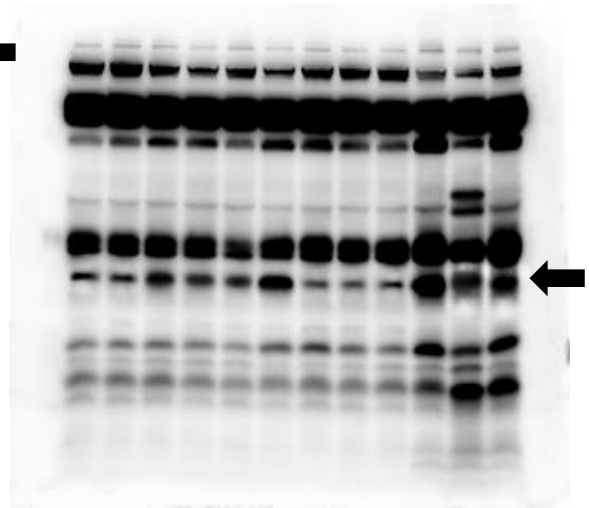
Atg-7 Western blot image



Beclin 1 Western blot image

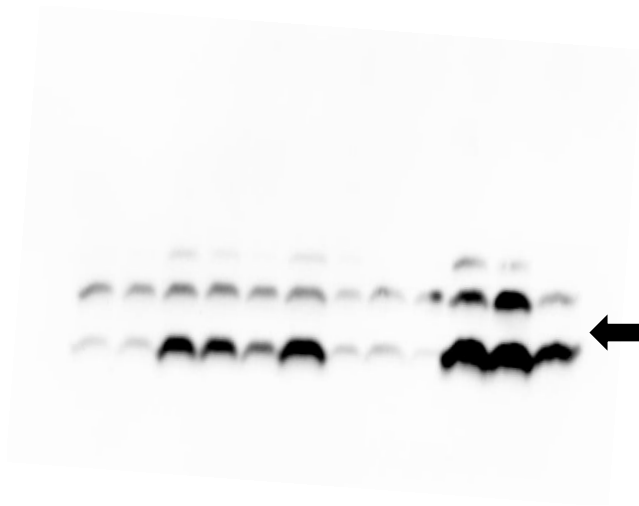


BIP Western blot image

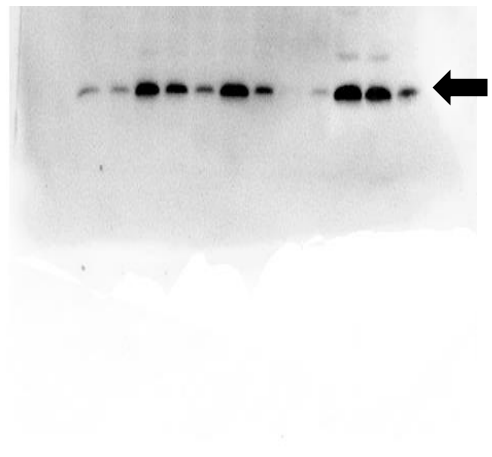


CHOP Western blot image

PC-3 Cell line

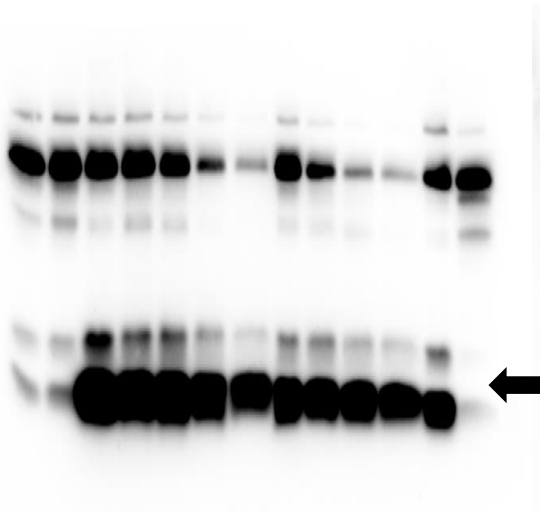


LC3 Western blot image

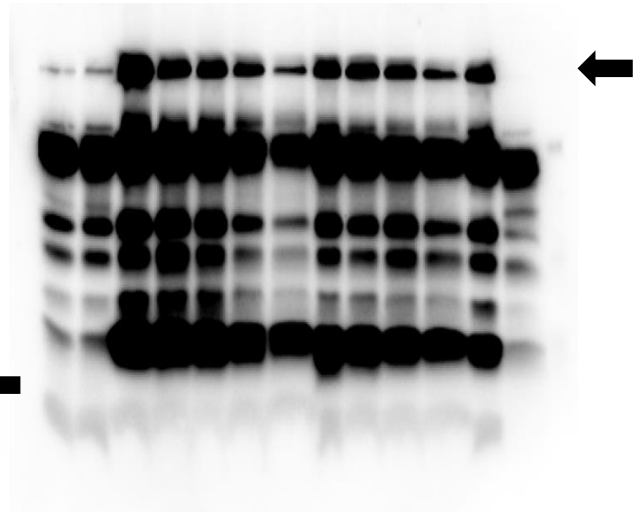


p62 Western blot image

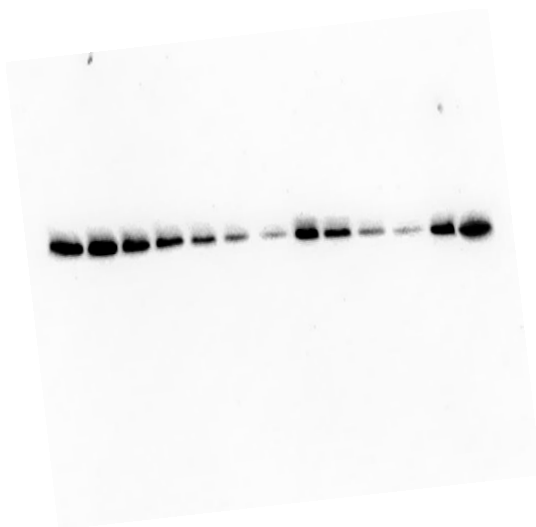
Dose response experiment Western blots (Whole membrane images)
HeLa Cell line



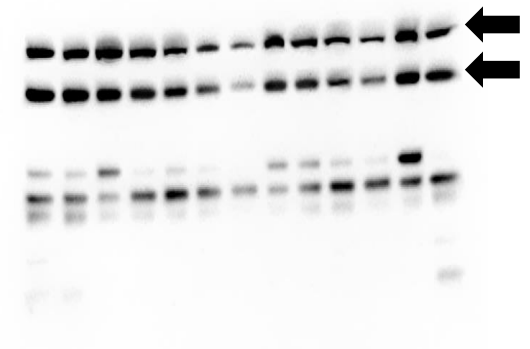
LC3 Western blot image



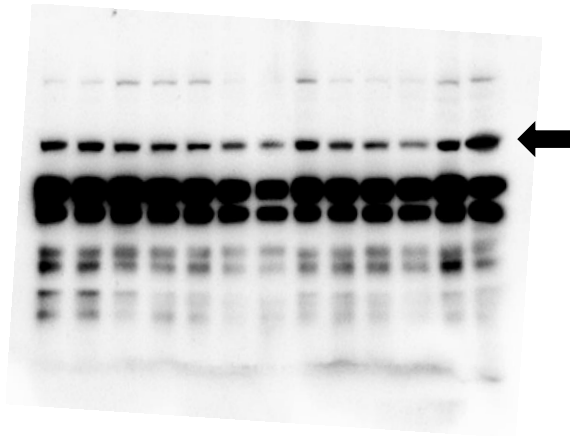
p62 Western blot image



Atg-3 Western blot image



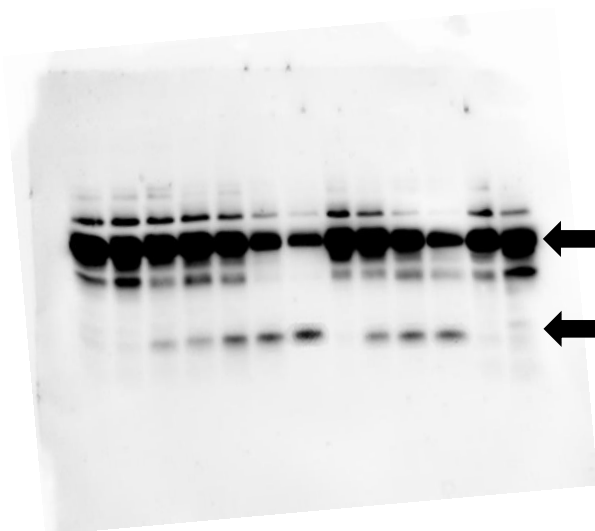
Atg-16L1 and Atg-5/12 Western blot image



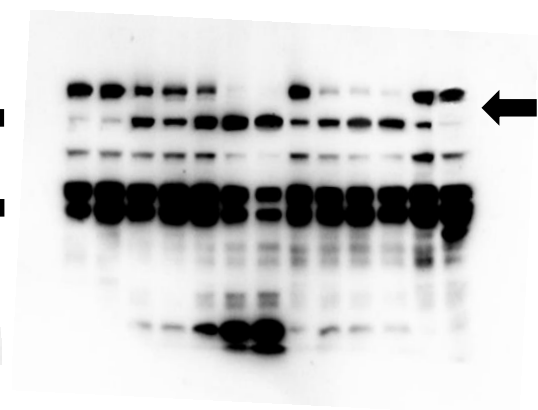
Atg-7 Western blot image



Beclin 1 Western blot image



Caspase 3 Western blot image



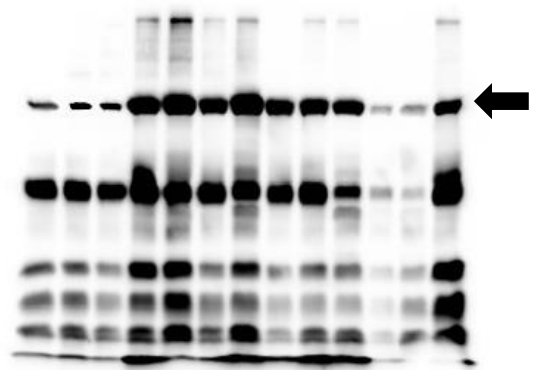
PARP Western blot image

Combine treatment experiment Western blots (Whole membrane images)

HeLa Cell line



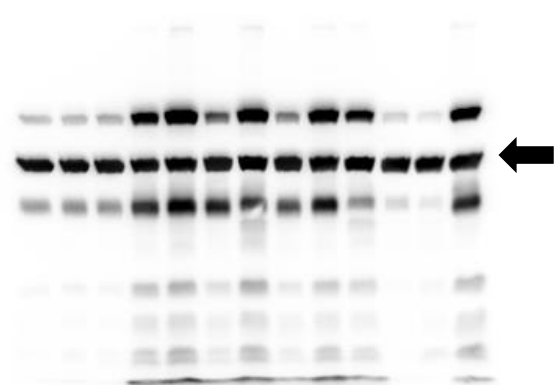
LC3 Western blot image



p62 Western blot image



Actin Western blot image



Actin Western blot image